TECHNICAL UNIVERSITY OF LIBEREC

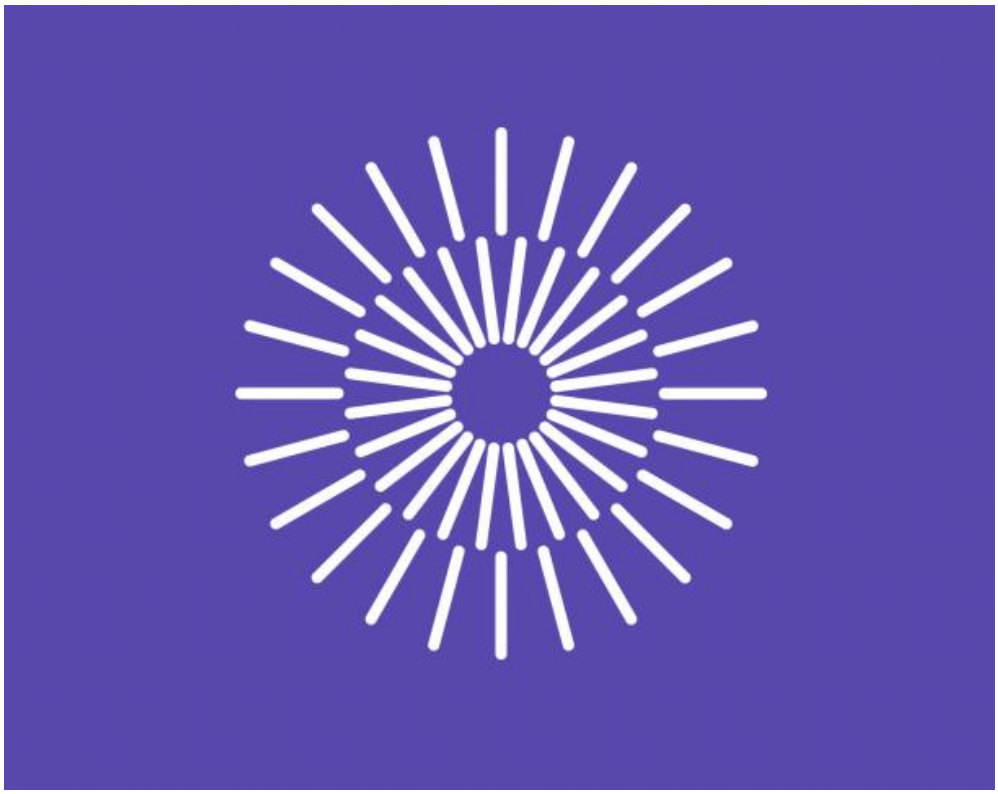

BIOREMEDIATION POTENTIAL OF MICROBIAL COMMUNITIES AND PLANTS IN ORGANOCHLORINE CONTAMINATED ENVIRONMENTS

Ph.D. Thesis

Study Program: **P 3901 Applied sciences in engineering**

Field of Study: 3901V055 Applied sciences

Liberec 2024

Author: MSc. Aday Amirbekov

Supervisor: RNDr. Alena Ševců, Ph.D

Workplace: Faculty of Mechatronics, Informatics and Interdisciplinary Studies
Technical University of Liberec
Studentská 1402/2
460 01 Liberec 1
Czech Republic

Declaration

I hereby certify that I have been informed that Act 121/2000, the Copyright Act of the Czech Republic, namely Section 60, School-work, applies to my Ph.D. thesis in full scope.

I acknowledge that the Technical University of Liberec (TUL) does not infringe on my copyrights by using my Ph.D. thesis for TUL's internal purposes.

I am aware of my obligation to inform TUL of having used or licensed to use my Ph.D. thesis, in which event TUL may require compensation for costs incurred in creating the work at up to their actual amount.

I have written my Ph.D. thesis myself using the literature listed therein after consulting with my supervisor and my tutor.

I hereby also declare that the hard copy of my Ph.D. thesis is identical to its electronic form as saved at the IS STAG portal.

Date:

Signature:

Acknowledgement

I extend my sincerest appreciation to my supervisor, Alena Ševců, whose unwavering encouragement and support, spanning from the initial stages to the final culmination, played a pivotal role in fostering my understanding of the subject matter. My heartfelt thanks are directed towards my consultant, Pavel Hrabák, for his valuable consultations, assistance, and wise counsel throughout my academic journey.

I am deeply thankful to Professor Miroslav Černík for instilling faith in my ability to undertake this Ph.D. study. Gratitude also goes to Jakub Říha for his assistance in bioinformatics, and a special acknowledgment is reserved for Carlos Arias from Aarhus University, Denmark, for graciously hosting me as an intern and providing the necessary resources for laboratory experiments in growth chambers and greenhouse settings.

My appreciation extends to my colleagues and the entire Department of Applied Biology for their unwavering support, particularly in gaining knowledge in the field of environmental microbiology. I would like to express my gratitude to Stanislava Vrchovecká and the entire Department of Environmental Chemistry for their collaboration and for facilitating chemical analysis.

I reserve special thanks for my parents, friends, and loved ones, whose kind understanding and all-encompassing support have been instrumental throughout the course of my studies. Your encouragement has been a guiding light, and I am truly grateful for your unwavering presence in my life.

Research funding

My research was supported by the following projects:

- Research Infrastructure **NanoEnviCz** (Project No. LM2018124 and Project No. LM2023066) supported by the Ministry of Education, Youth and Sports of the Czech Republic.
- Ministry of Education, Youth and Sports of the Czech Republic, and Investment Funds under the framework of Operational Programme Research, Development and Education—Project: Hybrid Materials for Hierarchical Structures "**HyHi**" (CZ.02.1.01/0.0/0.0/16_019/0000843).
- **SGS-**2021–3051 project of Student Grant Scheme of TUL: Olše lepkavá - genetická diverzita mikrobiomu rhizosféry při stresových podmínkách a expozici vůči polutantům.
- EC LIFE Programme within the framework of project ''Innovative technology based on constructed wetlands for treatment of pesticide contaminated waters (**LIFEPOPWAT**) ", registration number LIFE18 ENV/CZ/000374.

Abstract

Hexachlorocyclohexane (HCH) is a group of chemical compounds occurring in several isomers (α HCH to θ-HCH). HCH compounds were commonly used as pesticides, particularly γ-HCH as an insecticide. Even though the use of the HCH isomers has been prohibited for decades, their presence in the environment is still reported worldwide.

This thesis comprises an outline of bioremediation of HCH by: i) biochar-filled wetland beds, ii) Wetland+ treatment technology, iii) wetland plant species and *Alnus glutinosa* tree. The purpose of the dissertation was to investigate the removal efficiency of different systems, the effects of the HCH isomers on the growth, physiological parameters, and microbial communities in selected soil-plants and wetland systems.

The first study demonstrated that the biochar wetland beds achieved an impressive 96% efficiency in HCH removal and its transformation products from drainage water, a notable advancement compared to conventional wetland beds that typically remove an average of 68% of HCH.

Wetland+, a trademarked remedial technology, achieved an average efficiency of 96.8% for chlorobenzenes and 81.7% for HCH isomers, demonstrating effective integration of sedimentary tanks, PRBs, biosorption systems, and aerobic wetlands over its initial 12 months of operation.

The phytoremediation study's key findings demonstrate that selected wetland plants and trees, notably *A. glutinosa*, effectively remove HCH from the soil, efficiency is dependent on a particular isomer.

Key words: Hexachlorocyclohexane, phytoremediation, constructed wetlands, bioremediation, *lin* genes.

Abstrakt

Hexachlorocyclohexany (HCH) je skupina organochlorových sloučenin, které se vyskytují ve formě několika izomerů (α HCH až θ-HCH). HCH sloučeniny byly běžně používány jako pesticidy, zejména γ-HCH jako insekticid. I když je použití izomerů HCH zakázáno již desítky let, jejich přítomnost v životním prostředí je stále reportována po celém světě.

Tato disertační práce obsahuje výsledky výzkumu bioremediace HCH pomocí: i) biofiltru naplněném biouhlem (biochar), ii) komplexní technologie Wetland+, iii) mokřadních rostlin a olší (*Alnus glutinosa*) . Cílem disertační práce bylo zhodnotit účinnost odstraňování HCH v různých biologických systémech, dále vliv izomerů HCH na růst a fyziologické parametry vybraných rostlin a mikrobiální společenstva.

První studie prokázala, že biofiltr s biouhlem dosáhl účinnosti odstranění HCH a jeho transformačních produktů z odtokové vody až 96 %, což je pozoruhodný pokrok ve srovnání s konvenčními biofiltry, který odstranil průměrně 68 % HCH.

Wetland+, obchodně chráněná technologie, dosáhl průměrné účinnosti 96,8 % pro chlorbenzeny a 81,7 % pro izomery HCH během prvních 12 měsíců provozu, což bylo dosaženo účinnou integrací sedimentačních nádrží, reaktivních bariér, biosorpčních systémů a aerobních mokřadů.

Klíčové poznatky fytoremediační studie ukazují, že vybrané druhy mokřadních rostlin a stromů, zejména *A. glutinosa*, účinně odstraňují HCH z půdy, přičemž účinnost závisí i na druhu izomeru.

Klíčová slova: Hexachlorocyklohexan, fytoremediace, konstruované mokřady, bioremediace, *lin* geny.

Thesis structure

This thesis is divided into three main parts: Introduction, Experimental part (HCH removal by constructed wetlands, Phytoremediation) and Conclusions.

The introduction provides an overview of the research topic, its importance, the scope of the study, and the research objectives.

The experimental part represents the main part of the thesis. It contains both a methodical description of the experiments and results with summary. This key part is based primarily on published articles and is divided into two chapters:

- The **first chapter** focuses on the studies on constructed wetland beds for the removal of the HCH compounds and microbial analysis of the substrates and water from these constructed wetland beds. It is based on two published studies (Amirbekov et al., 2023, 2021): the first study tested HCH removal in a biochar-amended wetland bed where the outcomes served as a basis for the second and more complex study focused on the Wetland+ system established at Hajek site in Czechia.
- The **second chapter** focused on three phytoremediation studies. The first study demonstrated *A. glutinosa* efficacy in eliminating α, β, and δ isomers of HCH from freshly spiked soil. The results are based on a published study (Amirbekov et al., 2024). The second study was on the removal potential of one and two-year-old *A. glutinosa* planted on soil and sediments from the contaminated Hajek site. The results of the study were submitted to the journal. The third study compares the removal potential of *A. glutinosa* seedlings and three wetland plants: *Phragmites australis, Juncus effusus* and *Typha latifolia*. In addition, rhizosphere microbial communities were assessed. It is partially based on this study (Vrchovecká et al., 2024).

Conclusions summarize all important outcomes of this thesis.

Table of Contents

List of figures

List of tables

Abbreviations

1,4-TCDN	1,3,4,6-tetrachloro-1,4-cyclohexadiene
16S rRNA	16S ribosomal RNA
2,5-DDOL	2,5-dichloro-2,5-cyclohexadiene-1,4-diol
ABA	Abscisic acid
AG	*Alnus glutinosa*
ASV	Amplicon Sequence Variant
AUX	Auxin
BR	Brassinosteroids
CK	Cytokinin
Clb	Chlorobenzene
Clph	Chlorophenol
Ct	Cycle threshold value in real-time PCR
DDOL	Dichlorocyclohexadiene diol
DDT	Dichlorodiphenyltrichloroethane
DNA	Deoxyribonucleic acid
GA	gibberellic acid
GC-MS	Gas chromatography-mass spectrometry
HCH	Hexachlorocyclohexane
IAA	Indole-3-acetic acid
IDA	Information dependent acquisition
JA	Jasmonic acid
JE	*Juncus effusus*
K_{ow}	The ratio of the concentration of a chemical in n-octanol and water at equilibrium at a specified temperature.
LC/HRMS	Liquid chromatography–high-resolution mass spectrometry
LOD	Limit of detection
log K_{ow}	Relative indicator of the tendency of an organic compound to adsorb to soil and living organism.
MCPGM	monochlorophenyl-β-D-(6-O-malonyl) glucopyranoside
OCP	Organochlorine pesticide
OTU	Operational taxonomic unit
oxIAA	2-oxindole-3-acetic acid

PA	*Phragmites australis*
PCA	Principal component analysis
PCL	Pentachlorocyclohexanol
PCR	Polymerase chain reaction
POPs	Persistent Organic Pollutants
qPCR	Quantitative Polymerase chain reaction
SA	Salicylic acid
SD	Standard deviation
TCDN	Tetrachlorocyclohexadiene
t-HCH	Technical hexachlorocyclohexane
TL	*Typha latifolia*
TOC	Total organic carbon
U16SRT	Universal microbial recovery via gene 16s rRNA

Thesis aims

i. Method Optimization: The first objective of this thesis is to refine and standardize protocols for microbial DNA analysis, particularly focusing on quantitative polymerase chain reaction (qPCR) and next-generation sequencing (NGS) techniques. This optimization is crucial for ensuring the reliability and reproducibility of molecular biology results obtained from complex environmental samples contaminated with HCH compounds.

ii. Biodegradation Monitoring: A central aim is to systematically monitor specific enzymes and bacterial community associated with the biodegradation of HCH compounds, with a particular emphasis on evaluating ongoing processes within constructed wetlands. Through this investigation, we seek to elucidate the dynamics of bioremediation and its impact on natural microbial communities, thereby contributing to a deeper understanding of biodegradation phenomena.

iii. Phytoremediation Assessment: Another key goal is to assess the efficacy of phytoremediation technology in the removal of HCH compounds, while highlighting the essential role played by microbial communities in this remediation process. The aim is to describe the distribution of HCH isomers in plant roots, stems and leaves to understand the behavior of different isomers and the efficacy of their removal.

Introduction

Pesticides were invented to control pests for widespread use in agriculture. Trying to solve one problem, we spawned several new ones, sometimes the value of which we often underestimate. Hexachlorocyclohexane (HCH) isomers (especially lindane (γ-1, 2, 3, 4, 5, 6-hexachlorocyclohexane)) are highly persistent toxic compounds, three of which are included on the Stockholm convention list ("Stockholm Convention - an overview | ScienceDirect Topics," n.d.). Despite their known toxicity, HCH and its transformation products are virtually ubiquitous in the environment, with background concentrations at around ppb levels in a wide range of matrices (Bajpai et al., 2007; Chakraborty et al., 2019; Erkmen and Kolankaya, 2006; Rigét et al., 2019; Zhao et al., 2007). In the 1960s and 70s, when it became apparent just how toxic these substances were, large amounts of waste HCH isomers were disposed of into unsecured subsurface dumps (Directorate-General for Internal Policies of the Union (European Parliament), 2017) for an inventory of HCH sites from 15 EU countries). Nevertheless, around 382 000 t of technical HCH, and 81 000 t of γ-HCH, were used for agricultural purposes in Europe between 1970 and 1996 (Breivik et al., 1999). HCH polluted areas can be treated by technologies involving chemical reduction, sewage treatment works along with less costly biodegradation and phytoremediation approach of HCH isomers (Kumar and Pannu, 2018; Man et al., 2018; Wacławek, 2019).Various treatment technologies have been suggested for HCH-contaminated areas, and numerous studies focused on the chemical reduction and degradation of HCH isomers have been undertaken. Chemical reduction and degradation of HCH isomers are well studied (Dominguez et al., 2016; M. Homolková and Černík, 2015; Wacławek, 2019), for example, zero-valent iron nanoparticles showed effectiveness in the degradation of persistent HCH (Phenrat et al., 2019). Wang used alkaline cold-brew green tea to degrade HCH compounds (Wang et al., 2019). Over the last decade, however, increasing attention has been paid to the use of carbon-rich materials, such as charcoal, bio-coal, and activated carbon, for stabilizing organic pollutants in sediments and soils *in situ* (Beesley et al., 2011; Denyes et al., 2012; Paul et al., 2011). Biochar, a charcoal produced from plant biomass, is an inexpensive and renewable adsorbent that has been used for a variety of applications, including soil conditioning and remediation, carbon sequestration, water treatment and the absorption of a variety of pollutants (Mohan et al., 2014). However, while biochar is rapidly gaining popularity, only a limited number of studies have been published on the use of biochar for minimizing the bioavailability of pollutants, most of which have been laboratory based (Gomez-Eyles et al., 2011; Silvani et al., 2019; Xu et al., 2016; Zimmerman et al., 2011), and most concentrating on the factors affecting its ability to remove organic pollutants (Ahmad et al., 2014; Ali et al., 2012). One exception has been a recent study that sought to restore sediments contaminated by γ-HCH and hexachlorobenzene through amendment with carbon-

rich materials, with the aim of sequestering the contaminants and rendering them biologically unavailable (Grgić et al., 2019). To date, however, nothing has been published on the use of biochar in wetland beds for biodegradation and removal of pollutants, and particularly HCH isomers, at contaminated dumpsites. Theoretically, HCH accumulating in such biochar wetland beds could undergo degradation by indigenous bacteria; however, to the best of our knowledge, nothing is known about the development of microbial consortia in biochar wetland bed systems. On the other hand, detailed laboratory studies on aerobic (Lal et al., 2010) and anaerobic (Bala et al., 2010) microbial degradation of HCH isomers have been undertaken since the 1960s and a number of anaerobic bacteria capable of degrading HCH isomers have been identified, including *Clostridium sphenoids*, *Clostridium butyricum*, *Clostridium pasteurianum*, *Citrobacter freundii*, *Desulfovibrio gigas*, *Desulfovibrio africanus*, *Desulfococcus multivorans*, *Dehalobacter* sp., and *Clostridium rectum* (Lal et al., 2010), while strains of the *Sphingomonadaceae* family, capable of aerobic degradation of HCH, have been recorded as dominant at HCH dumpsites worldwide (Bala et al., 2010; Böltner et al., 2005; Mohn et al., 2006; Saxena et al., 2013). The primary reaction during HCH isomer degradation is dehydrochlorination, and functional genes in the genus *Sphingobium* encoding the key enzymes have now been identified as HCH dehydrochlorinase, haloalkane dehalogenase, and reductive dechlorinase, within *Sphingomonas paucimobilis* UT26 suggested as a possible γ-HCH degradation pathway (Nagata et al., 1999; Oakley et al., 2004; Okai et al., 2010). The dehydrochlorination reactions of γ-, α-, δ-, and β-HCH isomers catalyzed by dehydrochlorinase have also been described (Brittain et al., 2010). Most studies have recorded microbial biomass as increasing following biochar addition, with significant changes in microbial community composition and enzyme activity that may explain the biogeochemical effects of biochar. Nevertheless, very little is known about the mechanisms through which biochar affects microbial abundance and community composition. Changes in microbial community composition or activity induced by biochar may affect not only nutrient cycles and plant growth but also the cycling of soil organic matter (Cui et al., 2019; Deng et al., 2019; Odedishemi Ajibade et al., 2021).

Genes encoding enzymes involved in the HCH degradation process are named *lin* genes and were initially discovered in *S. japonicum* UT26. Currently, six structural *lin* genes *linA* (encoding a dehydrochlorinase), *linB* (a halidohydrolase), *linC* (a dehydrogenase), *linD* (a reductive dechlorinase) and *linE* (a ring-cleavage oxygenase) were described, all involved in the complete mineralization of γ-HCH in *S. japonicum* UT26 (Lal et al., 2006; Nagata et al., 1999). The *linA* is able to degrade α-, γ- and δ-HCH except for β-HCH (Kumari et al., 2002). Subsequent analysis revealed that *linA* requires the presence of a 1,2-biaxial HCl pair on a substrate molecule (Trantírek et al., 2001). The *linB* is responsible for the hydrolytic dechlorination of the chemically unstable intermediate 1,4-TCDN (1,3,4,6-tetrachloro-1,4-cyclohexadiene) to 2,5-DDOL (2,5-dichloro-2,5-cyclohexadiene-1,4-diol)

(Nagata et al., 1993). Unlike *linA*, which appears to be a unique dehydrochlorinase, *linB* is a haloalkane dehalogenase from the α/β-hydrolase family of enzymes. *linB* has been reported to convert β-HCH to 2,3,4,5,6-pentachlorocyclohexanol (PCL) (Nagata et al., 2005). *linD* and *linE* are associated with the downstream pathway of γ-HCH degradation (Lal et al., 2006). The accumulation of information on the genetic, molecular and physiological aspects of HCH degradation is necessary for the development of a bioremediation methods.

Phytoremediation is a promising way for contaminants removal as a sustainable, environmentally friendly and cost-effective method. In recent years, an increasing number of examples of HCH isomers uptake and accumulation by plants has become available from local flora adapted to the high toxicity of these sites (Kidd et al., 2008; Liu et al., 2021; Rissato et al., 2015; Zhang et al., 2013). Phytoremediation using species that are already adapted to the local conditions can be more effective. One of the dominant tree species in the highly contaminated site that was part of this study (Hajek near Karlovy Vary) is black alder (*Alnus glutinosa*). HCH represents an abiotic stress stimulus that can result in a change in the hormonal profile of plants. A similar abiotic stress stimulus is pruning. Plant hormones can be considered as a marker of the physiological state or adaptation of alder tree.*A. glutinosa* is a widespread and short-lived tree that grows in low-lying moist and coastal places. It is used in deluge control, stabilization of riverbanks, and the river ecosystems' functioning. To the best of our knowledge no report is available using this tree for the removal of HCH. Plant uptake of pesticides depends on several parameters as a physicochemical property of the compound, soil type, plant species, and climatic factors (Bromilow and Chamberlain, 1995). HCH and most of their metabolites are highly hydrophobic compounds: the log K_{ow} >3, therefore they are concentrated in roots and a little translocated to shoots (Briggs et al., 1982; Dettenmaier et al., 2009). Rhizosphere microorganisms play an important role in the organic transformation of the compounds. Due to of their activity, it can create more polar metabolites that can penetrate the root system and translocate to other parts of plants (Chaudhry et al., 2002; Schwitzguébel et al., 2006). Plants can release into soil a variety of substances such as root exudates, mucigel and root lysates. (Curl and Truelove, 2012; Dakora and Phillips, 2002; Pinton et al., 2007). These rhizodeposits provide a nutrient-rich habitat for microorganisms and can enhance the co-metabolic transformation of pollutants, induce genes encoding enzymes involved in the degradation process, and increase surfactant activity (Anderson and Coats, 1995; Miya and Firestone, 2001; Shaw and Burns, 2005). In addition, inoculation with rhizospheric microorganisms is reported to be a way of enhancing the degradation of HCH. Composition of the bacterial and fungal community of *A. glutinosa* root microsymbionts and endophytes depends on several parameters: salinity, phosphorus, pH, saturation percentage (SP) and total organic carbon (TOC) and seasonality is not an essential factor in the formation of microbial communities (Thiem et al., 2018).

EXPERIMENTAL SECTION

HCH removal by constructed wetlands

I. HCH Removal in Biochar-Amended constructed wetland

1. Materials and methods

1.1 Site Description and Experimental Design

This study took place in the Hajek, Czech Republic (50°17′31.5″ N 12°53′35.2″ E). The Hajek site is located in Western Bohemia near the Karlovy Vary spa. Since the 1960s, the site has been used as a waste repository for the nearby mine of uranium, kaolin, basalt, and bentonite. According to the decision of the state authorities, in 1966–1968, about 3,000–5,000 tonnes of residual ballast isomers of HCH and ClB from the production of lindane (γ-HCH) from the Spolana chemical plant (Neratovice, Czech Republic) were disposed into the Hajek quarry spoil heap. Nowadays, the long-term average concentrations in the outlet drainage channel reach 136, 605, and 28 µg L−1 sum of HCH, ClB and chlorophenols (ClPh), respectively. Annual temperatures at the site range from 17°C to -3°C and annual precipitation is around 849.3 mm (www.chmi.cz).

In 2018, two parallel constructed wetland beds (each 360 × 100 × 35 cm) were installed close to the waste sedimentation ponds (50°17'31.508"N, 12°53'34.348"E) in order to test potential water treatment measures against HCH contamination. In August 2018, one of the treatment beds was filled with a locally obtained soil/clay substrate with a shallow layer of natural water (control), while the other was filled with 750 kg of biochar (biochar wetland beds; Figure 1). Waste water from the industrial site was then allowed to trickle through the beds via gravitation, with water flow being assessed manually during sampling using stopwatches and calibrated vessels.

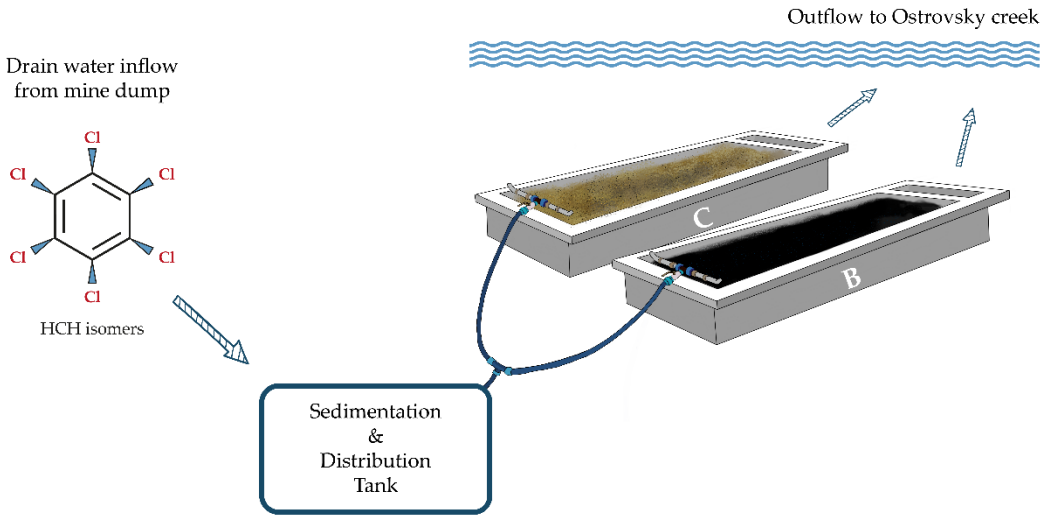

Figure 1. Schematic illustration of the artificial two-part wetland bed used in this study, B- biochar wetland bed, C- control bed filled with a soil/clay substrate and natural water.

The main objectives of this study, therefore were i) to evaluate and compare the efficiency of two horizontal flow constructed wetland bed systems with and without biochar at HCH removal, and ii) to

elucidate the HCH biodegradation potential of biochar wetland beds through the detection of HCH transformation functional genes, DNA sequencing and whole microbial community profiling.

1.2 Biochar characteristics

The biochar used in this study was produced by a commercial company (Biouhel, Zlin, Czech Republic) through pyrolysis of a mixture of waste agricultural biomass (one- to two-year plants) and digestate from a biogas plant, mixed at a ratio of 3:2. Pyrolysis was carried out for 50 min at a maximum temperature of 570 °C, producing a dry product (dry matter 99.9%) with a density of 0.59 kg L−1. Prior to installation of the biochar, laboratory tests were undertaken to determine the sorption capacity for chlorobenzenes (ClB) at 100 mg g^{-1} and HCH at 4 mg g^{-1}, and the presence of polyaromatic hydrocarbons (PAH; not detected). Elemental composition, determined using a Vario EL cube analyzer (Elementar, Langenselbold, Germany), was N (0.3%), C (88.8%), H (0.8%), S (0.1%), and O (10%).

1.3 Sampling

Each month, water from inflow and outflow from each bed was sampled from each bed for chemical analysis using glass vials. In total, 20 water samples were obtained from each wetland bed. Water (400 mL) was also sampled twice a year from the inflow and outflow of both beds for molecular biology analysis (i.e., amplicon 16S rRNA sequencing, qPCR; see below), while sediment samples for molecular biology analysis were taken from the control bed on 26 September 2018, and from the biochar test bed on 1 November 2019, with three samples taken in each case from different depths (i.e., upper inlet section—5 cm, middle section—15 cm, lower outlet section—30 cm). Water samples for molecular biology analysis were immediately filtered through a 0.2 µm membrane filter and later stored at −80 °C. All samples were transported to the laboratory in a cooled box.

1.4 Physical and chemical analysis

The concentration of HCH isomers and their ClB and ClPh byproducts in water were determined using two GC-MS assemblies, per a previous study (Wacławek et al., 2019). The first used an RSH/Trace 1310/TSQ 8000 GC-MS array (ThermoFisher Scientific, USA) with a Scion-5MS column for HCH, ClB and ClPh (Scion Instruments, Goes, The Netherlands), whereas the other was based on an CombiPal/CP3800/Saturn2200 GC-MS array (PAL, Zwingen, Switzerland; Varian, Palo Alto, USA) using a DB-624 column for benzene and monochlorobenzene determination (Agilent, Santa Clara, USA). In each case, limits of quantification (LOQ) were <0.005 µg/L for diClB, <0.015 µg/L for

1,2,4,5+1,2,3,5-tetraClB and pentaClB, <0.01 µg/L for 1,2,3,4-tetraClB, <0.25 µg/L for hexaClB, <0.025 µg/L for chlorophenols, and <0.01 µg/L for HCH. Samples were extracted using the headspace SPME technique, either using a PDMS/DVB fiber with a coating thickness of 100 µm (Supelco, Bellefonte, USA) or by directly injecting the sample in static headspace mode. Prior to extraction, samples were derivatized so that acetylated chlorophenols were formed (following EN 12673). Isotopically labeled compounds (γ-HCH D6, pentachlorophenol 13C6) were used as internal GC-MS/MS analysis standards.

1.5 Molecular genetic analysis

DNA extraction was undertaken on all duplicate samples using the DNeasy power Soil KIT (Qiagen, Netherlands). DNA yield and quality were then assessed using a Qubit fluorometer (Thermo Fisher Scientific, Waltham, USA) and agarose gel electrophoresis.

1.5.1 Real-Time Quantitative PCR

DNA was assessed for all samples using the primers LinA-F (5′AGCTCAACGGATGCATGAACT3′), LinA-R (5′ GGCGGTGCGAAATGAATG3′), LinB-F (5′ACCACGGGCCGAATGC3′), LinB-R (5′ACCGTGATTTCGGTCTGGTTT3′), LinB-RT-F (5′GCGATCCGATCCTCTTCCA3′) and LinB-RT-R (5′GCATGATATTGCGCCACAGA3′), LinD-F (5′GAACTGTTCCACTTCGTGTTCTCA3′), and LinD-R (5′GGTCACGCCCTTCTCCATTA3′) (Bala et al., 2010; Gupta et al., 2013; Suar et al., 2004). Total bacterial biomass was assessed by amplification of the 16S rDNA gene using the primers U16SRT-F (5′ACTCCTACGGGAGGCAGCAGT3′) and U16SRT-R (5′TATTACCGCGGCTGCTGGC3′) (Clifford et al., 2012). All qPCR reactions were run in the LightCycler 480 Real-Time PCR System (Roche, Basel, Switzerland) using white 96-well plates to increase sensitivity. Triplicate reactions of 20 µL consisted of 1 × SYBR Green I Master (Roche, Basel, Switzerland), 0.5 mM of both primers, and 2 mL of the template (0.4–16 ng). The program consisted of preincubation at 95 °C for 5 min, a melting cycle of 95 °C for 10 s, annealing for 15 s, elongation at 72 °C for 20 s, melting to 97 °C. Optimized annealing temperatures were 55 °C and 60 °C with a cycle number of 45. The data were displayed in the form of a heatmap of Ct values, the values of a particular primer being first divided into two sets comprised of values < 36 (low values) and ≥36, the latter being included in the detection boundary group. The second set, values < 36, was divided into three equally wide intervals, and gradually from the lowest values, the intervals were grouped into: high quantity, medium quantity, and small quantity. Ct values equal to 40 were considered below the *LOQ*. Individual

groups (intervals) are presented in heat maps in appropriate colors (Nechanická and Dolinová , 2018).

1.5.2 Amplicon 16S rRNA Sequencing

The V4 region of the bacterial *16S rDNA* gene was amplified using the primers 530F (5′TGCCAGCMGCNGCGG3′) and 802R (5′TACNVGGGTATCTAATCC3′) in a final volume of 50 µL (Claesson et al., 2010; Dowd et al., 2008). The initial PCR program consisted of preincubation at 95 °C for 3 min, 15 cycles of melting at 98 °C for 20 s, annealing at 50 °C for 15 s, elongation at 72 °C for 45 s, and final elongation at 72 °C for 1 min. PCR conditions for the second reaction consisted of preincubation at 95 °C for 3 min, 35 cycles of melting at 98 °C for 20 s, annealing at 50 °C for 15 s, elongation at 72 °C for 45 s, and a final elongation at 72 °C for 1 min. The amplicons were cleaned up using the Agencourt Ampure XP system (Beckman Coulter, Brea, USA). Barcoded sequencing adapters were ligated to the PCR products using the Ion Xpress Plus gDNA fragment library kit with Ion Xpress barcode adapters (Thermo Fisher Scientific, Waltham, MA, USA). Sequencing was performed using an Ion PGM Hi-Q Sequencing Kit with an Ion 314 Chip (Thermo Fisher Scientific, Waltham, MA, USA). Raw reads were then split into samples using Mothur software (Schloss et al., 2009) and subsequently processed by the DADA2 software package, following the suggested pipeline for single-end reads (Callahan et al., 2016). Preprocessing of reads included the removal of low-quality and short reads and chimeric sequences, based on taxonomy classification by DADA2 against the SILVA database v.132 (www.arb-silva.de (accessed on 20 September 2020)). Classification accuracy was evaluated against an artificial MOCK community sample created from four different species. OTU relative frequency was visualized on a heatmap showing only those OTUs with a frequency of relative abundance >5% at the genus and family level. Correlations between taxa and environmental data on 16S rRNA results were calculated using the microbiome Seq R library (Ssekagiri et al., 2017; Torondel et al., 2016) and visualized as a bar chart with p-values calculated using Pearson's correlation coefficient).

1.6 Statistical Analysis

Significant differences in pollutant concentrations in water, sediment, and biochar samples at the inlet, mid-point, and outlet of each bed were assessed using multivariate analysis of variance (MANOVA) based on the pairwise-adonis implementation with Bonferroni *p*-value correction in the R vegan package (Oksanen et al., 2009). Correlations between values for chemical analysis and the most abundant taxa were identified using Spearman's correlation, and correlations between taxa and environmental data or 16S rRNA results were calculated using the microbiome Seq R library (Ssekagiri et al., 2017; Torondel et al., 2016), and visualized as a bar chart with *p*-values calculated using Pearson's

correlation coefficient. In all cases, a significant difference was assumed at $p < 0.05$, $p < 0.01$, and $p < 0.001$.

2. Results and Discussion

The inflow drainage water had a long-term average pH value of 7.3, while the other chemical parameters were somewhat typical of kaolin mine water, with high conductivity (1350 µS cm^{-1}), high sulfate concentration (650 mg L^{-1}), high total Fe concentration (20 mg L^{-1}), and low F^{-}, NO^{2-}, and NO^{3-} concentrations (below limit od detection (LOD)). The average HCH, ClB, and ClPh concentrations in inflow water were 635.5 µg L^{-1}, 13 µg L^{-1}, and 115.5 µg L^{-1}, respectively (Figure 2).

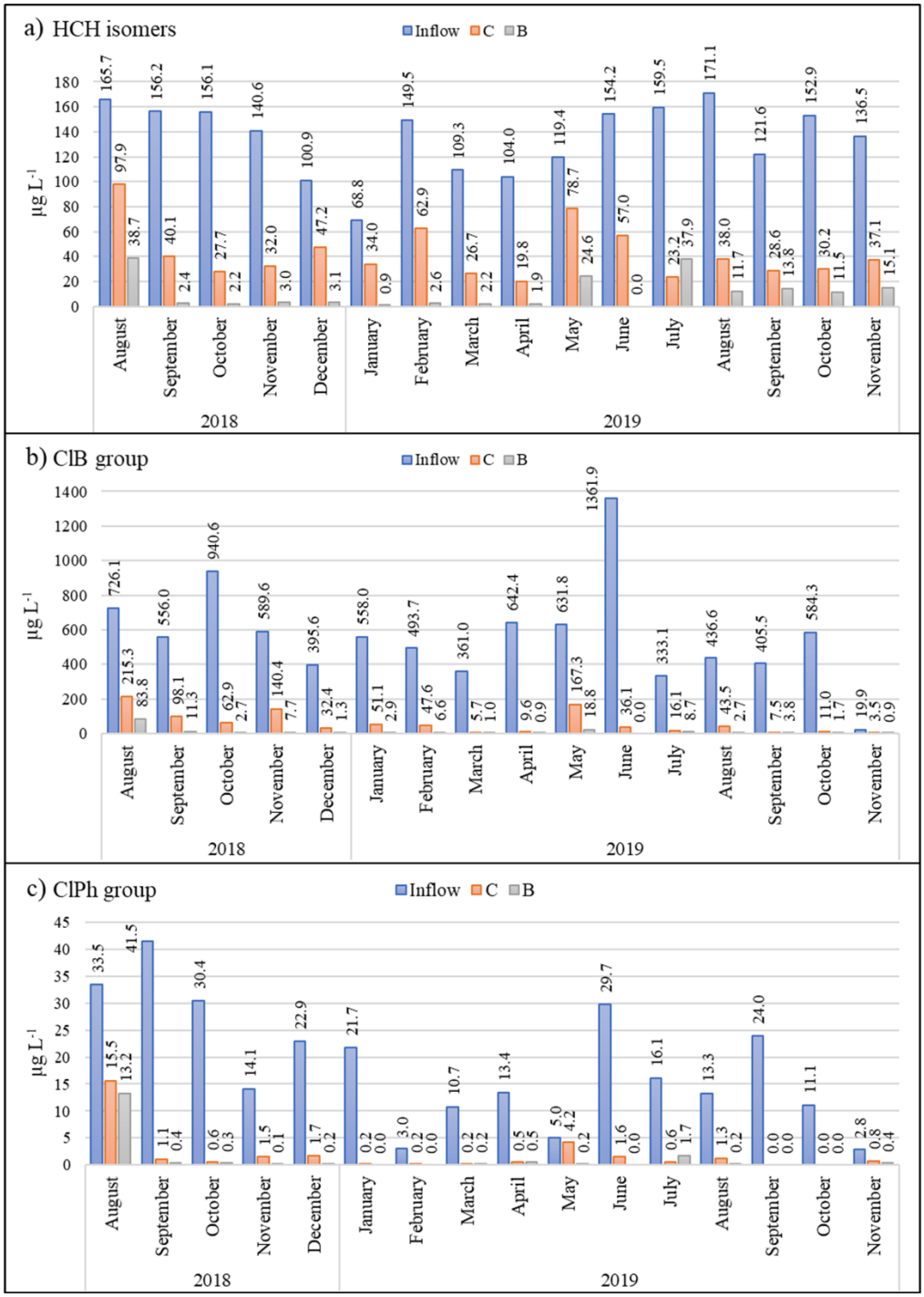

Figure 2. Monthly measurements of (a) HCH isomers (b) ClB, and (c) ClPh in polluted inflow water (blue), the control bed (C, orange), and the biochar test bed (B, gray) over the course of the experiment.

2.1 Pollutant removal efficiency

After passing through the biochar test bed, 90% of the HCH and other target pollutants had been removed from the drainage water (Figure 2). This already high efficiency was further increased to 96% after the initial high flow rate (15 L min^{-1}) had decreased to 5 L min^{-1}. In comparison, the classically

constructed control wetland bed with the clay/soil substrate removed around 80% of the HCH (Figure 2).

During analysis, the chemical compounds in outlet water samples of both wetland beds were divided into three main groups, i.e., ClB, ClPh, and HCH. Approximately 98% of the total concentration of the ClB group comprised 1.4-diClB > chlorobenzene > 1.3-diClB > 1.2.4-triClB > 1.2-diClB > 1.3.5-triClB, with benzene, 1.2.3-triClB, 1.2.4.5+1.2.3.5-tetraClB, 1.2.3.4-tetraClB, penta-ClB, and hexa-ClB found at < 1% of total concentration. In the ClPh group, approximately 89% of the total concentration was represented by 4-ClPh > 2-ClPh; 2.4+2.5-diClPh > 3-ClPh > 3.5-diClPh. Finally, the average percentage content of each HCH isomer in the HCH group was δ-HCH (76.1%), ε-HCH (10%), α-HCH (6.7%), γ-HCH (5.1%), and β-HCH (2.1%).

While we recorded no significant difference ($p > 0.05$) in outlet water ClB and ClPh concentrations between the control and biochar wetland beds, there was a significant difference in HCH concentration ($p < 0.01$), with an average difference in removal efficiency of 45.3% between the control and biochar beds (see Figure 2), clearly indicating biochar's greater ability to remove HCH.

In both the control bed and biochar bed, the degradation of pollutants is most likely to have resulted from microbial degradation, with biochar being the more successful of the two methods. Previous studies have shown that the organic pollutant removal efficiency (sorption rate) depends a great deal on its origin (harvest waste, wood, rice husk, sugar industry wastes, etc.), along with its surface area, porosity, hydrophobicity, polarity, and pyrolysis temperature (Ahmad et al., 2014; Ali et al., 2012). It has been shown, for example, that biochar's obtained at temperatures > 500℃ become less polar and more aromatic than those obtained at 300℃ due to the loss of O- and H-containing functional groups (Ahmad et al., 2014). Since the biochar used in this study was prepared at 570℃, this would suggest that it had a lower polarity surface and was more aromatic, resulting in decreased sorption.

2.2 HCH isomers

Concentration of the HCH isomers during experiment presented in Table 1. In the first month of the experiment, the total concentration of HCH in the biochar wetland bed decreased by 40.9%, compared with 76.6% in the control (Figure 2). A minor decrease was observed in β-HCH and ε-HCH for ten months in wetland beds. These two isomers are the most hydrophobic of all the HCH isomers analyzed (*log* K_{ow} 3.85 and 4.14, respectively), possibly explaining their low removal rate; however, their degradation rate could also have played a role. A previous study described the HCH isomer degradation rate as γ-HCH > α-HCH > δ-HCH > β-HCH (Buser and Mueller, 1995), which partly confirms our own

data. However, these authors did not analyze ε-HCH degradation times; hence, we would suggest an augmented sequence of γ-HCH > α-HCH > δ-HCH > β-HCH > ε-HCH. Removal of β-HCH and ε-HCH in the biochar bed had reached 91.8% by the fourth month, and continued to increase as time went on, while removal of the same two isomers in the control bed was the lowest than all other isomers, reaching just 60.9% and 20.1%, respectively, after ten months. Thus, the decrease of these compounds repeated the tendency of ClB. Interestingly, the decline in total HCH concentration in the control bed showed a non-linear trend, with percentage removal increasing from 40.9% to 82.2% over the first three months, then decreasing from 82.2% to 50.6% over the next four months, then increasing again from 50.6% to 81% over the next four months (Figure 2). This wave-like dynamic appeared to be dependent on monthly temperature differences, with temperatures ranging from 24.0°C to 13.0°C in the first quarter of the experiment, from 6.0°C to 0.7°C over the second quarter, and from -1.5°C to 5.5°C over the third quarter. In comparison, the concentration of α-HCH decreased by more than 99.7% in the biochar bed over the first ten months (except August), β-HCH by 88.5%, γ-HCH by 98.4% or they were not detected at all (α-HCH in 6 months, β-HCH and γ-HCH in 5 months). This peculiarity can be explained by the presence of *Sphingorhabdus* in the inflow water samples. The genus belongs to the *Sphingomonadaceae* family, which representatives are common in HCH-contaminated soils and able to transform the β-HCH and δ-HCH to the pentachlorocyclohexanols (*Sphingobium* sp., *S. indicum*, *S. japonicum*, and *S. francense*) (Nagata et al., 2007; Sharma et al., 2006; Verma et al., 2017).

Table 1. Concentration of HCH isomers during experiment (LOQ < 0.01 µg L-1).

Month		HCH isomers concentration, µg L^{-1}				
		α-HCH	**β-HCH**	**γ-HCH**	**δ-HCH**	**ε-HCH**
August, 2018	Inflow	14.0	2.8	15.1	118.3	15.5
	C	7.8	1.5	8.9	67.3	12.4
	B	3.6	0.8	3.9	26.4	4.1
September, 2018	Inflow	10.3	2.2	8.5	122.2	13.2
	C	1.2	1.5	1.3	23.6	12.5
	B	**< LOQ**	0.2	**< LOQ**	1.0	1.1
October, 2018	Inflow	7.4	1.6	3.8	131.0	12.3
	C	0.4	1.2	0.5	14.9	10.8
	B	**< LOQ**	**< LOQ**	**< LOQ**	1.2	1.0
November, 2018	Inflow	7.5	3.6	4.7	110.4	14.3
	C	0.9	2.1	0.7	16.7	11.6
	B	0.0	**< LOQ**	0.0	1.7	1.3
December, 2018	Inflow	5.2	1.4	2.1	79.8	12.4
	C	1.5	1.4	1.3	32.0	11.1
	B	**< LOQ**	0.2	**< LOQ**	1.9	1.1
January, 2019	Inflow	4.5	1.9	3.0	51.3	8.2
	C	1.1	1.3	1.0	22.6	8.0
	B	**< LOQ**	**< LOQ**	**< LOQ**	0.4	0.6
February, 2019	Inflow	8.6	2.6	6.3	117.7	14.3
	C	2.2	1.7	2.4	44.9	11.7
	B	**< LOQ**	0.3	0.1	1.5	0.7
March, 2019	Inflow	10.9	4.4	8.4	74.1	11.5
	C	0.7	1.7	0.8	14.6	8.8
	B	0.0	**< LOQ**	**< LOQ**	1.2	1.0
April, 2019	Inflow	8.1	2.4	7.4	76.1	10.1
	C	0.4	1.1	0.4	9.9	8.1
	B	**< LOQ**	0.2	0.1	0.7	1.0
May, 2019	Inflow	9.8	2.0	9.6	84.9	13.2
	C	6.1	1.4	6.5	53.4	11.3
	B	1.7	0.9	1.5	16.5	3.9

2.3 Chlorobenzenes

Concentration of the chlorobenzenes during experiment presented in Table 2. In the ClB group, the following dynamics was observed: starting from August the effieciency was by 99.5% and 96.6% in control and biochar wetland beds, respectively. Moreover, ClB were not detectable in all outflow water samples during the following ten months. The explanation of this pattern could be that chlorobenzene is less hydrophobic (*log* K_{ow} 2.84) and volatile within the ClB group. During the following months the most significant decrease in concentrations in all wetland beds was for 1.2-diClB (*log* K_{ow} 3.43) and 1.2.4-triClB (*log* K_{ow} 4.02), while a minor decrease was detected for 1.3-diClB (*log* K_{ow} is 3.53) and 1.3.5-triClB (*log* K_{ow} 4.19). Adsorption of organic compounds by biochar depends not only on the level of hydrophobicity but also on their polarity. Furthermore, there are two different mechanisms for the adsorption of two different types of compounds (polar and hydrophobic). Although the biochar applied to the restoration of the aquatic system was produced at 570℃ and became less polar and more aromatic, polar chemical compounds such as 1.2-diClB (0.91) (Wypych, 2001) and 1.2.4-triClB (0.98) (Arey et al., 2005) were better adsorbed by biochar. At the same time, the adsorption and removal of the less polar compounds such as 1.3-diClB (0.85) (Lamarche et al., 2001) and 1.3.5-triClB (0.7) (Chen et al., 2018) were relatively smaller. The first month of the experiment (August 21st, 2018) showed decreasing the total concentration of ClB in the control wetland bed by 70.4%, in B - by 88.5% (Figure 2). Pairwise comparison evidenced the difference between two wetland beds, and p-value was less than 0.001. Unlike biochar wetland bed, the decrease of ClB in the control wetland bed exceeded 90% only after four months (December 2018), and at the end of the experiment was 98.5%. This peculiarity can be explained by the drop-down in average monthly temperature from 24.0°C to 3.8°C and decreasing outflow rate (from 6.2 to 2.3 L min^{-1}). While in the biochar wetland bed, the decrease was more than 96% by the second month and at the end of the experiment almost reached 100% (99.9%).

Throughout the experiment, the behavior of 1.3.5-triClB in control wetland bed was interesting and might be explained by the fact that this compound is the most hydrophobic within the group (*log* K_{ow} is 4.19):

The decrease of 1.3.5-triClB concentration remained the smallest during whole period. Thus, it reduced the decrease percentage of the total concentration of ClB. From August to November, the decrease was oscillatory (58.2%, 28%, 57.4%, and 41%, respectively). From December (8.3%), its removal consistently increased and in April reached 84.4%. Therefore, soil and clay substrate are not suitable for natural attenuation of high concentrations of 1.3.5-triClB. The biochar wetland bed showed better efficiency 98.2% throughout the ten-month experiment.

Table 2. Concentration of Chlorobenzenes (ClBs) during experiment.

Month		Chlorobenzenes' concentration, µg L^{-1}										
		Benzene	**ClB**	**1.3-diCLB**	**1.4-diCLB**	**1.2-diCLB**	**1.3.5-triCLB**	**1.2.4-triCLB**	**1.2.3-triCLB**	**1.2.4.5+1.2.3.5-tetraCLB**	**1.2.3.4-tetraCLB**	**penta-CLB**
	LOQ	**< 1**	**< 0.2**	**< 0.005**	**< 0.005**	**< 0.005**	**< 0.005**	**< 0.005**	**< 0.005**	**< 0.015**	**< 0.01**	**< 0.015**
August, 2018	Inflow	4.8	268.0	57.9	260.7	62.7	9.2	43.2	18.5	0.6	0.4	**< LOQ**
	C	**< LOQ**	1.3	26.9	128.6	27.1	3.9	19.1	8.0	0.3	0.2	**< LOQ**
	B	**< LOQ**	9.2	10.7	37.3	11.8	1.9	9.8	3.0	0.1	0.1	**< LOQ**
September, 2018	Inflow	**< LOQ**	23.2	129.3	120.5	102.6	19.2	139.1	17.2	2.9	1.7	0.4
	C	**< LOQ**	**< LOQ**	33.5	20.2	8.9	13.8	9.6	11.2	0.3	0.6	**< LOQ**
	B	**< LOQ**	**< LOQ**	0.6	0.6	1.6	**< LOQ**	6.4	2.1	**< LOQ**	**< LOQ**	**< LOQ**
October, 2018	Inflow	1.0	143.0	168.4	415.0	81.4	41.6	70.9	4.6	9.6	2.8	2.3
	C	**< LOQ**	**< LOQ**	22.8	14.6	2.3	17.7	1.4	2.2	0.5	0.8	0.6
	B	**< LOQ**	**< LOQ**	0.4	0.6	1.1	0.2	**< LOQ**	0.4	**< LOQ**	**< LOQ**	**< LOQ**
November, 2018	Inflow	**< LOQ**	**< LOQ**	328.1	**< LOQ**	75.3	50.9	114.0	3.2	10.2	3.9	4.1
	C	**< LOQ**	**< LOQ**	92.2	1.3	3.6	30.1	7.6	2.1	0.9	1.5	1.2
	B	**< LOQ**	**< LOQ**	0.4	0.5	3.6	0.2	2.5	0.4	**< LOQ**	0.0	0.1
December, 2018	Inflow	**< LOQ**	101.0	44.5	170.7	35.2	5.0	37.8	0.4	0.6	0.3	**< LOQ**
	C	**< LOQ**	**< LOQ**	21.0	2.3	1.6	4.6	2.2	0.4	**< LOQ**	0.2	**< LOQ**
	B	**< LOQ**	**< LOQ**	0.1	**< LOQ**	0.6	0.1	0.4	0.1	**< LOQ**	**< LOQ**	**< LOQ**
January, 2019	Inflow	**< LOQ**	25.0	87.2	313.4	45.1	16.3	64.1	2.8	1.6	2.1	0.4
	C	**< LOQ**	**< LOQ**	21.6	8.5	3.2	8.9	6.7	1.3	**< LOQ**	0.7	0.3
	B	**< LOQ**	**< LOQ**	0.1	**< LOQ**	0.2	0.2	2.5	**< LOQ**	**< LOQ**	**< LOQ**	**< LOQ**
February, 2019	Inflow	**< LOQ**	93.0	55.0	251.5	45.3	6.9	36.9	4.0	0.4	0.7	**< LOQ**
	C	**< LOQ**	**< LOQ**	19.3	6.8	7.2	3.1	9.5	1.2	0.1	0.4	**< LOQ**
	B	**< LOQ**	**< LOQ**	0.2	0.4	1.0	0.2	4.8	**< LOQ**	**< LOQ**	**< LOQ**	**< LOQ**
March, 2019	Inflow	3.0	136.0	32.8	111.1	27.0	3.7	37.4	3.2	0.5	0.8	**< LOQ**
	C	**< LOQ**	**< LOQ**	2.9	0.5	**< LOQ**	1.4	0.2	0.5	**< LOQ**	0.2	**< LOQ**
	B	**< LOQ**	**< LOQ**	0.1	0.1	**< LOQ**	**< LOQ**	0.7	0.0	**< LOQ**	**< LOQ**	**< LOQ**
April, 2019	Inflow	10.7	341.5	37.7	115.7	26.3	7.4	94.1	7.1	0.8	0.8	0.4
	C	**< LOQ**	**< LOQ**	4.2	2.9	1.2	1.2	**< LOQ**	0.2	**< LOQ**	**< LOQ**	**< LOQ**
	B	**< LOQ**	**< LOQ**	0.1	0.1	0.4	0.2	0.2	**< LOQ**	**< LOQ**	**< LOQ**	**< LOQ**
May, 2019	Inflow	8.4	214.4	45.6	203.8	38.9	8.1	101.6	10.0	0.5	0.5	**< LOQ**
	C	**< LOQ**	**< LOQ**	29.7	56.8	18.1	5.1	50.8	6.3	0.3	0.3	**< LOQ**
	B	**< LOQ**	**< LOQ**	3.04	8.49	1.83	0.54	4.4	0.53	**< LOQ**	**< LOQ**	**< LOQ**

2.4 Chlorophenols

Concentration of the chlorophenols during experiment presented in Table 3. Five dominant compounds (2-ClPh, 3-ClPh, and 2.4+2.5-ClPh) represent the group of detected ClPh. Total concentration of ClPh in control wetland bed decreased within the first month by 53.9% and by 60.8% in biochar wetland (Figure 2). During the following ten months, the decrease of ClPh total concentration was not lower than 89.7% in the control and 96.4% in the biochar wetland. The smallest decrease was observed for 4-ClPh being the only detected ClPh from September in biochar wetland with the exception in January and February - in these months, it was not detected at all. This tendency can be also explained by the polarity/polarizability level (π) and volatility of the compounds: 4-ClPh is a less polar contaminant within the group (0.72), while the π values of 2-ClPh, 3-ClPh, and 2.4+2.5-ClPh are 0.82, 0.77 and 0.87, respectively (Marcus, 1991; Yang et al., 2008).

Table 3. Concentration of Chlorophenols (ClPhs) during experiment.

Month		Chlorophenols' concentration, µg L^{-1}														
		2-ClPh	3-ClPh	4-ClPh	2.3-diClPh	2.4+2.5-diClPh	2.6-diClPh	3.4-diClPh	3.5-diClPh	2.3.5+2.3.4-triClPh	2.3.6-triClPh	2.4.5-triClPh	2.4.6-triCLF	3.4.5-triCLF	2.3.4.5+2.3.4.6-tetraCLF	2.3.5.6-tetraCLF	PentaCLF
	LOQ	**< 0.025**	**< 0.025**	**< 0.025**	**< 0.025**	**< 0.05**	**< 0.025**	**< 0.025**	**< 0.025**	**< 0.05**	**< 0.025**	**< 0.025**	**< 0.025**	**< 0.025**	**< 0.05**	**< 0.025**	**< 0.025**
August, 2018	Inflow	8.4	2.6	6.9	0.3	7.9	**< LOQ**	0.6	1.3	2.2	0.6	0.7	0.2	**< LOQ**	1.8	**< LOQ**	**< LOQ**
	C	4.0	0.9	3.5	**< LOQ**	3.4	**< LOQ**	0.2	0.8	1.1	0.3	0.3	**< LOQ**	**< LOQ**	1.0	**< LOQ**	**< LOQ**
	B	3.2	0.9	5.4	**< LOQ**	1.8	**< LOQ**	**< LOQ**	0.5	0.6	0.2	0.2	**< LOQ**	**< LOQ**	0.5	**< LOQ**	**< LOQ**
September, 2018	Inflow	7.2	4.2	21.9	0.1	4.5	**< LOQ**	0.4	1.9	0.7	**< LOQ**	0.3	**< LOQ**	**< LOQ**	0.4	**< LOQ**	**< LOQ**
	C	**< LOQ**	**< LOQ**	0.4	**< LOQ**	**< LOQ**	**< LOQ**	**< LOQ**	0.7	**< LOQ**	**< LOQ**	**< LOQ**	**< LOQ**	**< LOQ**	**< LOQ**	**< LOQ**	**< LOQ**
	B	**< LOQ**	**< LOQ**	0.4	**< LOQ**	**< LOQ**	**< LOQ**	**< LOQ**	**< LOQ**	**< LOQ**	**< LOQ**	**< LOQ**	**< LOQ**	**< LOQ**	**< LOQ**	**< LOQ**	**< LOQ**
October, 2018	Inflow	2.7	1.8	13.5	**< LOQ**	2.9	8.1	0.2	0.7	0.4	**< LOQ**	0.2	**< LOQ**	**< LOQ**	**< LOQ**	**< LOQ**	**< LOQ**
	C	**< LOQ**	**< LOQ**	0.3	**< LOQ**	**< LOQ**	0.3	**< LOQ**	**< LOQ**	**< LOQ**	**< LOQ**	**< LOQ**	**< LOQ**	**< LOQ**	**< LOQ**	**< LOQ**	**< LOQ**
	B	**< LOQ**	**< LOQ**	0.3	**< LOQ**	**< LOQ**	**< LOQ**	**< LOQ**	**< LOQ**	**< LOQ**	**< LOQ**	**< LOQ**	**< LOQ**	**< LOQ**	**< LOQ**	**< LOQ**	**< LOQ**
November, 2018	Inflow	0.1	0.1	0.1	0.0	1.5	4.2	0.5	5.2	0.3	0.2	0.3	0.2	0.1	0.4	0.1	0.8
	C	**< LOQ**	**< LOQ**	0.1	0.0	0.2	0.6	0.0	0.3	**< LOQ**	**< LOQ**	0.1	**< LOQ**	0.0	**< LOQ**	**< LOQ**	0.1
	B	**< LOQ**	**< LOQ**	0.1	**< LOQ**	**< LOQ**	0.0	**< LOQ**	**< LOQ**	**< LOQ**	**< LOQ**	**< LOQ**	**< LOQ**	**< LOQ**	**< LOQ**	**< LOQ**	**< LOQ**
December, 2018	Inflow	0.8	1.8	17.4	**< LOQ**	2.0	0.2	**< LOQ**	0.7	**< LOQ**	**< LOQ**	**< LOQ**	**< LOQ**	**< LOQ**	**< LOQ**	**< LOQ**	**< LOQ**
	C	**< LOQ**	**< LOQ**	0.2	**< LOQ**	0.5	**< LOQ**	**< LOQ**	0.8	**< LOQ**	**< LOQ**	0.2	**< LOQ**	**< LOQ**	**< LOQ**	**< LOQ**	**< LOQ**
	B	**< LOQ**	**< LOQ**	0.2	**< LOQ**	**< LOQ**	**< LOQ**	**< LOQ**	**< LOQ**	**< LOQ**	**< LOQ**	**< LOQ**	**< LOQ**	**< LOQ**	**< LOQ**	**< LOQ**	**< LOQ**
January, 2019	Inflow	**< LOQ**	8.5	10.0	**< LOQ**	0.6	1.4	**< LOQ**	**< LOQ**	**< LOQ**	**< LOQ**	**< LOQ**	1.2	**< LOQ**	**< LOQ**	**< LOQ**	**< LOQ**
	C	**< LOQ**	**< LOQ**	**< LOQ**	**< LOQ**	**< LOQ**	0.2	**< LOQ**	**< LOQ**	**< LOQ**	**< LOQ**	**< LOQ**	**< LOQ**	**< LOQ**	**< LOQ**	**< LOQ**	**< LOQ**
	B	**< LOQ**	**< LOQ**	**< LOQ**	**< LOQ**	**< LOQ**	**< LOQ**	**< LOQ**	**< LOQ**	**< LOQ**	**< LOQ**	**< LOQ**	**< LOQ**	**< LOQ**	**< LOQ**	**< LOQ**	**< LOQ**
February, 2019	Inflow	0.6	0.4	1.2	**< LOQ**	0.8	**< LOQ**	**< LOQ**	**< LOQ**	**< LOQ**	**< LOQ**	**< LOQ**	**< LOQ**	**< LOQ**	**< LOQ**	**< LOQ**	**< LOQ**
	C	**< LOQ**	**< LOQ**	**< LOQ**	**< LOQ**	**< LOQ**	**< LOQ**	**< LOQ**	0.2	**< LOQ**	**< LOQ**	**< LOQ**	**< LOQ**	**< LOQ**	**< LOQ**	**< LOQ**	**< LOQ**
	B	**< LOQ**	**< LOQ**	**< LOQ**	**< LOQ**	**< LOQ**	**< LOQ**	**< LOQ**	**< LOQ**	**< LOQ**	**< LOQ**	**< LOQ**	**< LOQ**	**< LOQ**	**< LOQ**	**< LOQ**	**< LOQ**
March, 2019	Inflow	0.6	0.7	7.1	**< LOQ**	1.3	**< LOQ**	**< LOQ**	0.3	0.2	**< LOQ**	**< LOQ**	**< LOQ**	**< LOQ**	0.2	**< LOQ**	0.3
	C	**< LOQ**	**< LOQ**	0.2	**< LOQ**	**< LOQ**	**< LOQ**	**< LOQ**	**< LOQ**	**< LOQ**	**< LOQ**	**< LOQ**	**< LOQ**	**< LOQ**	**< LOQ**	**< LOQ**	**< LOQ**
	B	**< LOQ**	**< LOQ**	0.2	**< LOQ**	**< LOQ**	**< LOQ**	**< LOQ**	**< LOQ**	**< LOQ**	**< LOQ**	**< LOQ**	**< LOQ**	**< LOQ**	**< LOQ**	**< LOQ**	**< LOQ**
April, 2019	Inflow	1.5	1.6	7.0	**< LOQ**	1.7	**< LOQ**	**< LOQ**	0.5	0.4	**< LOQ**	0.3	**< LOQ**	**< LOQ**	**< LOQ**	**< LOQ**	0.5
	C	**< LOQ**	**< LOQ**	0.5	**< LOQ**	**< LOQ**	**< LOQ**	**< LOQ**	**< LOQ**	**< LOQ**	**< LOQ**	**< LOQ**	**< LOQ**	**< LOQ**	**< LOQ**	**< LOQ**	**< LOQ**
	B	**< LOQ**	**< LOQ**	0.5	**< LOQ**	**< LOQ**	**< LOQ**	**< LOQ**	**< LOQ**	**< LOQ**	**< LOQ**	**< LOQ**	**< LOQ**	**< LOQ**	**< LOQ**	**< LOQ**	**< LOQ**
May, 2019	Inflow	0.4	0.3	2.8	**< LOQ**	0.7	**< LOQ**	**< LOQ**	0.3	0.3	**< LOQ**	**< LOQ**	**< LOQ**	**< LOQ**	**< LOQ**	**< LOQ**	0.3
	C	**< LOQ**	**< LOQ**	**< LOQ**	**< LOQ**	0.7	**< LOQ**	0.2	2.9	**< LOQ**	**< LOQ**	0.3	**< LOQ**	**< LOQ**	**< LOQ**	**< LOQ**	0.2
	B	**< LOQ**	**< LOQ**	**< LOQ**	**< LOQ**	**< LOQ**	**< LOQ**	**< LOQ**	0.2	**< LOQ**	**< LOQ**	**< LOQ**	**< LOQ**	**< LOQ**	**< LOQ**	**< LOQ**	**< LOQ**

2.5 Microbial community structure and function

The microbial community was analyzed in samples from inflow, control, and biochar wetland beds in September 2018 and November 2019. Sediments for molecular biology analyses were taken from both wetland beds.

The relative representation of microorganisms at the family level is shown in Figure 3. The dominant families in inflow water was *Flavobacteriaceae* together with *Sporithyaceae* and *Comamonadaceae*. Population of *Flavobacterium* reached 26.1% of total biomass in the inflow, while in outflow water from control wetland bed its percentage decreased to 0.3% and from biochar wetland bed it was as low as 0.1%. *Flavobacterium* might be well adapted to higher HCH concentrations due to its possible ability to degrade high concentrations of tech-HCH (25 mg kg^{-1}) in a microbial consortium containing *Pseudomonas* spp., *Burkholderia*, and *Vibrio* (Murthy and Manonmani, 2007).

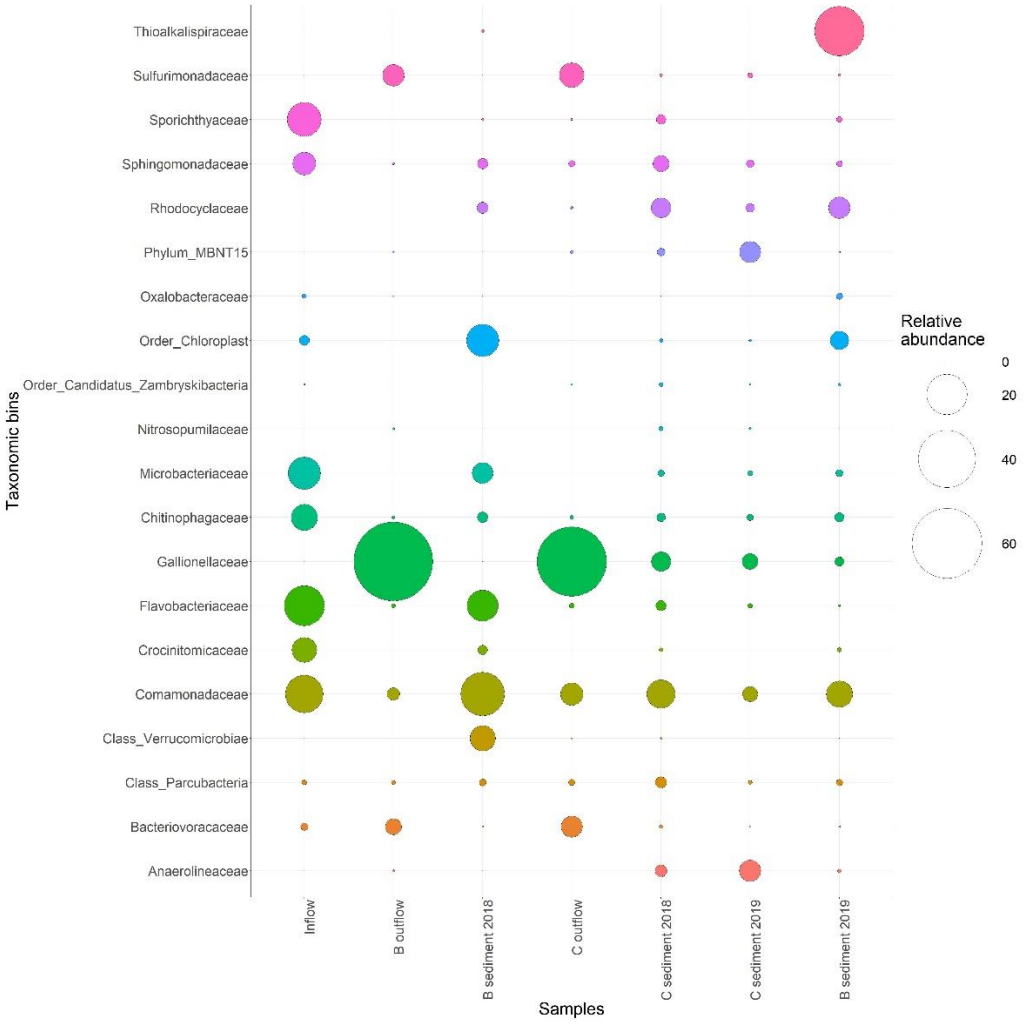

Figure 3. Relative abundance (> 5%) of microorganisms (family level) in water and sediment samples. B = biochar test bed, C= control bed.

Gallionellaceae family dominated water outflow samples of control and biochar wetland beds (71.2% and 84.6%, respectively) in September 2018, most probably due to high level of Fe^{2+} in the inflow water. *Gallionella*, *Geobacter*, and *Sulfuricurvum* appeared only in outflows due to a decrease in the pollutant's total concentration. The genus *Gallionella* is characterized by its chemolithotrophic growth with ferrous iron as a donor of electrons. Chemical dichloroelimination of γ-HCH is relatively pH insensitive and can be mediated by iron sulfides (FeS) and activated carbon to generate di- and trichlorobenzene isomers as end products. Liu et al. (Liu et al., 2003) reported that the reducing agent FeS enhanced elimination of γ-HCH at a concentration of 10 g L^{-1}.

The abundance of microorganisms in the control wetland bed was very diverse in sediment and water samples (September 2018). In the sediment sample, there was detected aryl-halorespiring facultative anaerobic myxobacterium – *Anaeromyxobacter* while in the water the dominant genus was *Sideroxydans* that is able to oxidize Fe^{2+}(Liu et al., 2012). Abundance of the microbial community changed dramatically after one year. The presence of *Gallionella* increased from 0.9% to 5% in sediment samples in the control wetland bed. For the biochar wetland bed, *Gallionella* was not detected in sediment samples in 2018, while in 2019, it increased to 1.2%. The abundance of the rest microbial populations was different between the years. Sediment of the biochar wetland bed hosted more *Rhodocyclaceae* (7.1%) than of the control wetland bed (1.5%). Dadwhal et al. (Dadhwal et al., 2009) isolated *Rhodocyclaceae* from HCH contaminated soil and suggested that members of this family might be involved in the removal of HCH.

Spearman correlation analysis demonstrated correlation between several families and chemical compounds (Figure 4). *Parcubacteria* and *ZhambryskiiBacteria* families negatively correlated with 2.6-diClPh and 2.3.6-triClPh ($p < 0.05$). *Nitrosarchaeum* has a stronger negative correlation with the above compounds ($p < 0.01$) while its correlation with 2.3-diClPh and 2.4.5-triClPh was significant but weaker ($p < 0.05$). *Rhodoferax* family negatively correlated with ClB and 4-ClPh ($p < 0.05$). Thus, all detected correlations were negative and three of five families correlate with the 2.6-diClPh and 2.3.6-triClPh. Interestingly, three bacterial groups positively (although not significantly) correlated with all targeted pollutants. *Candidatus Aquiluna* (*Microbacteriaceae)* was reported from wide range of aquatic habitats from freshwaters to hypersaline waters (Leoni et al., 2020). *Hgcl clade (Actinobacteria)* associated with soil and eutrophic waters is being able to use organic compounds for their metabolism and most importantly *Sphingorhabdus* that is able to metabolize HCH.

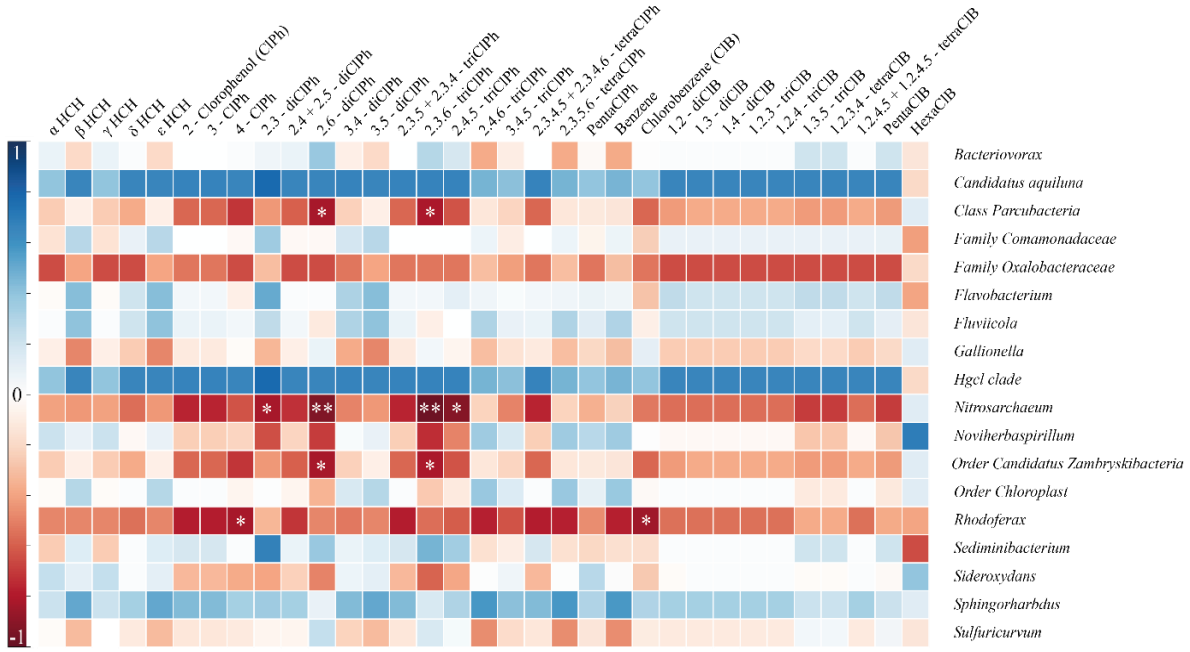

Figure 4. Spearman correlation between relative taxa abundance and chemical compounds. *** p < 0.001, ** p < 0.01, * p < 0.05

2.6 Functional genes involved in HCH biodegradation

The functional genes *linA*, *linB*, *linB-RT*, and *linD* encoding enzymes involved in aerobic and anaerobic *γ*-HCH biodegradation were detected in all sediment samples except those taken from the freshly installed biochar wetland bed in 2018 (Table 4), suggesting that the microbial community was still not well developed one month after installation. In comparison, the highest levels of *U16SRT*, *linA*, *LinB-RT*, and *LinD genes* were detected in sediment from the control bed in 2018. By 2019, however, the situation had switched, with However, it was the opposite in samples from the same wetland bed in 2019 except for *U16SRT* gene. There is clear experimental evidence that *linA* encodes enzyme that dehydrochlorizes γ-, α- and δ-HCH, while *linB* hydrolytically dechlorines β- and δ-HCH in all strains studied (Lal et al., 2010). Within HCH isomers, the γ-HCH displaying the fastest degradation rate.

linB gene was detected in high amounts in all samples except in early biochar samples from 2018. The highest amount of this gene was in sediment samples from biochar wetland bed in 2019. The highest amount of the *linB-RT* gene was found in sediment samples from the control wetland bed in 2018 and sediment from biochar wetland bed in 2019. In 2018 *linD* genes were highest in sediment samples taken from the control wetland bed, but in 2019 the amount is decreased, unlike in biochar wetland bed, is highest quantity. *linD* encoding reductive dechlorinase was first isolated from *Sphingobium japonica* UT26 (Miyauchi et al., 1998). Dehalogenation of HCH isomers and byproducts is also a significant reaction. *linB* and *linB-RT* encode haloalkane dehalogenase and catalyzes the HCH hydrolytic

dechlorination of 1.4-TCDN to 2.5-DDOL (Nagata et al., 1993).

Overall, in 2019, *lin* genes were found in all samples, and the maximum amount was found in samples taken from the biochar wetland bed in 2019. Therefore, the removal of HCH isomers and their byproducts was not driven by sorption on biochar but by biodegradation.

Table 4. Relative abundance of genes indicating total bacterial biomass (U16SRT), dehydrochlorinase (linA), haloalkane dehalogenase (linB, linB-RT), and reductive dechlorinase (linD) in the control wetland bed (C, average of duplicate samples) and biochar sediments (B, average of duplicate samples). The color scale indicates the relative quantity of a given marker: red (+++) highest, orange (++) high, and yellow (+) intermediate quantity, ND = not detected or below the LOQ.

		gene				
Wetland bed		U16SRT	linA	linB	linB-RT	linD
2018	C	+++	+++	++	+++	+++
	B	+	ND	ND	ND	ND
2019	C	+++	++	++	++	++
	B	+++	+++	+++	+++	+++

3. Summary

In this study, we compared efficiency of HCH and related compounds removal in biochar wetland bed and control wetland bed at historically polluted site. Biochar wetland bed was more efficient (98.2%) in the removal of HCH than control wetland (81.0%), whereas higher efficiency was reached at a lower inflow water rate.

The interesting point is that the chemical analysis of biochar showed the absence of any adsorbed HCH-related compounds. It can be therefore assumed that there were microorganisms able to degrade HCH, ClB, and ClPh. Analysis of sediment samples taken at the end of the study confirmed the presence of functional genes and bacterial genera capable of degrading HCH isomers and their byproducts. Most were detected in the lower part of the biochar wetland bed and the control wetland bed. In control wetland bed, the abundance of functional genes encoding key enzymes involved in the degradation of HCH isomers and their byproducts under aerobic conditions was significantly reduced after a year. At the end of the study, ClB and ClPh removal reached 98.5% and 96.0% in control and 99.9% and 96.4% in biochar wetland bed respectively. Therefore, for these groups of compounds, there was no significant improvement when using biochar.

The main advantage of a biochar wetland bed is its simplicity, effectivity and speed of its installation in

the field. In contrast to wetland bed modules with surface vegetation, a high-water purification function is immediately achieved. This may encourage the use of biochar beds, for example, for temporary installations for water purification during the construction of other wastewater treatment technologies as final solutions at contaminated sites.

II. Wetland+ system

1. Materials and methods

1.1 Site Description and Experimental Design

This study took place in Hajek, Czech Republic (50°17′31.5″ N 12°53′35.2″ E). Details are described in the section 1.1 of *I. HCH Removal in constructed wetland beds*. The Wetland+ system was installed in September 2021. It consists of the following parts, connected in series: an aeration and sedimentation module (A), a permeable reactive barrier (B), a biosorption module (C), and an aerobic wetland system (D) (Figure 5). The aeration and sedimentation module (A) consist of three compartments connected in series of an area of 313 m^2 to enhance precipitation and sedimentation of dissolved iron, which is at a relatively high concentration in the inflow water (see below). The next module (B) of an area of 540 m^2, with the total volume of the module of 360 m^3 is filled with zerovalent iron (ZVI) chips. Here, a part of HCH is transformed to ClB by dehalogenation due to strong anaerobic conditions. The B module consists of six compartments B1–B6. The individual compartments are interconnected in three parallel branches and each branch consists of two compartments connected in series. The water flows through this system in a longitudinal direction, where the inflow is introduced beneath the surface of the layer of iron chips and the outflow is collected at the bottom by a perforated pipe located in the central longitudinal axis of the B module. Following is the C module, where a mix of gravel, soil, peat, and wooden chips form a bed. This biosorption module consists of two compartments with parallel connections, the total volume of the reactor is 480 m^3. Common wetland species (*Phragmites* sp. and *Phalaris* sp.) were planted in the C module at a density of 4 plants m^{-2} in a total area of 650 m^2. Splitting of the flow in B and C modules enables to refill of the substrate without any break in the system's operation. The final treatment takes place in module D, a surface flow aerobic wetland with an area of 2,669 m^2, and a total aerobic wetland volume: of 1,600 m^3. This stage serves for the final removal of organic substances, suspended solids and the decomposition products of HCH, especially ClB. This aerobic wetland is filled with soil/gravel and planted with common wetland species (*Typha* spp., *Spargamium erectum, Juncus* spp., *Glyceria fluitans*) enriched by rare and protected species supplied by the local botanical garden (Dalovice) and from nearby natural reserves, such as *Hippuris vulgaris,*

Calla palustris, or *Menyanthes trifoliata*. Part of the D area was left unplanted for testing purposes to observe the spontaneous succession of wetland plants from natural seed. In contrast to previous modules, in module D, aerobic transformation pathways of HCH and ClB are employed by bacterial enzymes, in addition to adsorption and bioaccumulation.

Figure 5. Wetland+ modules. The inlet (S), aeration system including sedimentation (A), permeable reactive barrier remedial system (B), biosorption module (C), and aerobic wetland system (D).

1.2 Sampling

The water samples for chemical analyses and biology analyses (i.e., amplicon 16S rRNA sequencing, qPCR; see below) were collected from outflows of each Wetland+ module. Physical-chemical

parameters of water (temperature, pH, electrical conductivity, redox potential and dissolved oxygen concentration) were measured using Multi 3430 SET C (WTW, Weilheim, Germany) directly on site. All samples were transported to the laboratory in a cooled box, water samples for molecular biology analysis were immediately filtered through a sterile 0.2 µm membrane filter and stored at −80 °C.

1.3 Physical and chemical analysis

Concentrations of HCH isomers and their ClB and ClPh byproducts in water were determined According to a previous study, the concentration of HCH isomers and their ClB and ClPh byproducts in water were determined using two GC-MS assemblies (Wacławek et al., 2019). The first used an RSH/Trace 1310/TSQ 8000 GC-MS array (ThermoFisher Scientific, USA) with a Scion-5MS column for HCH, ClB and ClPh (Scion Instruments, Goes, The Netherlands), whereas the other was based on a CombiPal/CP3800/Saturn2200 GC-MS array (PAL, Zwingen, Switzerland; Varian, Palo Alto, USA) using a DB-624 column for benzene and monochlorobenzene determination (Agilent, Santa Clara, USA). Samples were extracted using the headspace SPME technique, either using a PDMS/DVB fiber with a coating thickness of 100 µm (Supelco, Bellefonte, USA) or directly injecting the sample in static headspace mode. Prior to extraction, samples were derivatized to form acetylated chlorophenols (following EN 12673). Isotopically labelled compounds (γ-HCH D6, pentachlorophenol 13C6) were used as internal GC-MS/MS analysis standards.

1.4 Molecular biology and bioinformatic analysis

DNA extraction, real-time qPCR and amplicon 16s rRNA sequencing were described in previous study in the section 1.5 Molecular genetic analysis of *I. HCH Removal in constructed wetland beds*. The obtained data were processed with QIIME 2 2021.8 software (Bolyen et al., 2019). Raw sequence data were demultiplexed and quality filtered using the q2-demux plugin followed by denoising with DADA2 (via q2-dada2) (Callahan et al., 2016). Taxonomy was assigned to ASVs (Amplicon Sequence Variant) using the q2-feature-classifier (Bokulich et al., 2018), and classified by classify-sklearn naïve Bayes against the Silva 138 database (Quast et al., 2013) and then mitochondria and chloroplast were removed. The accuracy of classification was evaluated against an artificial MOCK community sample. QIIME 2 outputs were processed using the phyloseq R package (McMurdie and Holmes, 2013).

1.5 HCH and ClB removal efficiency

The overall removal efficiency of the Wetland+ treatment system was calculated from the difference in HCH or ClB concentration in inflow water (S) and outflow water (D). The removal efficiency of individual modules of the system was calculated from the difference in pollutant concentrations in inflow and outflow to/from the respective module. The average removal efficiency was calculated as the arithmetic mean of efficiency values from the 12 different sampling campaigns performed in the period September 2021–September 2022.

2. Results

2.1 General Characteristics of Inflow Water

The inflow drainage water (S) had a long-term average pH value of 6.6, with average conductivity of 1719 µS cm^{-1}, redox potential l,182 mV (original S water is anoxic with a low redox potential, but due to contact with atmosphere the redox and oxygen content increases), high sulfate concentration 598 mg L^{-1}, high total Fe concentration 24.3 mg L^{-1}, and low F^-, NO_2^-, and NO_3^- concentrations (below LOD). Average concentrations of HCH and ClB in inflow water were 136.2 and 604.6 µg L^{-1}, respectively, with the average flow of approx. 2 $L.s^{-1}$. The physicochemical parameters of water are given in Table 5.

Table 5. Physicochemical parameters of inflow and outflow water from individual modules of Wetland+

Module	pH	Eh	O_2
	[-]	[mV]	[mg/l]
S (inflow)	6.6	182	2.65
A	6.7	283	4.26
B	7.2	110	2.76
C	7.3	187	7.00
D	7.4	356	9.00

2.2 Pollutant Removal Efficiency

The average removal efficiencies of individual modules are given in Table 6.

Table 6. Average removal efficiency of individual modules and of the whole Wetland+ treatment system in the period September 20021 – September 2022

Module	∑HCH	∑ClB
A	3.9%	34.3%
B	45.0%	94.7%
C	21.2%	53.1%
D	37.3%	74.0%
Whole system	81.7%	96.8%

In total, 5.9 kg of HCH and 26.0 kg of ClB were eliminated from the drainage water within the 12-month operation of the system. Individual HCH isomers were not removed evenly but followed the pattern: $\alpha = \gamma = \delta > \varepsilon = \beta$. As a result, while δ-HCH dominated at the inflow to the system covering more than 60% of the total HCH concentration, ε-HCH prevailed at the outflow from the system.

Approximately 98% of the inflow total concentration of the ClB group comprised 1.4-diClB > 1.3-diClB > 1.2.4-triClB > 1.2-diClB > 1.3.5-triClB with 1.2.3-triClB, 1.2.4.5+1.2.3.5-tetraClB, 1.2.3.4-tetraClB, penta-ClB, and hexa-ClB found at <1% of the total concentration. The removal of individual di-ClB compounds by the treatment system was more intensive than tri-ClB compounds, thus their mutual ratio in the outflow balances out.

2.3 Functional Genes Involved in HCH Biodegradation

The functional genes *linA*, *linB, linB-RT,* and *linD* encoding enzymes involved in aerobic HCH biodegradation were detected in all samples (Table 7). The highest level of the *U16SRT* gene, representing the total microbial biomass, was detected in the outlet from the aerobic wetland (module D). The relative abundance of the *linA*, *linB-RT*, and *linD* genes was the highest in the outlet. The quantity of the *lin* genes in the samples from modules S, A and B was similarly low, but in samples from module C were *lin* genes elevated.

The highest relative abundance of *Dehalococcoides* spp. (DHC), was found in the inflow water (profile S) and in modules A and B. In direction of water flow (modules C and D), the abundance of DHC was decreasing.

Table 7. Relative abundance of *Dehalococcoides* spp. and genes indicating total bacterial biomass (16S rDNA), dehydrochlorinase (*linA*), haloalkane dehalogenase (*linB, linB-RT*), and reductive dechlorinase (*linD*) in individual modules of Wetland+. The color scale indicates the relative quantity of a given marker: red (+++) highest, orange (++) high, yellow (+) intermediate quantity, (+-) low quantity, ND = not detected or below the LOQ.

	Total bacterial biomass	**organohalide respiring bacteria**	**Lindane-degrading bacteria**			
	16S rDNA	*Dehalococcoides* spp.	dehydrochlorinase	haloalkane dehalogenase	haloalkane dehalogenase	reductive dechlorinase
	U16SRT	**DHC**	**linA**	**linB**	**linB-RT**	**linD**
S	++	+++	+	+	+	+
A	+	+++	+	+	+	+
B	++	+++	+++	+	++	++
C	++	++	+++	++	++	++
D	+++	+	+++	+++	+++	+++

2.4 Microbial abundance

The microbial profile demonstrates the high abundance bacteria belonging to genus *Galionella* and *Canditatus Omnitrophus* but with decreasing trend to the end of the wetland system (Figure 6). The D module were rich on bacteria of genera *Massilia, Rhodoferax, Hydrogenophaga, Flavobacterium, Caulobacter* and *Bacteriovorax* comparing to another modules. The abundance bacteria of the sulfate-reducing genera *Desulfovibrio* and *Desulfosporosinus* was found is become higher elevated in all module's profiles except for the inlet water S and A module. The abundance of the family *Oxalobacteraceae*, family *Comamonadaceae* and *Pseudarcobacter* increased in modules C1, C2 and D comparing to other.

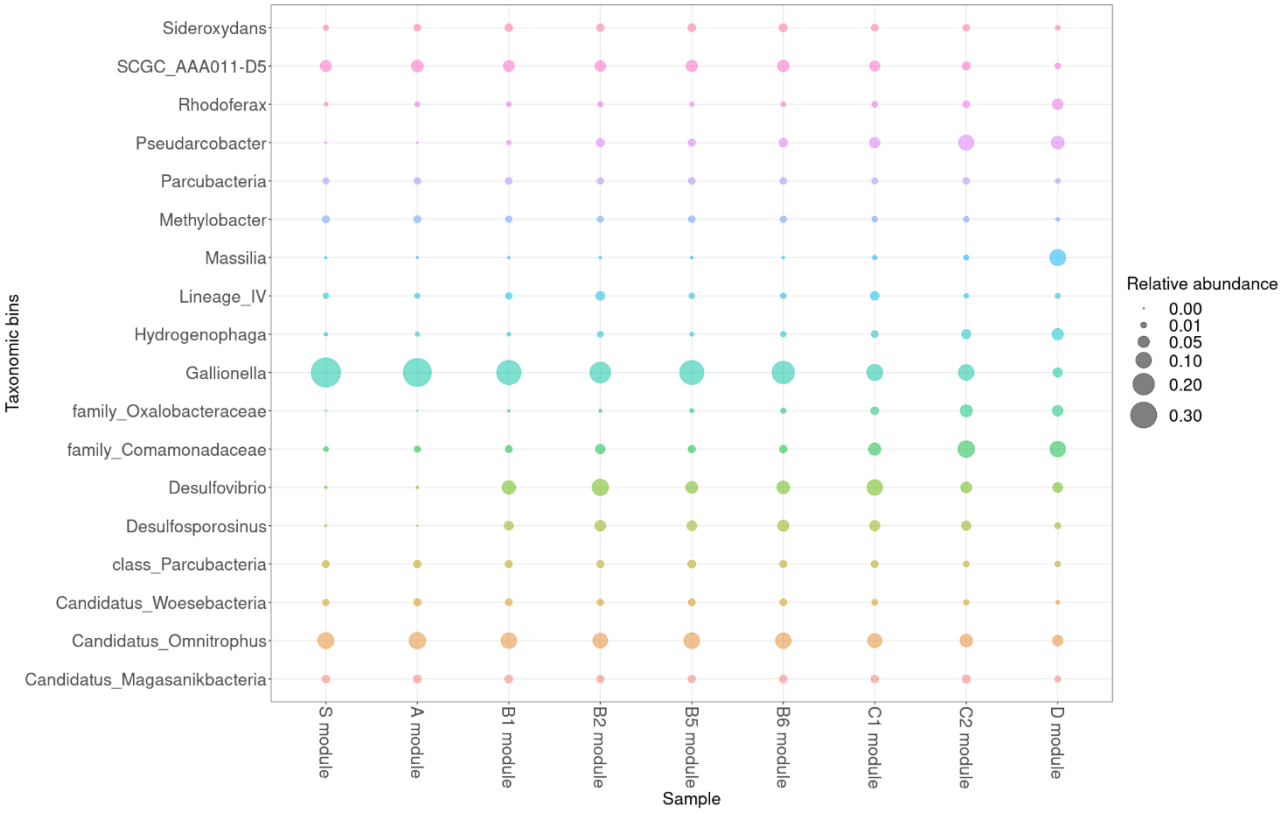

Figure 6. Relative abundance of taxonomic bins in the individual modules the Wetland+ system.

3. Discussion

This study assessed the Wetland+ efficiency in removing HCH and ClB from Ostrovský Creek springs in the historically polluted area, role of bacteria in biodegradation and its effect on diversity of diatoms. As most of the ClB compounds are volatile and are more readily subject to aerobic degradation (Monferrán et al., 2005), a higher ClB removal rate (96.8%) of these compounds was observed. HCH isomers are more persistent compared to ClB, therefore the average HCH removal rate was 81.7%. This disparity in removal rates emphasizes the need for tailored treatment strategies within the Wetland+ system to effectively address these distinct contaminants.

Analysis of water samples confirmed the presence of functional genes and bacterial genera capable of degrading HCH isomers and their byproducts. Whereas the abundance of *Dehalococcoides* spp., the microorganism capable of anaerobic dechlorination of HCH, was lower in the downgradient profiles C and D, the abundance of the functional genes *linA*, *linB*, *linB-RT*, and *linD* encoding enzymes involved in aerobic HCH biodegradation displayed an opposite trend and in general followed the trend of increasing concentration of O_2 in water in the direction of water flow. These different patterns indicate prevailing HCH biodegrading processes in the Wetland+ treatment system in addition to chemical reduction in module B and other attenuation processes such as chemisorption, biosorption,

bioaccumulation and evapotranspiration.

The most likely explanation for cooccurrence of both aerobic and anaerobic biomarkers of HCH degradation is that the inflow drainage water originates in an environment with low redox conditions, but on the way through the system, especially through modules A, C and D, is exposed to the atmosphere and oxidation - reduction conditions change, see Table 5. Additionally, the flow through individual modules of the Wetland+ system is not homogenous with different pathways of different hydrogeochemical conditions including stagnation zones. Similar cooccurrence of anaerobic and aerobic bacteria degrading chlorinating ethenes was observed in groundwater (Liang et al., 2017; Němeček et al., 2017), and discrete aquifer soil samples (Richards et al., 2019) as well as in surficial riverbed sediment samples (Atashgahi et al., 2013). Understanding the composition and dynamics of microbial communities within the system is essential for its efficient operation. The coexistence of both aerobic and anaerobic bacteria for HCH degradation suggests the need for tailored management strategies. By harnessing this knowledge, it is possible to optimize the conditions that favor specific microbial populations, thereby enhancing the removal of HCH and ClB contaminants.

The analysis of microbial community revealed the high abundance of iron oxidizing *Galionella* with a noticeable decreasing trend in direction of water flow through the system. The presence of these iron oxidizing bacteria were predicted due to high iron content of water, and it was reported in our previous study (Amirbekov et al., 2021). This trend corresponds with the decreasing content of dissolved (i.e. ferrous) iron (data not shown). The increased abundance of the sulfate-reducing *Desulfovibrio* and *Desulfosporosinus* in module B may be related to the higher content of sulfate and ferrous iron as available electron acceptor and donor, respectively. While sulfate-reducing bacteria do not directly degrade HCH themselves, they contribute to HCH degradation through their metabolic activities and interactions with other microorganisms. Particularly their production of H_2S can stimulate the activity of reductive dechlorinators, including dehalogenases. H_2S can act as a co-substrate, supporting the reductive dechlorination reactions and promoting the stepwise dechlorination of HCH compounds (Boyle et al., 1999). Further research could explore how these bacteria can be used to enhance the wetland's performance. For instance, controlling the availability of ferrous iron may be a strategy to modulate the activity of these bacteria and, in turn, enhance HCH degradation.

The D modules were rich in bacteria of genera *Massilia, Rhodoferax, Hydrogenophaga, Flavobacterium, Caulobacter* and *Bacteriovorax* comparing to another modules. *Massilia* sp. is common environmental bacterium often associated with plants and roots (Baek et al., 2022; Heo et al., 2022; Johnston-Monje et al., 2021) (Li et al., 2021) and was described as characteristic for HCH-contaminated rhizospheres (Balázs et al., 2021). *Massilia* also have the potential to degrade many

pollutants present in the environment, such as *Massilia* sp. WF1 degrading the polycyclic aromatic hydrocarbon phenanthrene (Gu et al., 2021).

Fahy et al. (2006) states that a benzene degradation occurred after a community shift from a *Rhodoferax*-dominated community to a mix of *Rhodococcus* and *Hydrogenophaga* spp. (Fahy et al., 2006). Certain species of *Flavobacterium* have been reported to possess the ability to degrade HCH compounds. These bacteria may participate in the biodegradation of HCH and contribute to its removal from the environment (Amirbekov et al., 2021; Lata et al., 2012; Murthy and Manonmani, 2007; Ramteke and Hans, 2008). Kaur et al. reported that the abundance of *Caulobacterales* increased with the increasing HCH content in soil (Kaur et al., 2021). It is important to note that the ability of these bacteria to degrade HCH compounds can vary among species and strains. Further investigation and characterization of the specific strains present in the contaminated samples would provide a clearer understanding of their potential roles in HCH degradation or adaptation. The findings of this study will help to shape and optimize the design of future Wetland+ systems. Adaptive systems that adjust to changing pollution levels and environmental circumstances may be conceivable.

4. Summary

This study assessed the efficiency of the Wetland+ system to treat water heavily contaminated by HCH and ClB after one year of operation. Successful chemical removal of pollutants was supported by biodegradation by indigenous bacterial community.

The main findings of this study are:

1. The average efficiency of the system during twelve months of operation was 96.8% for ClB and 81.7 % for HCH. Rate of the removal of individual HCH isomers followed the pattern: $\alpha = \gamma = \delta > \varepsilon = \beta$
2. The highest total microbial biomass was in the outlet from the aerobic wetland (module D). Similarly, the abundancy of the *linA, linB, linB-RT*, and *linD* genes was the highest in this outlet along with the highest level of dissolved O_2 in water. Therefore, the best conditions for aerobic biodegradation of HCH isomers and their metabolites were in the aerobic wetland.
3. The highest abundance of *Dehalococcoides*, capable of anaerobic dechlorination of HCH, was found in the inflow water (profile S), in aeration system with sedimentation (A), and in permeable reactive barrier remedial system (module B).
4. High abundance of iron oxidizing *Galionella* corresponded to the level of dissolved iron in water flowing through the system. Similarly, the increased abundance of the sulfate-reducing

Desulfovibrio sp. and *Desulfosporosinus* sp. in module B may be related to the higher content of sulfate and ferrous iron as available electron acceptor and donor, respectively. The D module exhibited a high abundance of *Massilia, Rhodoferax, Hydrogenophaga, Flavobacterium, Caulobacter,* and *Bacteriovorax* demonstrating a range of metabolic capabilities and interactions that may contribute to the degradation of HCH and other pollutants. Further research is warranted to investigate the specific mechanisms and contributions of these bacteria in HCH degradation.

This study not only sheds light on the Wetland+ system's efficiency in eliminating HCH and ClB pollutants, but it also delves deeply into the delicate microbial and ecological processes involved. The complex relationships within microbial populations, redox conditions, and pollutant removal rates provide potential for wetland design optimization. The research establishes the groundwork for future research and development targeted at improving the efficiency of wetland-based remediation technologies and increasing environmental recovery in historically contaminated regions.

PHYTOREMEDIATION

I. A. glutinosa and soil microbial community response to HCH contamination

1. Background

A. glutinosa is the dominant tree species at the Hajek site in the Czech Republic highly contaminated with HCHs (50°17′31.5″ N 12°53′35.2″ E). The species is a widespread, short-lived tree that grows in low-lying, moist areas and, as such, has proven useful for flood control, riverbank stabilisation and river ecosystem functioning. Desai et al. (2019) were able to show that the species was effective at taking up lead (Pb) from contaminated soils (Desai et al., 2019), while Tischer & Hübner proposed its use for degrading mineral oil hydrocarbons, phenol and polycyclic aromatic hydrocarbons (PAHs) through promotion of microbial activity via mycorrhizal nitrogen fixation (Tischer and Hübner, 2002). While, to the best of our knowledge, no full-scale study has yet been published on HCH uptake by *A. glutinosa*, our own preliminary studies have demonstrated that presence of 12-day-old *A. glutinosa* seedlings enhances δ-HCH removal by 21–36% compared to control plots without seedlings (Košková et al., 2022).

In this study, we aim to describe the uptake and transformation of HCH isomers by *A. glutinosa* saplings planted in freshly contaminated soil and compare the development of associated rhizosphere and soil microbial communities. In doing so, we also determine the physiological response of *A. glutinosa* to HCH isomers by measuring sapling biomass and phytohormonal activity. In the first exterior study described below, we aimed to determine the bioaccumulation potential of α, β, and δ isomers of HCH by *A. glutinosa* seedlings. Control was prepared with the same soil without HCH. All variants were set in triplicate and had instant access to water for three months. HCH was analyzed in soil and sections of seedlings (roots, trunks, branches, leaves) on GC/MS. Amplicon 16S rRNA and ITS region sequencing was applied to study the microbial and fungal community in rhizosphere samples.

2. Material and Methods

2.1 Chemicals

The standarts α HCH, β HCH, and δ HCH isomers, LC grade acetone and hexane were purchased form Merck (Merck, St. Louis, Missouri, United States). The deuterated γ-HCH standard and ClB standards were obtained from Neochema (Neochema GmBH, Bodenheim, Germany). Anhydrous sodium sulphate was provided by Lach-ner s.r.o. (Neratovice, Czech Republic). Deionized water was prepared by Millipore Direct Q® 3 UV system (Merck, St. Louis, MO, USA). Acetonitrile and formic acid were purchased from Merck (Merck, St. Louis, MO, USA). Phytohormonal standards and isotopic labelled internal standards were provided by Olchemim Ltd. (Olomouc, Czech Republic).

2.2 Experimental design and sample processing

For this study, experimental substrates were prepared by mixing clean soil and standard α-HCH, β-HCH and δ-HCH isomers to achieve 50 mg/kg dry weight of each, with a control soil sample prepared in the same way but without HCH. Next, 2-year-old *A. glutinosa* saplings were planted in triplicate for all experimental and control variants and then placed outdoors in unshaded place with instant access to water (Figure 7).

After three months, 10.0 ± 0.5 g of soil was sampled from each pot for analysis of α-HCH, β-HCH and δ-HCH isomers, with an equal amount of soil used for dry mass determination (see below). The *A. glutinosa* saplings were then removed from the pots, and divided into four sections, i.e. root, trunk, branches and leaves. Each part of the sapling was then weighed, after which it was milled in liquid nitrogen and the resultant fine powder used for HCH analysis, dry weight determination (both using 5.0 ± 0.5 g of biomass) and phytohormonal analysis (see below).

Samples for HCH extraction were agitated in a horizontal shaker at 200 rpm for 24 hrs in 10 ml of a 1:1 (v/v) acetone: hexane mixture for soil, and 5 mL of 1:1 (v/v) acetone: hexane for sapling biomass. The supernatant was then collected and anhydrous sodium sulphate added, after which the mixture was vortexed. One ml of extract was then taken and enriched with 10 μl of internal deuterated γ-HCH standard to cover the ionization instability prior to analysis (see below). Samples for dry mass determination were dried in dryer for 3 hrs at 105°C and then weighted for dry mass calculation.

Phytohormone analysis performed to describe adaptation of *A. glutinosa* to phytoremediation. Rhizosphere soil obtained by shaking roots to remove bulk soils, and the remaining soils stuck to roots were placed in a 50-ml test tube containing 35 ml of sterile phosphate buffer and then shaken for 5 min. The resultant solution was then centrifuged 10 min at 4,000 × g at a temperature of 4 °C to obtain biomass for DNA extraction (see below).

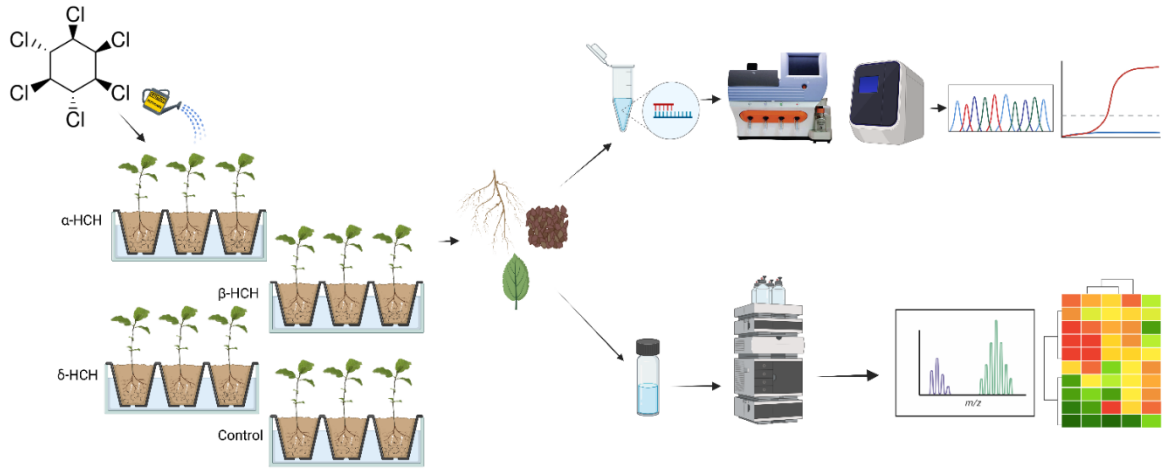

Figure 7. Schematic illustration of the experiment: Alnus glutinosa and soil microbial community response to HCH contamination

2.3 Chemical analysis

Prior to mixing the experimental substrates, the purity of the standard isomer solutions was assessed using an RSH/Trace 1310/TSQ8000 Gas chromatography–tandem mass spectrometry (GC-MS/MS) assembly with a DB-5ms column (PAL, Switzerland; ThermoFisher Scientific, USA). The same assembly was also used to assess the concentrations of HCH and ClB isomers in the various experimental samples. In each case, the limit of quantification (LOQ) was set at < 0.01 µg/g (dw) for all analytes.

Hormone analysis was performed using an Acquity® I-Class ultra-high-performance liquid chromatograph (UHPLC; Waters, Milford CT, USA) coupled with a Xevo TQ-XS MS/MS assembly (Waters, UK) according to previously published methodology (Šimura et al., 2018). Briefly, 15 mg FW of homogenized plant material was extracted in 60% acetonitrile with the mixture of isotopic labeled internal standards. The samples were shaken in the oscillation bead mill (Retch MM400, Haan, Germany), sonicated, incubated for 30 min at 4 °C and centrifuged at 20,000 rpm, 4 °C for 15 min (Allegra 64R benchtop centrifuge, Beckman Coulter, USA). The supernatant was collected and purified with Oasis® HLB 30 mg/1 ml extraction cartridges (Waters, Milford, CT USA). Flowthrough fraction was collected, evaporated to dryness using SpeedVac concentrator (RC1010 Centrivap Jouan, ThermoFisher, USA). The sample was dissolved in 40 µl 25% acetonitrile (v/v), 5 µl was injected into Acquity UPLC® CSHTM C18 2.1×150 mm, 1.7 µm chromatographic column and analysed under the operating conditions as described in Šimura et al., 2018 (Šimura et al., 2018). Concentrations of phytohormonal metabolites were calculated using the isotope dilution method.

2.4 Molecular genetic analysis

DNA extraction, real-time quantitative PCR, amplicon 16S rRNA sequencing and bioinformation analysis were described in previous study in section 1.5 of *I. HCH Removal in constructed wetland beds*.

2.5 Statistical Analysis

The effect each HCH isomer on sapling growth parameters was evaluated using one-way ANOVA with post-hoc Tukey tests, using the Origin software package v.2019b (OriginLab Corporation, USA). Prior to analysis, all data were subjected to Levene‘s test to test for homogeneity of variance. All statistical analyses were performed with a significance level of $\alpha > 0.05$. Data for phytohormonal analysis were first log-transformed and then subjected to principal components analysis (PCA) to describe the general data structure. Values under the limit of detection (LOD) were replaced by 95% of the respective detection limit. The non-parametric Mann-Whitney test was then used to calculate significant differences in phytohormonal content between the control and HCH-polluted saplings.

3. Results and discussion

3.1 Growth parameters

Though there were noticeable differences in sapling height and biomass of individual sapling parts compared to the control in those samples subjected to HCH-pollution, none of the differences observed were statistically significant (Figure 8).

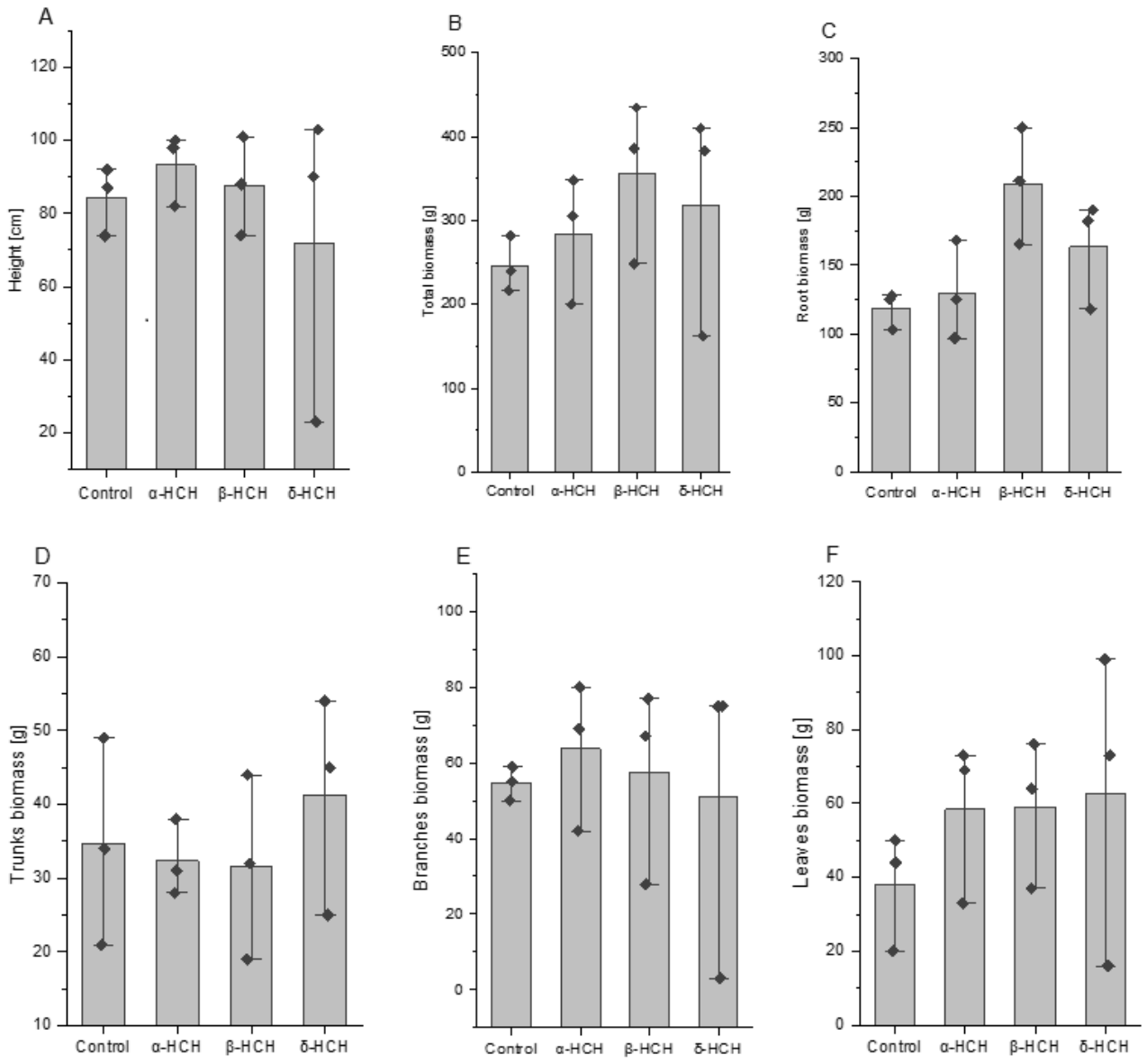

Figure 8. Effect of HCH -pollution on *A. glutinosa* growth parameters; (A) sapling height; (B) root biomass; (C) trunk biomass; (D) branch biomass; (E) leaf biomass.

3.2 HCH treatment

3.2.1 Soil remediation

HCH removal efficiency varied depending on the type of isomer, the degradation of each HCH isomer differing with its persistence and physiological properties (e.g. solubility, volatility). Its important to note that seedlings were exposed to freshly dissolved HCH isomers. In contaminated site the HCH isomer may have undergone chemical transformations due to interactions with the soil, water, air, and other environmental factors. For example, HCH isomers can undergo biodegradation, photodegradation, hydrolysis, and other chemical reactions that can change their properties and affect their availability to plants for uptake. Highest removal efficiency was observed in the group treated with β-HCH (90.26%),

followed by α-HCH (64.85 %) and δ-HCH (57.08 %) (Figure 9).

Highest ClB metabolite levels in soil were registered for α-HCH, with 10 metabolites (1,2-; 1,3-; 1,4-diClB, 1,2,3 -;1,2,4-triClB 1,2,4,5-; 1,2,3,5-; 1,2,3,4-tetraClB, pentaClB; hexaClB) found at a total concentration of 802.90 ng/g (Figure 8). In comparison, lowest ClB metabolite levels were recorded in β-HCH polluted soils, with a total concentration of 12 ng/g dominated by hexaClB. It is important to note here that transportation of HCH does not always follow the 'water diffusion pattern' through the environment as its octanol-water partition coefficient is close to 4 (*log Kow*). This isomer can show the tendency to bind to the root lipid membrane. It also has a lower vapour pressure than the other two isomers. Consequently, the β-HCH isomer is the least soluble in water, which may have resulted in precipitation despite the soil being thoroughly homogenised. While soils with δ-HCH also contained 16.70 ng/g of ClB metabolites, mainly comprising the pentaClB and hexaClB isomers, soils with β-HCH contained very few as β-HCH is relatively stable and degradation to ClB metabolites only occurs at very low levels (Bachmann et al., 1988; Kaushik, 1989). In comparison, α-HCH is more susceptible to metabolic transformation in soils, most likely through bacterial activity in cooperation with plants. Indeed, numerous studies have reported high degradation rates of α-HCH through a range of microorganisms (Huntjens et al., 1988; Okeke et al., 2002; Sineli et al., 2016).

In the environment, removal of HCH from the soil occurs primarily through uptake by plants, trees and microbiota and through the influence of environmental conditions. However, it is also possible that trans-isomerisation occurs, especially in soil and root tissue. Under experimental conditions, isomer stability tends to follow the route δ-HCH > α-HCH > β-HCH.

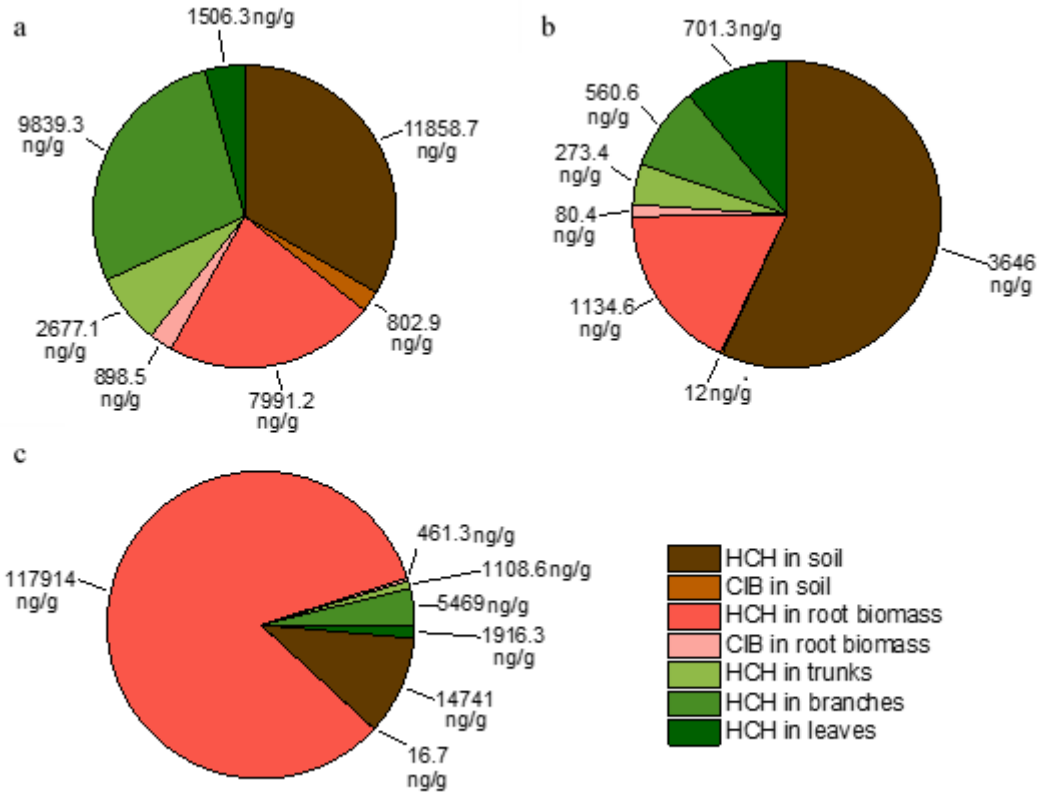

Figure 9. Concentrations of HCH isomers and metabolites (dry weight) in leaves, branches, roots and trunks of *A. glutinosa*. (a) α-HCH; (b) β-HCH; (c) δ-HCH.

3.2.2. Sapling root biomass

The root biomass of saplings treated with α-HCH contained 7991.2 ng/g α-HCH and a total ClB concentration of 898.5 ng/g (Figure 9a), both metabolites matching those found in the soil. In this group, a rapid decrease in the concentration gradient of metabolites was observed compared to their concentration in soil, possibly due to low uptake of metabolites formed in the soil or their rapid degradation, transportation or transformation to unknown products in the root biomass. A similar decrease in metabolite concentrations was also observed for the β-HCH isomers (Figure 9b). For example, its concentration in root reached 1134.6 ng/g while total metabolite levels were just 80.4 ng/g (primarily hexaClB, pentaClB and 1,2,4-triClB).

3.2.3 Above-ground sapling parts

In general, concentrations of HCH were low in trunks, branches and leaves. But for saplings exposed to α-HCH, concentrations reached 2677.2 ng/g in trunks, 9839.3 ng/g in branches and 1506.3 ng/g in leaves, indicating that, once taken up by the roots, the isomer is subsequently transported throughout

the sapling (Figure 9a). Interestingly, high concentrations were determined in branches where, presumably, no further processing of the original substance takes place as no metabolites were detected. On the other hand, the isomer is then transported to the leaves, where further metabolism or volatilization does occur. It should be noted, however, that there is a possibility that hitherto unknown metabolites are formed in all sapling parts.

Overall, less HCH and metabolites were recorded in sapling parts treated with the β-HCH isomer, with levels reaching just 273.36 ng/g in trunks, 560.60 ng/g in branches and 701.30 ng/g in leaves (Figure 9b). Likewise, total metabolite concentrations were negligible, with just a 1,2- and 1,4-diClB and 1,2,4-triClB detected in the trunks and hexaClB in the branches.

Results for the δ-HCH isomer were similar to those for the α-HCH isomer, with trunks containing 1108.63 ng/g, branches 5469 ng/g and leaves 1916.30 ng/g (Figure 9c). Likewise, there were higher levels in the branches than in other aboveground parts, though metabolites were only detected in trunks and not in branches or leaves.

3.3 Phytohormones

Overall, 72 plant hormones and metabolites in eight classes were identified in tissues growing in contaminated and control soils. As expected, most differences in concentration levels were observed between the various sapling organs (Figure 10), most likely due to differences in organ function and developmental patterns over time and space. The roots, for example, were characterised by highest concentrations of 2-methylthio CK and indole-3-acetamid, indicative of bacterial activity in the rhizosphere (Mano and Nemoto, 2012; Podlešáková et al., 2013). In comparison, highest concentrations of IAA (bioactive AUX) and the majority of CK were detected in sapling trunks. Indeed, several studies have shown that homeostasis between trunk AUX and CK orchestrate several physiological functions, including apical dominance (Kotov et al., 2021). The phytohormonal pattern in branches and leaves, however, was characterised by BR, which typically occurs in the meristems of young proliferating organs (Planas-Riverola et al., 2019), while increased levels of ABA, JA and SA in the branches and leaves suggest a response to abiotic stress (Waadt et al., 2022).CK in all sapling organs was downregulated in trees growing on polluted soil, whatever the isomer (Figure 10), possibly in relation to early senescence as a response to stress induced by phytoremediation(Ha et al., 2012). The only exceptions were isopentenyladenine and isopentenyladenosine in sapling trunks, which was probably related to CK transport(Osugi and Sakakibara, 2015; Zürcher et al., 2016). Also identified in *A. glutinosa* samples were metabolites of GA, which have previously been described as components of the

13-hydroxy biosynthetic GA pathway in buds of mountain alder *Alnus incana* subsp. *tenuifolia* (Hedden, 2020; Zanewich and Rood, 1994), with a significantly increase in the precursor GA53 and the catabolite GA29 in stressed trees, along with upregulated JA and downregulated abscisates (Figure 11 A). In our own study, the high concentrations of JA would suggest that the signalling pathways involved in abiotic stress had been activated. Components of the JA signal pathway have previously been reported as interacting antagonistically with ABA in *Arabidopsis (Brassicaceae)*, which could explain the lower concentration of ABA metabolites observed in our own study on *A. glutinosa* (Anderson et al., 2004; Proietti et al., 2018). Abscisates are also known to act antagonistically with GA, which would increase the level of GA in stressed trees (Yuan et al., 2011).

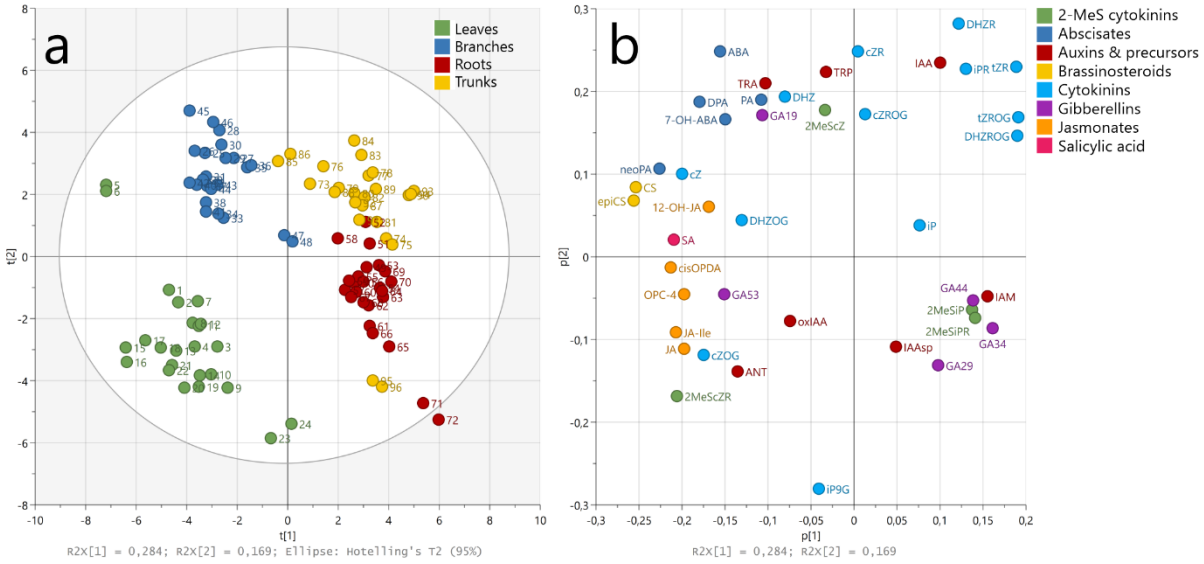

Figure 10. Variability of A. glutinosa saplings in plant hormone concentrations calculated by principal component analysis (PCA). In the score plot (a), each data point represents an individual plant sample coordinated by the principal components PC1 and PC2, both expressing total variability 45.3%. The similar samples, each coloured by a plant organ, are clustered close to each other. The numbers nearby the data points express the sample identifiers, whose meanings are explained in Table S1. The ellipse expresses the 95% limit of multivariate t-distribution (Hotelling's T-squared distribution). The similarities of the samples are given by the concentrations of plant hormones depicted in the loading plot (b). The plant hormones co-localising with the samples on the same side of the scatter plot are abundant in these samples. Conversely, the plant hormones on the opposite side of the scatter plot are low in their concentration. The plant hormones are coloured by the corresponding phytohormonal group.

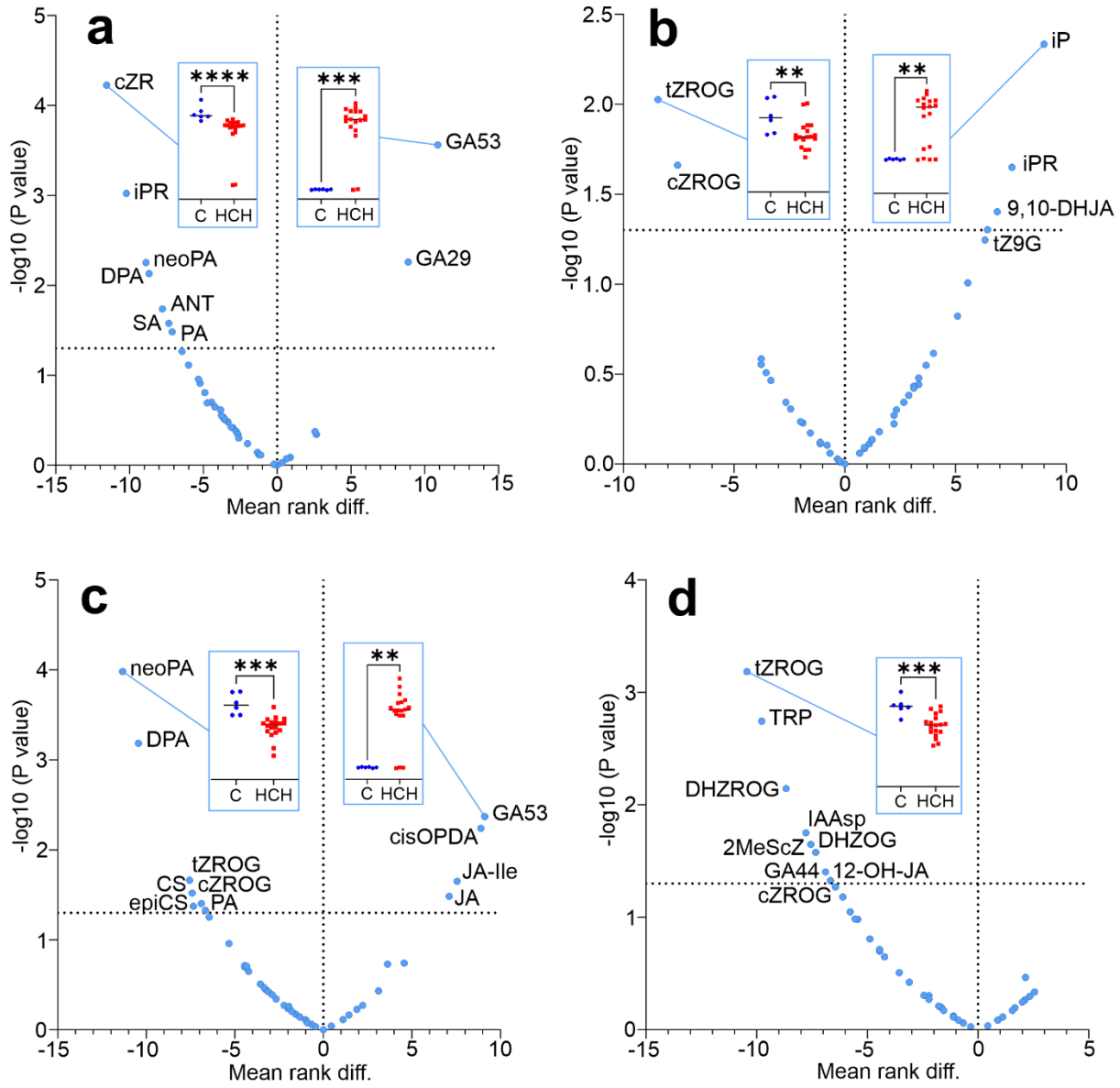

Figure 11. Effect of HCH on phytohormone concentration levels in the different parts of A. glutinosa; (a) branches, (b) trunk, (c) leaves and (d) roots. The blue circles in each volcano plot represent the plant hormones distributed according to the mean rank difference of the concentration between control (C) and HCH-treated groups (horizontal axis) and the negative logarithm of p-value calculated by Mann-Whitney test (vertical axis). The horizontal dashed line delimits the significance level of α = 0.05. The blue boxes inside each volcano plot shows the data distribution of the most significantly different plant hormone concentrations (with the highest absolute value of both mean rank difference and negative logarithm of p-value) in each individual sapling. The asterisks indicate the statistical significance at level of α = 0.05 (p-value 0 '**' 0.0001 '***' 0.001 '**' 0.01).**

3.4 Bacteria

Soil and rhizosphere samples contained 530 common bacterial taxa. Of these, 93 taxa were found in the rhizosphere but not in the soil, 126 taxa in soil samples only (Figure 12). Soil bacterial community structure was similar in all samples treated with HCH.

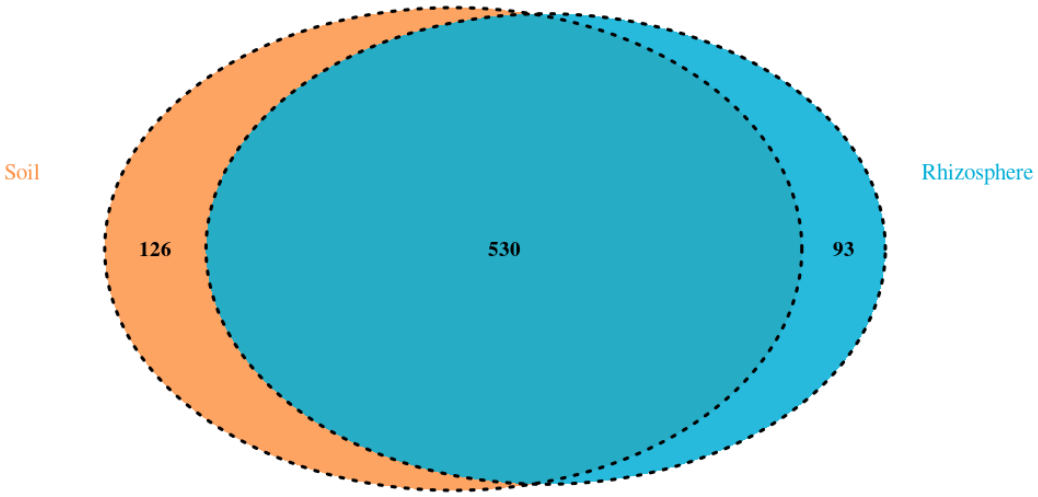

Figure 12. Venn diagram showing common microbial populations shared by the soil and rhizosphere samples.

In soil samples, the dominant bacterial groups, in order, were *Pseudomonas*, the unclassified *Chloroflexi* group *KD4-96*, *Comamonadaceae, Nocardioides* and *Gemmatimonadetes*. While *Pseudomonas* was dominant, with abundance levels highest in control samples, levels decreased noticeably in samples treated with HCH (Figure 13). The *Nocardioides* along with *Chloroflexi* and *Gemmatimonadetes,* have also been reported as abundant taxa in OCP contaminated soils (Zheng et al., 2022), while *Chloroflexi KD4-96* are frequently been detected in soils contaminated with heavy metals (Gołębiewski et al., 2014). In the latter case, its abundance has been found to correlate highly with iron and aluminium concentrations (Wegner and Liesack, 2017).

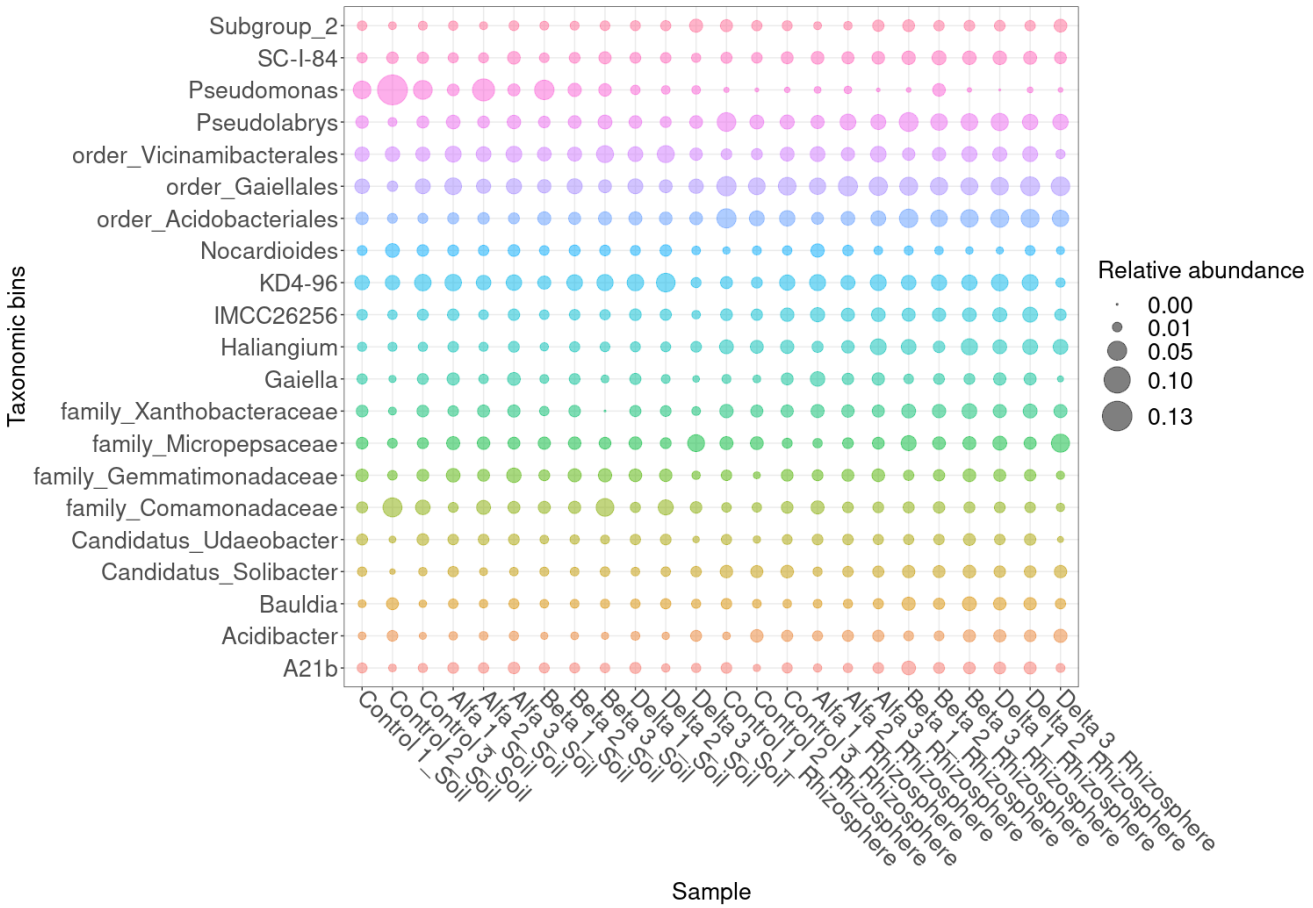

Figure 13. Relative abundance (mean > 0.05) of bacteria in soil and rhizosphere samples.

HCH isomer abundance was similar in all rhizosphere population samples, though with some exceptions. For example, *Pseudomonas* levels were significantly lower than in soil samples in all HCH treatments, with lowest abundance for the δ-HCH isomer, despite this being detected at highest levels in the root biomass (Figure 13). In contrast, *Pseudolabrys*, *Gaiellales (Gaiella)*, *Acidobacteriales*, *Haliangium* and *Bauldia* were the dominant contributors to biomass in the rhizosphere. *Pseudolabrys*, of the order *Rhizobiales*, are nitrogen-fixing bacteria that have a symbiotic relationship with plant roots, as does *Bauldia*. *Gaiella*, on the other hand, is an important decomposer of organic matter and is heavily involved in carbon cycling (Albuquerque and da Costa, 2014).

3.5 Fungi

Soil and rhizosphere samples contained 138 common fungal taxa, with 33 taxa found in the rhizosphere but not in soil and 86 taxa found only in soil samples (Figure 14).

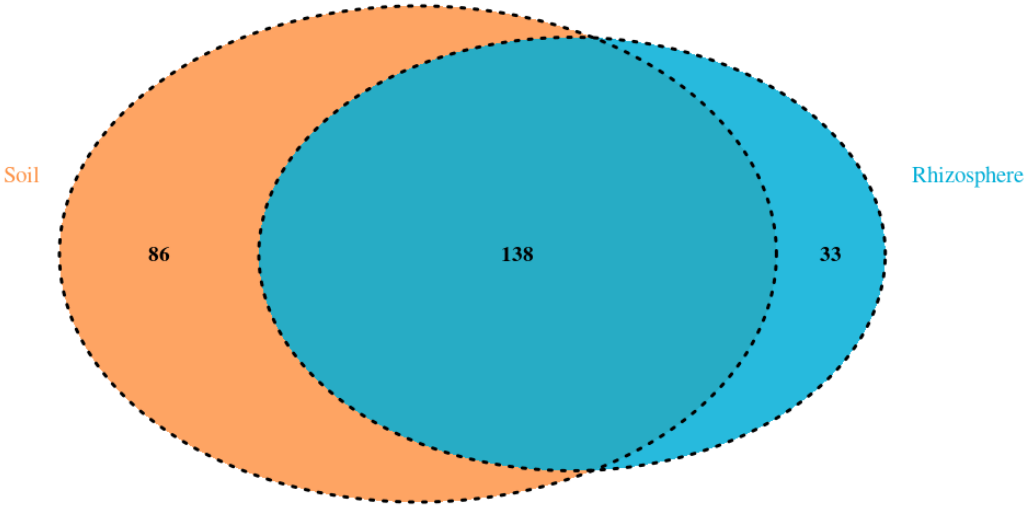

Figure 14. Venn diagram showing common fungal populations shared by the soil and rhizosphere samples.

The abundance of *Penicillium* and *Coleophoma* was higher in the soil than in the rhizosphere, while levels of *Moritella* were higher in the rhizosphere (Figure 15). While *Tomentella* was generally dominant in rhizosphere samples, samples treated with δ-HCH had the lowest concentrations and β-HCH samples and the control the highest. Tedersoo et al. (Tedersoo et al., 2009) identified 40 species of putatively ectomycorrhizal fungi from seven sites dominated by *A. glutinosa*, with the ectomycorrhizal fungi *Tomentella* aff. *Sublilacina* most prevalent under saline stress conditions. *Tomentella* contains melanins, which may act as a boundary between fungal cells and their environment, protecting them against physical, chemical and/or biological stressors (Vrålstad et al., 2002).

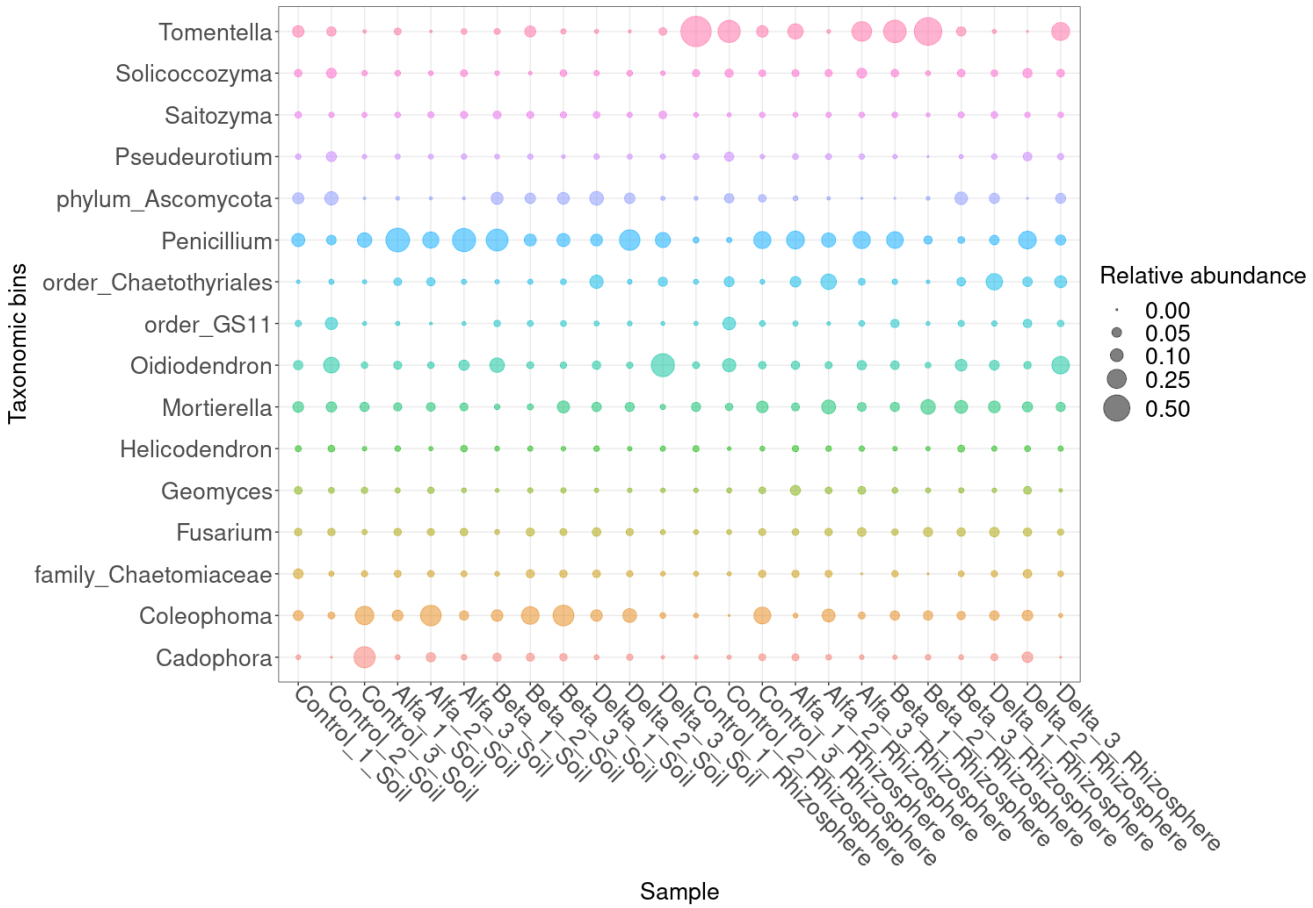

Figure 15. Relative abundance (mean > 0.05) of fungi in soil and rhizosphere samples.

3.6 Functional genes involved in HCH biodegradation

Lin genes were found in all samples, with higher relative quantities in soil than the rhizosphere (Table 5). Interestingly, the *linA* gene was not detected in most rhizosphere samples but was present in low quantities in all soil samples. The *linB* gene was detected in high amounts in soil samples, especially in samples treated with β-HCH. Lal et al. (Lal et al., 2010) also reported *linB* as occurring at higher levels than *linA* in most soil samples from a highly contaminated HCH dump site. The key function of *linB* is in the breakdown of the most resistant β-HCH isomer (Sharma et al., 2006). Furthermore, the similarity of *linB* to other enzymes, as opposed to *linA*, which is unique, may result in the selection of more *linB* genes from unidentified bacteria present at the samples (Lal et al., 2010). Overall, highest levels of the *linB-RT* gene were found in soil samples treated with the β-HCH isomer, while very little was recorded in control samples and none at all in soil treated with α-HCH, suggesting that the β-HCH isomer biodegrades in soil (Lal et al., 2010). Finally, *linD* genes were detected at intermediate relative quantities in all rhizosphere samples, but were rarely detected in soil samples.

Table 8. Relative abundance of genes indicating total bacterial biomass (16S rDNA), dehydrochlorinase (linA), haloalkane dehalogenase (linB, linB-RT) and reductive dechlorinase (linD) in rhizosphere and soil samples (average of duplicate samples). The color scale indicates the relative quantity of a given marker: red (+++) highest, orange (++) high, yellow (+) intermediate, (+-) low and ND = not detected or below the LOQ.

			Gene			
		U16SRT	**linA**	**linB**	**linB-RT**	**linD**
Rhizosphere	Control 1	+++	+-	+-	+-	+-
	Control 2	+	ND	+-	+-	+-
	Control 3	+	+-	+-	+-	+-
	α-HCH 1	++	+-	+-	+-	+-
	α-HCH 2	++	+-	+-	+-	+-
	α-HCH 3	++	ND	+-	ND	+-
	β-HCH 1	+++	ND	+-	+-	+-
	β-HCH 2	+++	ND	+-	+-	+-
	β-HCH 3	+++	+-	+-	+-	+-
	δ-HCH 1	++	ND	+-	+-	+-
	δ-HCH 2	+++	+-	+-	+-	+-
	δ-HCH 3	+	ND	+-	+-	+-
Soil	Control 1	+	+-	+++	ND	ND
	Control 2	+	+-	+-	ND	ND
	Control3	++	+-	+++	+-	+-
	α-HCH 1	++	+-	++	ND	+-
	α-HCH 2	++	+-	++	ND	ND
	α-HCH 3	+++	+-	+++	ND	ND
	β-HCH 1	++	+-	++	+++	ND
	β-HCH 2	++	+-	+++	+-	ND
	β-HCH 3	+++	+-	+++	+++	+-
	δ-HCH 1	++	+-	+	ND	ND
	δ-HCH 2	+++	+-	+++	+-	ND
	δ-HCH 3	+++	+-	+	+-	ND

4. Summary

Owing to its physicochemical properties, the δ-HCH isomer was the most persistent in soils and the most strongly bound to *A. glutinosa* roots, with α-HCH the second major isomer recorded in soils treated with β-HCH and δ-HCH. All monitored metabolites were present at highest concentrations in the α-HCH isomer treatment, suggesting that α-HCH may be subject to degradation over the longer term. All HCH isomers were found at highest proportions in the soil, with relatively little found in root biomass, suggesting that degradation of HCH isomers by bacteria in the soil occurs mainly through the aerobic upstream pathway. In rhizosphere bacteria, however, high amounts of the *linD* gene confirmed HCH degradation via downstream pathways. Overall, there was no significant difference in the abundances of bacterial and fungal consortia between treated and control samples. Similarly, there were no significant differences between soil and rhizosphere microorganisms. Phytohormone analysis indicated that *A. glutinosa* reacts to HCH contamination through changes in the stress hormones CK, JA, abscisate and GA. To conclude, *A. glutinosa* saplings showed clear uptake of all HCH isomers, with highest quantities detected in the roots and lowest in the leaves. While our pot experiment with freshly dissolved HCH isomer provide useful information about the potential of alder trees for phytoremediation, it is important to recognize the limitations of the experiment and the extent to which it can represent the real-life conditions. The results of the study provided preliminary information about the phytoremediation potential of the alder trees, but further studies in real contaminated sites would be necessary to fully understand their ability to remediate contaminated soils.

II. Performance of the one year and two-year *Alnus glutinosa* saplings in HCH contaminated soil and -evaluation of microbial community in soil and rhizosphere.

1. Background

The bioaccumulation experiment was set up with 34 selected 1- and 2-year-old *A. glutinosa* saplings in quadruplicate. The saplings were randomly divided in two groups – the control group and the treated group. Within each group, saplings were divided into two subgroups - pruned and unpruned to simulate establishing the short rotation coppice culture. The following samples were prepared: unpruned 1-year-old control (U1C), pruned 1-year-old control (P1C), unpruned 2-year-old control (U2C), pruned 2-year-old control (P2C), unpruned 1-year-old treated (U1T), pruned 1-year-old treated (P1T), unpruned 2-year-old treated (U2T), pruned 2-year-old treated (P2T). Contaminated sediment was obtained from polluted locality Hájek (Czech Republic) (50°17′31.5″ N 12°53′35.2″ E). Where the average concentrations of HCH and ClB as their main degradation products from the outlet drainage channel were 635.5 for HCH and 13 μg L^{-1} for ClB respectively (Amirbekov et al., 2021). The fresh wet sediment was properly homogenized in concrete mixer to ensure similar pesticide exposure. The control unpolluted soil was taken near the locality to retain the composition of the soil as similar as possible. Both homogenized sediment and soil were sampled before experiment to verify the soil purity and determined the contamination level in sediment. The seedlings were planted into plastic pots containing 500 g of soil prepared in this way. Simultaneously with the control and treated group, pots contained only sediments (S) were prepared to evaluate the environmental effect on HCH concentrations. The prepared pots were placed on a sunny outdoor location and regularly irrigated with tap water during 90 days.

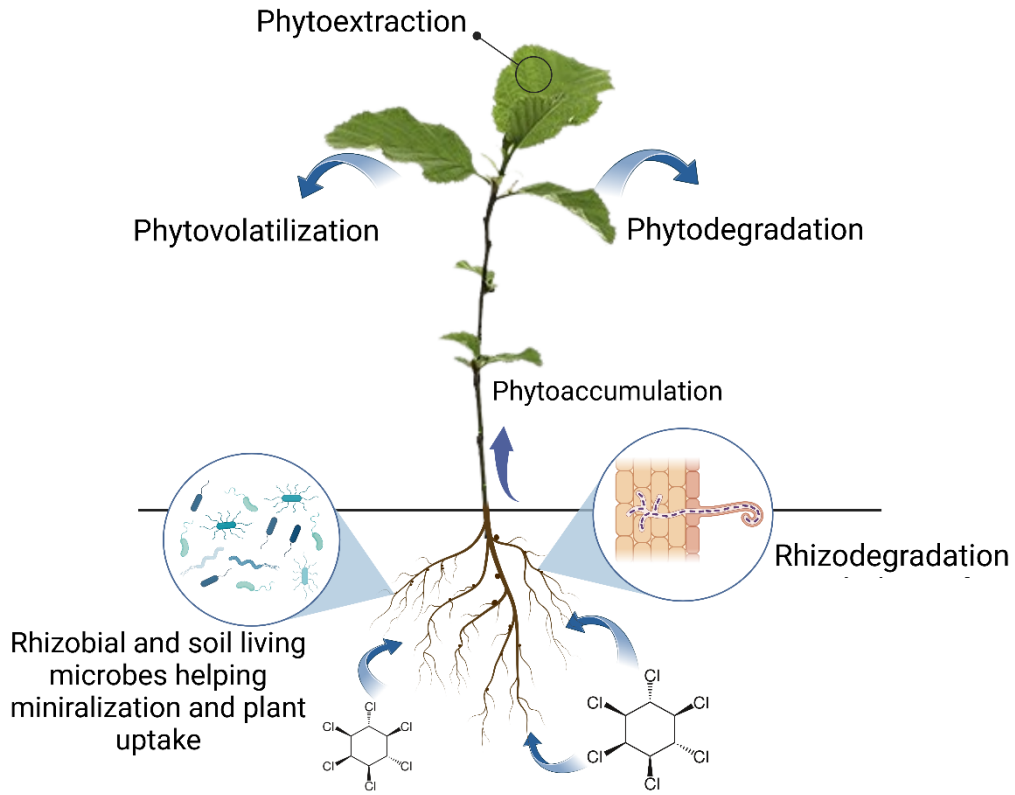

Figure 16. Phytoremediation routes in plants

2. Materials and methods

2.1 Sample collecting and pre-treatment

At the end of experiments, all seedlings were collected, for the molecular biology analysis. The bulk soil were removed by shaking and the rhizosphere soil were collected after that roots were washed repeatedly in tap water, weighted and measured. The biomass of the all plant was collected at the end of experiment. The soil was carefully removed from the root part to avoid the affecting the HCH analysis. The plant biomass was divided into root and above-ground part. Subsequently, all the plant samples were ground in a presence of liquid nitrogen, homogenized and analysed for HCH and phytohormones determination.

2.2 GC/MS analysis

Concentrations of all HCH isomers and selected metabolites were measured by Varian Saturn 2200 GC/MS in the SIM mode with the spitless liquid injection. Analysis of HCH and related metabolites: The sample processing was performed as previously described (Balázs et al., 2018; Košková et al., 2022) with some modifications. The soil (10 ± 0.5 g) and plant biomass (were 1 ± 0.1 g) were extracted

using 10 ml and 1 ml of acetone: hexane 1:1 (v/v) solution, respectively. The extraction was carried out for 24 hours using horizontal shaker at 300 rpm. Subsequently, the supernatant was collected and transferred to the clean 4 ml vials with 500 mg of anhydrous sodium sulphate followed by vortexing. In this way prepared extract was used for GS/MS analysis using tetrachloro-m-xylene as the internal standard. The dry masses were determined using dryer for 3 hours at 105 °C.

2.3 LC/HRMS analysis

The plant hormones analysis was performed according the study of authors (Košková et al., 2022). The plant biomass of all alder seedlings was divided into two groups - roots and above-ground parts. After extraction and purification of samples, the obtained extracts were measured using LC/HRMS ExionLC system with X500R QTOF and Turbo V ion source from AB SCIEX company were used. The phytohormones separation was carried out using the column Kinetex Evo C18 (100 mm; 2.1 mm; 2.6 μm; Phenomenex) and binary gradient consisted from 0.1% formic acid with 5 % of methanol (A) and pure methanol (B). The other separation conditions were as follows: flow rate - 0.300 $ml.min^{-1}$, column compartment temperature - 40 °C, and injection volume - 25 μl. The analysis lasted 9.5 min. and for the detection was used ESI in negative mode. Identification and quantification of the selected hormones were performed using multiple reaction monitoring (MRM) mode.

2.4 Molecular genetic analysis

DNA extraction, real-time quantitative PCR, amplicon 16S rRNA sequencing were described in previous study in section 1.5 of I. HCH Removal in constructed wetland beds

2.5 Bioinformatic analysis

The raw Ion Torrent reads were processed with QIIME 2 2021.8 software (Bolyen et al., 2019). Raw sequence data were demultiplexed and quality filtered using the q2-demux plugin followed by denoising with DADA2 (Callahan et al., 2016). Reads below 250 bp were removed. Taxonomy was assigned to ASVs using the q2-feature-classifier (Bokulich et al., 2018) classifysklearn naive Bayes taxonomy classifier against the Silva 138 database (Quast et al., 2013) and then Mitochondria and Chloroplast were removed. The accuracy of classification was evaluated against an artificial MOCK com-munity sample. QIIME 2 outputs were processed using the phyloseq R package (McMurdie and Holmes, 2013).

2.6 Statistical analysis

The software Origin, Version 2019b (OriginLab Corporation, Northampton, MA, USA) was used for the statistical evaluation of differences and visualization of the results. The biomass, remediation efficiency and HCH uptake were analyzed using one-way and two-way ANNOVA at the significance level of 0.05. The Levene‘s test for homogeinety of variance were used prior the analysis.

3. Results and Discussion

3.1 Biomass

The obtained values were highly variable and there was no statistically significant difference in biomass between the different groups consisting of 1-year-old plants (Figure 17a). In the case of 2-year-old plants (Figure 17b), HCH and metabolites presence did not show the negative effect. The significant negative root effect was caused by pruning (Figure 17b).

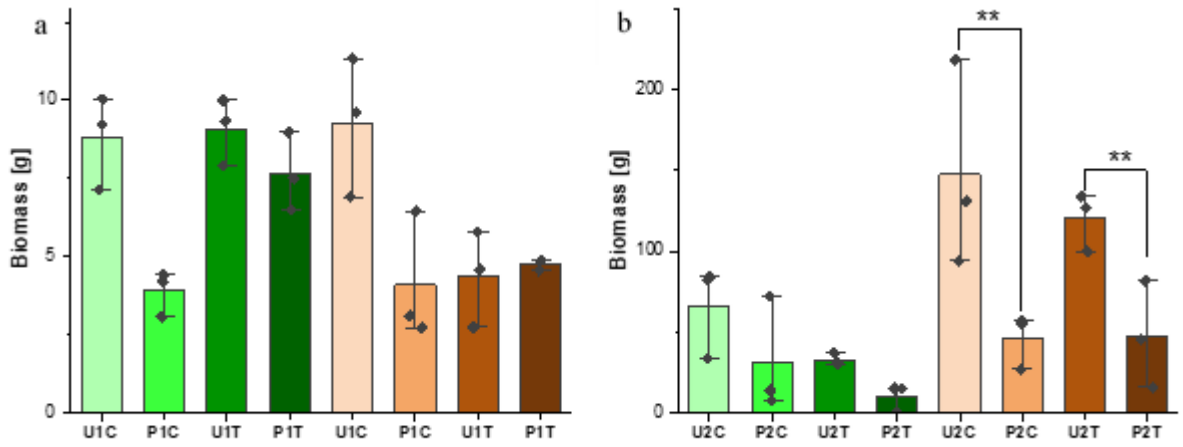

Figure 17. Biomass of all plants divided according the plant parts and treatment; a) 1-year-old plants, green color = above-ground part, brown colour - root biomass; b) 2-year-old plants, green colour = above-ground part, brown color - root biomass; Statistical evaluation - two-way Anova, significance level α = 0.05; *p < 0.05; ** p < 0.01, ***p < 0.001

3.2 Remediation efficiency and HCH uptake

Remediation effectiveness in the experimental groups was determined by comparing planted pots with unplanted sediment. The sediment was analysed before the establishment of the experiment. All stable isomers of HCH were present in the sediment at an average concentration of 1.53 ± 0.22 μg. g^{-1}. The used plants were exposed to 765 ± 110 μg of HCH in total. Percentage wise, the ε-isomer was the most represented (61.15 ± 7.17 %), followed by δ-HCH (33.79 ± 4.32 %), β-HCH (4.84 ± 0.40), and α-HCH

(1.52 ± 0.07 %). At the end of the experiment, the all samples of biomass and sediment were collected. Analysis of the unplanted sediment revealed that there was a decrease in HCH concentration. The difference was 14.6 ± 1.8 % probably caused by the environmental conditions and soil bacterial activity. The presence of plants increased the removal of HCH from the soil and by 6.8 - 24.4 % (Figure 18a). Higher remediation efficiency for unpruned 1-year-old plants was expected due to higher root biomass, but unexpectedly higher efficiency was observed for 1-year-old plants after pruning. This phenomenon can be explained by hormesis, where the plant responds positively to a stress stimulus induced by the presence of a pesticide and pruning. Plant uptake of HCH follows the trends in remediation efficiency. The highest pesticides concentrations were detected in root biomass (Figure 18b). In particular, ε-HCH followed by δ-HCH and β-HCH were present. Other isomers were not present in the samples with a few exceptions. Furthermore, the HCH were detected in isolated branch samples. An interesting fact was that HCH concentrations in 1-year-old branches without pruning were many times higher (923.1 ± 21.1 ng. g^{-1}) (Table 9) than in 2-year-old branches (detected only in one sample at concentration 19.8 ± 2.2 ng. $g.^{-1}$). Also, the HCH concentration were affected by pruning, with higher concentrations in 1-year-old alders (1338.4 ± 161.0 ng. g^{-1}) and lower concentrations in 2-year-old alders (113.1 ± 24.8 ng. g^{-1}). The β-HCH was not present in the branch samples and δ-HCH was observed in very low concentration. It can be assumed that δ-HCH is transpired due to vapour pressure (Calvelo Pereira et al., 2006) or transisomerised to ε-HCH. The β-HCH is assumed to remain bound to the root tissue; whether trans isomerization or the formation of unobserved degradation products occurs is not clear. HCH isomers were not detected in leaves tissue and no metabolites were found in plant biomass.

Table 9. Concentration of the HCH isomers in soil and plant parts

	Soil								Plants	
	Start of experiment (ng·g)				End of experiment (ng·g)				Roots	Branches
	α-HCH	β-HCH	δ-HCH	ε-HCH	α-HCH	β-HCH	δ-HCH	ε-HCH	Sum of HCH (ng·g)	Sum of HCH (ng·g)
P1T	24±3	81±12	616±83	1077±166	17±2	78±4	314±34	647±87	7751±2160	1338±160
U1T	22±3	68±13	451±33	789± 97	18±1	84±7	311±15	627±49	11813±3175	923±21
P2T	24±1	80±10	464±17	881± 62	16±1	76±5	319±31	651±52	5032±5485	113±24
U2T	24±2	69±8	538±27	996± 70	15±2	85±13	273±18	632±41	13015±970	20±2
Unplanted sediment	22±2	43±11	431±40	766± 99	13±2	53±8	311±25	693±58	---	---

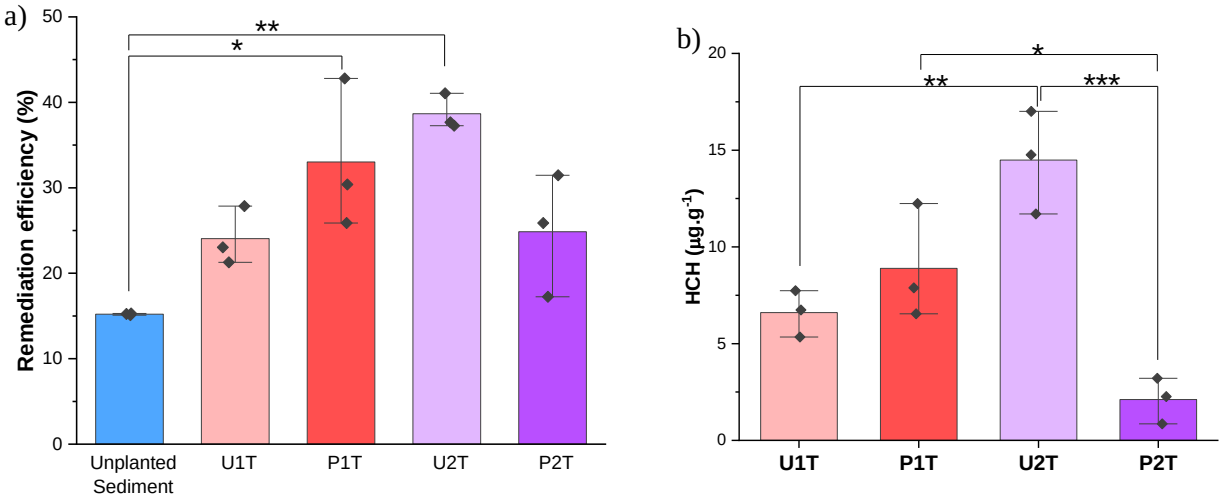

Figure 18. a) Removal efficiency [%] for unplanted sediment (blue), 1-year-old plants (red) and 2-year-old plants (purple); b) sum of HCH isomers in roots of 1-year-old plants (red) and 2-year-old plants (purple) Statistical evaluation - one-way Anova, two-way Anova, significance level α = 0.05; *p <0.05; ** p < 0.01, ***p < 0.001

3.3 Plant hormones

Eight basic plant hormones were selected for analysis and determined in the root and leaf parts of the plants. Although the results are variable, it is possible to observe changes in both matrices depending on the type of treatment. The results of the selected hormones are shown in Figure 19. Indole-3-acetic acid and its metabolite, 2-oxindole-3-acetic acid (oxIAA), have been reported mainly in root biomass, where it is one of the main sites of synthesis (Le Bris, 2017). In both age A. glutinosa groups, both pruning and the application of HCH were found to lower IAA levels, which corresponded with a decrease in biomass. Simultaneously, a significant increase in oxIAA concentration was observed in the root biomass of plants exposed to both stress stimuli.

One of the crucial mediators for regulating the stress response in plants is ABA. Abiotic stresses can be accompanied by cell desiccation and osmotic imbalance. These phenomena are regulated by ABA in cooperation with other elements in signaling pathways (Hsu et al., 2021; Sah et al., 2016; Tuteja, 2007). In the case of this experimental set up, a concentration trend in leaf biomass was observed. In both age groups, there was a decrease in ABA at pruning and in the presence of HCH. The overall reduction in co-occurrence after pruning and HCH treatment was approximately threefold in both groups. At simultaneous antagonism in concentration changes between ABA and JA was observed. Other hormones monitored were SA and JA. The relationship between these hormones was monitored mainly in the leaf part of the plants. The results suggest that the response to mechanical stress is mainly realized by an increase in JA concentration and a decrease in SA concentration, independent of plant age or the presence of the chemical. In the case of the response to chemical stress, the response differed, with a

significant increase in the concentration of SA accompanied by an increase in JA in 1-year-old plants, whereas a decrease in the concentrations of both these phytohormones was observed in 2-year-old plants. Under both stress stimuli, an increase in SA and JA was observed for 1-year-old plants. For 2-year-old plants, the concentrations of both hormones studied were reduced when compared to the unpruned uncontaminated group.

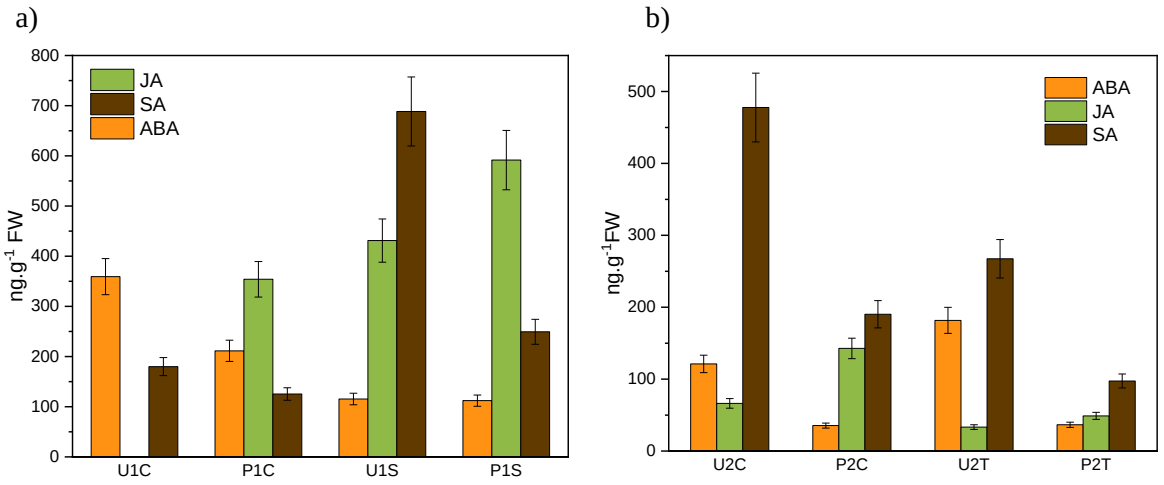

Figure 19.Concentration of selected hormones in leaves of a) 1-year-old and b) 2-year-old Alnus glutinosa plants; U - unpruned; C - control without HCH; P - pruned; T - treated with HCH

3.4 Microbial community

Plants increased the richness of bacterial community. It is important to note that before planting we detect high amount *lin* genes in polluted sediment, but when the experiment was terminated, there were no *lin* genes in unplanted control (Table 10). We can conclude that plant itself increased the richness of bacterial abundance especially species involved in degradation of HCH compounds. Exudates from the plant have been shown to influence the rhizosphere bacteria (Schnoor et al., 2008). The high relative quantity of the *linA* genes detected in all treated samples was presumably due to the high content of ε-HCH in the soil. Bala et al demonstrated conversion of the ε-HCH to a mixture of 1,2,4-, 1,2,3-, and 1,3,5-trichlorobenzenes without the accumulation of pentachlorocyclohexene as intermediate by LinA enzymes (Bala et al., 2012).

It is also interesting that the relative abundance of *linA* was higher compared to *linB* and *linD* in both the planted and unplanted samples. This observation may suggest that *linA* is the dominant gene involved in the degradation of HCH compounds in the soil samples. As well as the relative abundance of the *linA* gene is higher in the rhizosphere sample compared to the soil sample. This suggests that the presence of plant roots may have a positive effect on the abundance of *linA* genes involved in the degradation of the pesticide.

Rhizosphere samples showed higher bacterial abundance and *lin* genes than soil samples (Table 10, 11). As expected, *lin* genes were detected in a low quantity in control samples or not detected at all. In the treated rhizosphere samples *lin* genes were present in all samples, but behavior is quite different. *LinA* was detected in highest quantity in sample of 1-year old pruned saplings, which shows better removal efficiency comparing to unpruned one. Opposite trend was for *linB* genes, highest quantity was detected from samples in 2 years old unpruned saplings. *LinB-RT*, and *linD* were detected in all samples, but highest quantity is in samples from 1-year old sapling samples which shows higher removal efficiency comparing to 2-year-old saplings.

Overall, the qPCR results suggest that planting has an impact on the abundance of *lin* genes in the soil samples and may potentially enhance the degradation of HCH compounds.

Table 10. Relative abundance of genes indicating total bacterial biomass (16S rDNA), dehydro-chlorinase (*linA*), haloalkane dehalogenase (*linB, linB-RT*), and reductive dechlorinase (*linD*) in the soil samples (average of triplicate samples). The color scale indicates the relative quantity of a given marker: red (+++) highest, orange (++) high, yellow (+) intermediate quantity, (+-) low quantity and ND = not detected or below the LOQ.

		Total bacterial biomass	Lindane-degrading bacteria			
		16S rDNA	dehydrochlorinase	haloalkane dehalogenase	haloalkane dehalogenase	reductive dechlorinase
		U16SRT	*linA*	*linB*	*linB-RT*	*linD*
Control	U1C	++	+-	ND	+-	ND
	P1C	++	+-	ND	+-	ND
	U2C	+++	+-	ND	+-	ND
	P2C	++	++	ND	ND	ND
	Control, before planting	++	+-	+-	+	+-
Treated	U1C	++	+++	ND	ND	ND
	P1C	++	+++	ND	ND	++
	U2C	++	+++	ND	ND	+-

	P2C	++	+++	ND	+++	++
	Sediment unplanted	+-	ND	ND	ND	ND
	Sediment before planting	++	+++	+++	+++	+++

Table 11. Relative abundance of genes indicating total bacterial biomass (16S rDNA), dehydro-chlorinase (***linA***), haloalkane dehalogenase (***linB, linB-RT***), and reductive dechlorinase (***linD***) in the rhizosphere samples (average of triplicate samples). The color scale indicates the relative quantity of a given marker: red (+++) highest, orange (++) high, yellow (+) intermediate quantity, (+-) low quantity and ND = not detected or below the LOQ.

		Total bacterial biomass	Lindane-degrading bacteria			
		16S rDNA	dehydrochlorinase	haloalkane dehalogenase	haloalkane dehalogenase	reductive dechlorinase
		U16SRT	*linA*	*linB*	*linB-RT*	*linD*
Control	U1C	+++	ND	ND	ND	ND
	P1C	+++	+-	ND	+-	ND
	U2C	+++	ND	+-	+-	ND
	P2C	++	ND	+-	+-	ND
	1-year-old before planting	+	ND	+-	ND	+-
	2-year-old before planting	++	+-	+-	+-	ND
Treated	U1C	++	++	+-	+++	+++
	P1C	+++	+++	+-	+++	+++
	U2C	+++	++	+-	+-	++
	P2C	+++	++	+++	++	++

Rhizosphere 1-year-old A. glutinosaThe abundance of the *Comamonadaceae* in treated samples is increased comparing to control samples (Figure 20). *Flavobacterium* decreased in all samples. *Desulfocapsaceae, Ferribacterium, Sideroxydans, Sulfuricurvum, WCHB1-32* increased in treated samples comparing to control samples and they were not detected in unplanted rhizosphere samples. Liu demonstrated that natural iron oxides could enhance the reductive dichlorination of DDT under submerged condition, attributed to the production of reductive Fe^{2+} as an electron donor for reductive dechlorination. In addition, iron-oxides could stimulate iron reducing bacteria to conduct dissimilatory iron reduction, which could promote the reductive dechlorination of OCP either by transferring the electrons to OCP directly or by acting as a conductor to accelerate the interspecific electron transfer of microorganisms and then stimulate activity of different anaerobic microorganisms by the mechanism of microbial mutualism (Cruz Viggi et al., 2014; Maphosa et al., 2010).

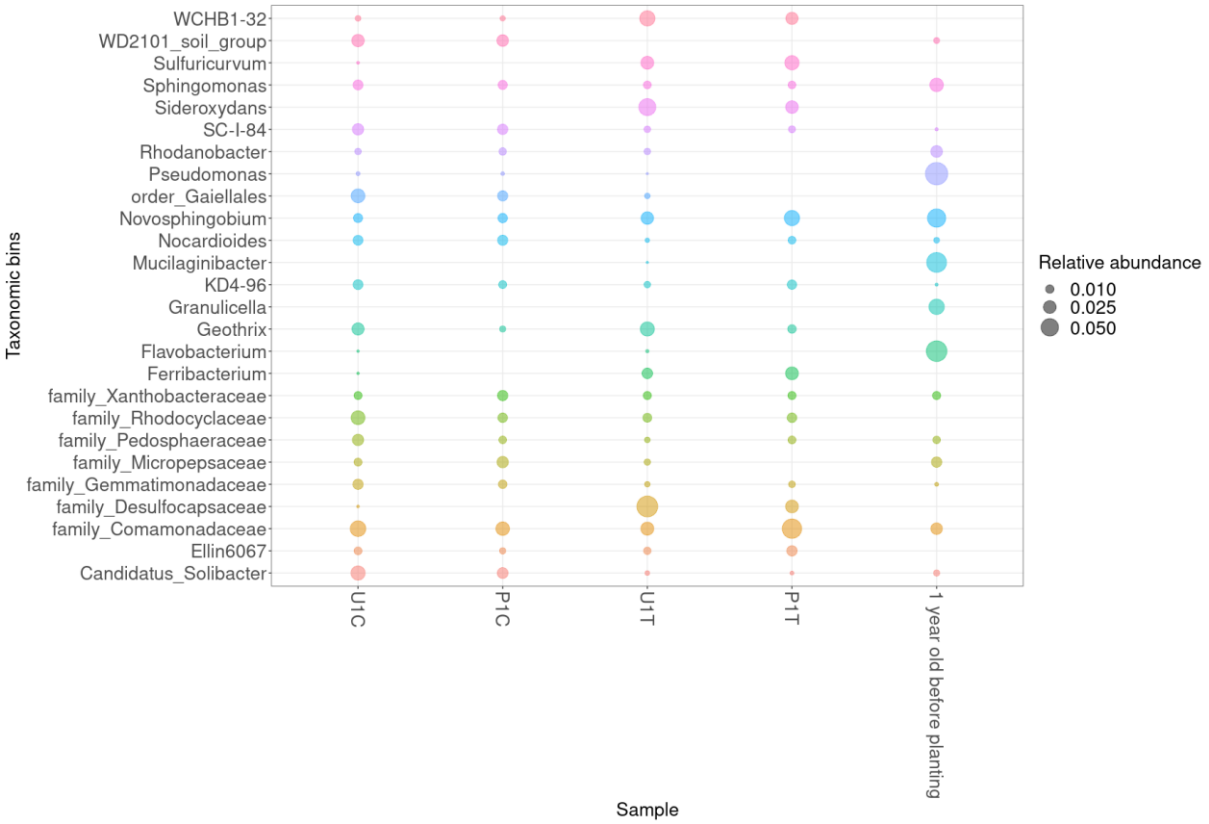

Figure 20. Relative abundance (mean > 0.0075) of bacteria in 1 year old sapling rhizosphere samples.

Rhizosphere 2-year-old A. glutinosa

Burkholderia-Caballeronia-paraburkholderia, class_Acidimicrobiia, family_Caulobacteraceae, Xanthobacteraceae, Granulicella, Occallatibacter, Gaiellales were mostly abundant in control samples than in treated samples (Figure 21). On the other hand, *Commamonadacea, Rhodoferax* was

more abundant in treated samples. *Sulfuricurvum* detected in highest abundance in unpruned treated samples.

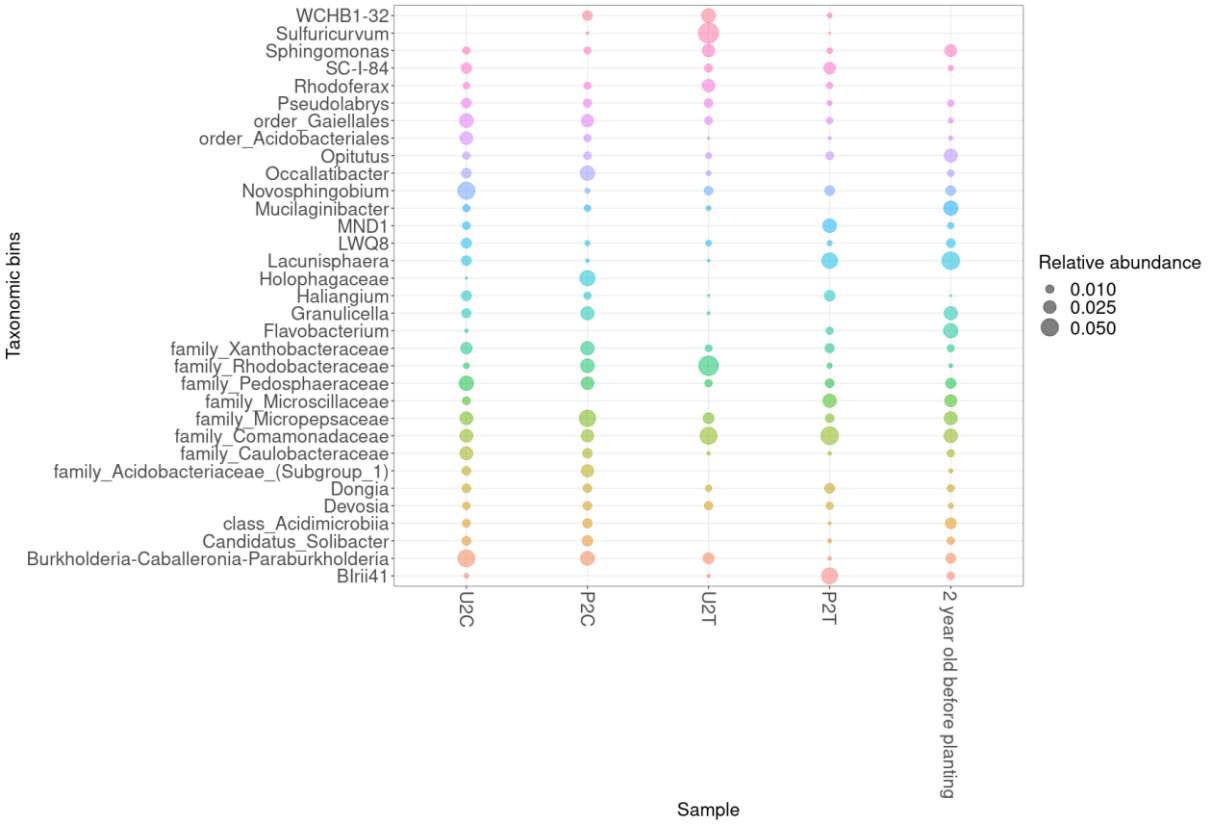

Figure 21. Relative abundance (mean > 0.0075) of bacteria in 2 year old saplings rhizosphere

Soil 1-year-old

During the 3 month of the experiment there were no significant changes in bacterial community for unplanted samples (Figure 22). Planting slightly changed the composition of the microbial community. P9x2b3d02 abundance increased in planted samples while in unplanted it was not detected. Overall treated soil samples were rich on *aminicenantales, bacteroids_vadinha17, thermosulfovibrionia, kd4-90, anaerolineacea,* etc.

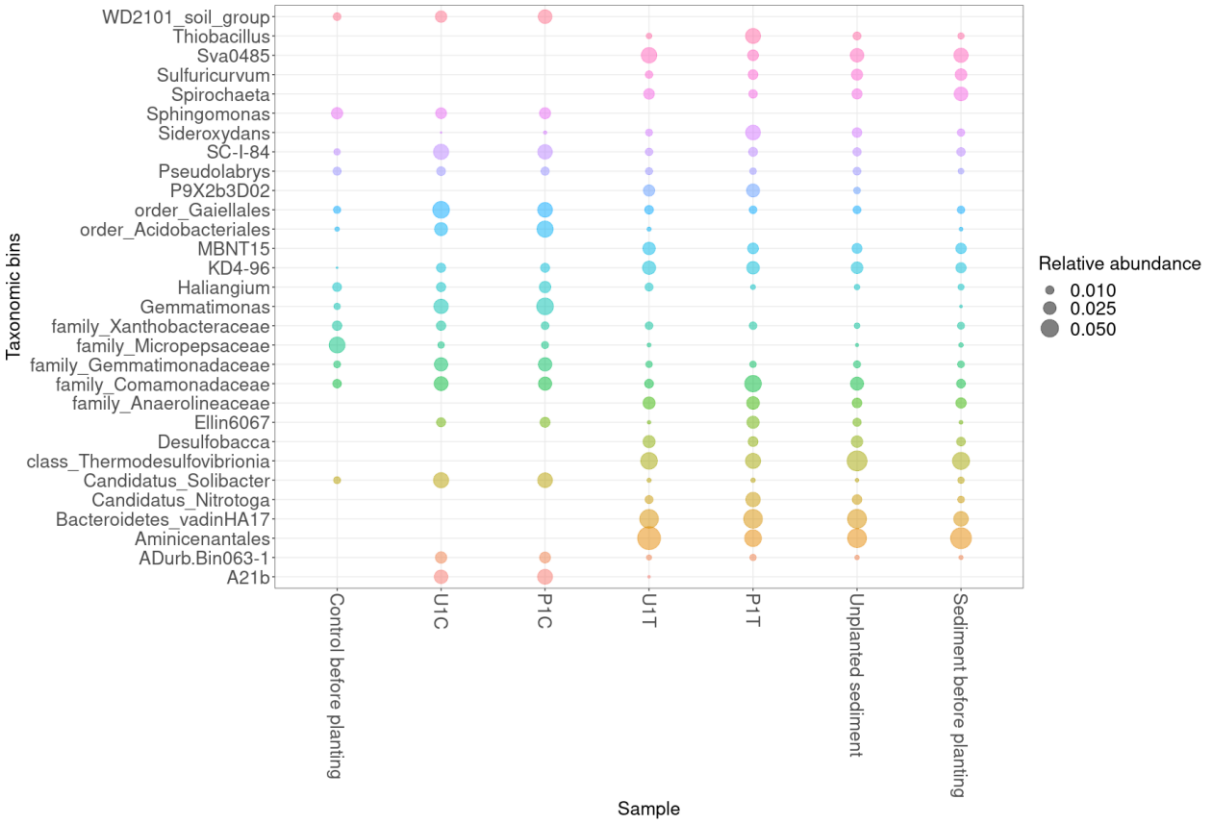

Figure 22. Relative abundance (mean > 0.0075) of bacteria in soil samples planted with 1 year old saplings.

Soil 2-year-old

Comamonadaceae increased in planted treated samples (Figure 23). The plant might positively influence this species same as to *KD4-96; MBNTI5; P9x2b3d02* and S*ulfuricurvum*.

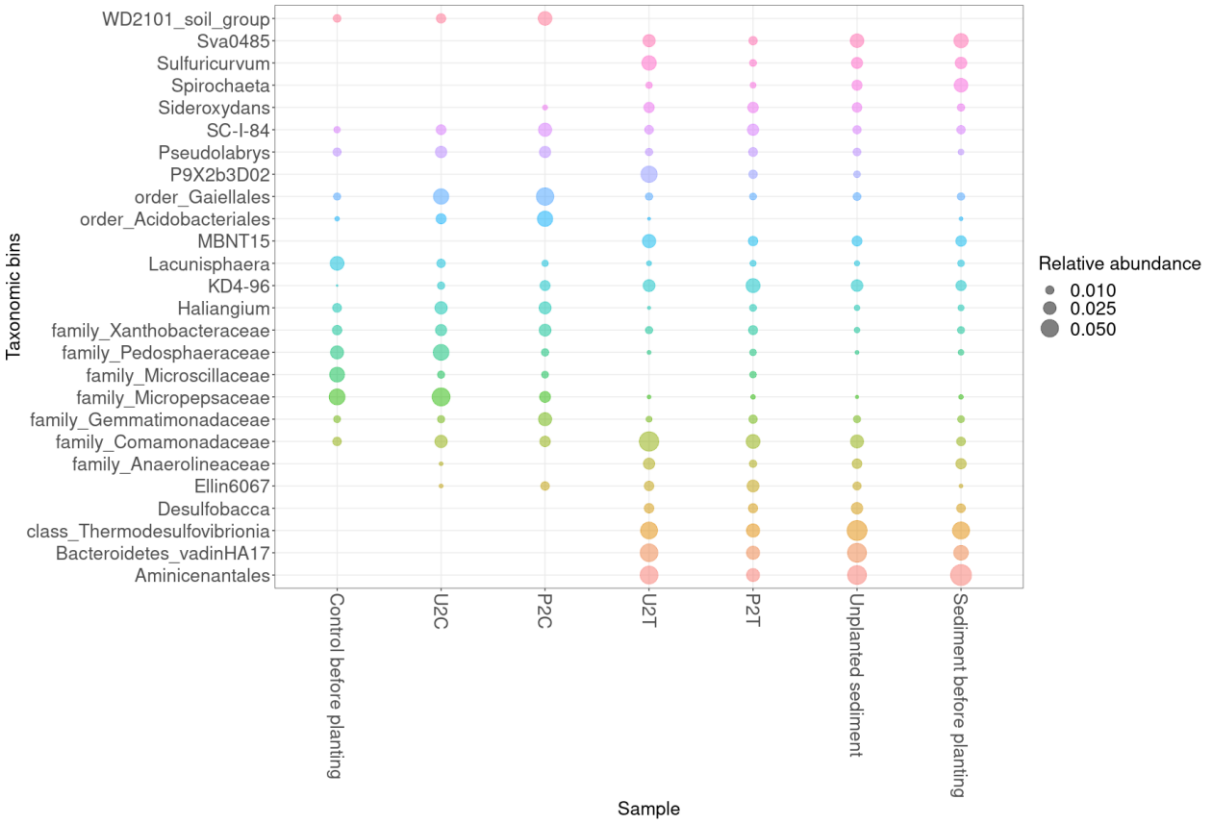

Figure 23. Relative abundance (mean > 0.0075) of bacteria in soil samples planted with 2 year old saplings.

In the rhizosphere PCoA plot, the samples from each group tend to cluster together, indicating that the microbial community composition was different between the treatment groups (Figure 24). In the soil PCoA plot, there is some overlap between the treatment groups, but they still appear to be somewhat separated (Figure 25). This suggests that the soil microbial community composition may also be influenced by the treatment, but to a lesser degree than in the rhizosphere. Overall, these plots provide a visual representation of the differences in microbial community composition between the samples and can help identify potential patterns or relationships in the data.

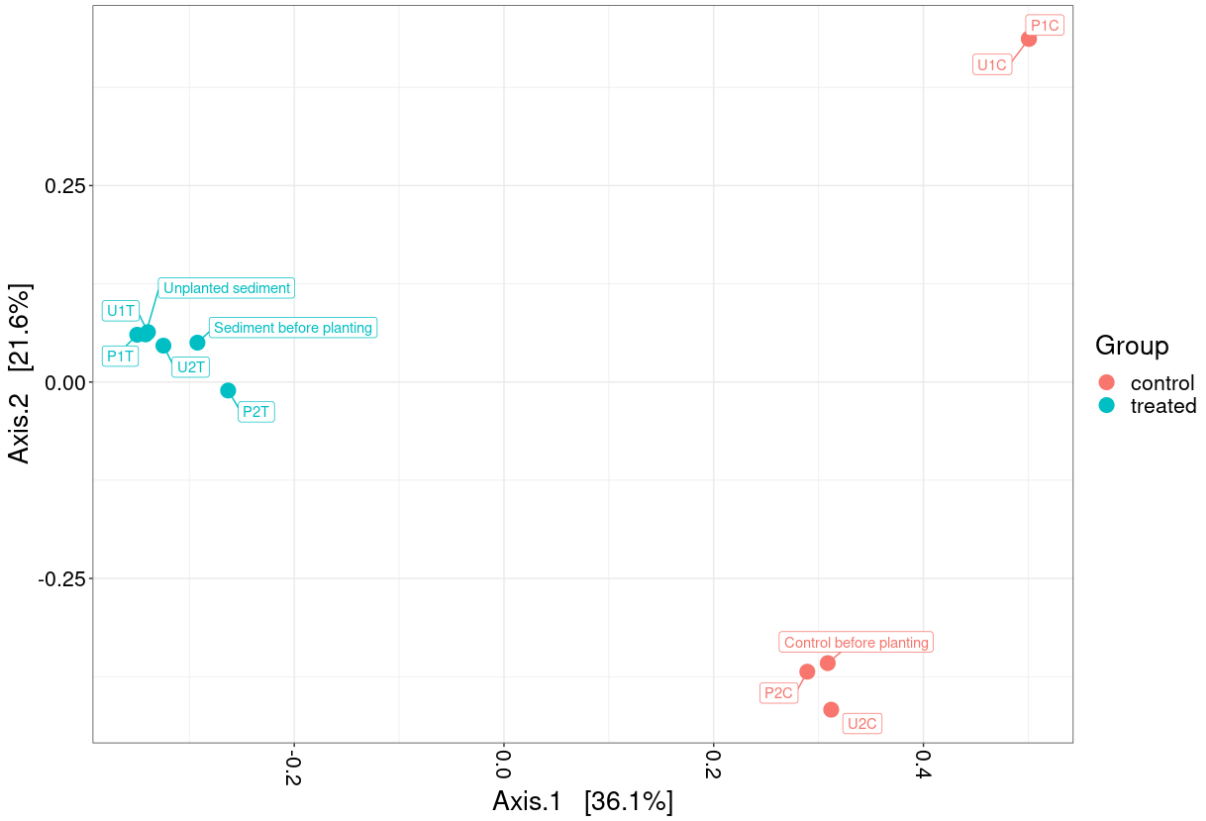

Figure 24. PCoA of the rhizosphere samples

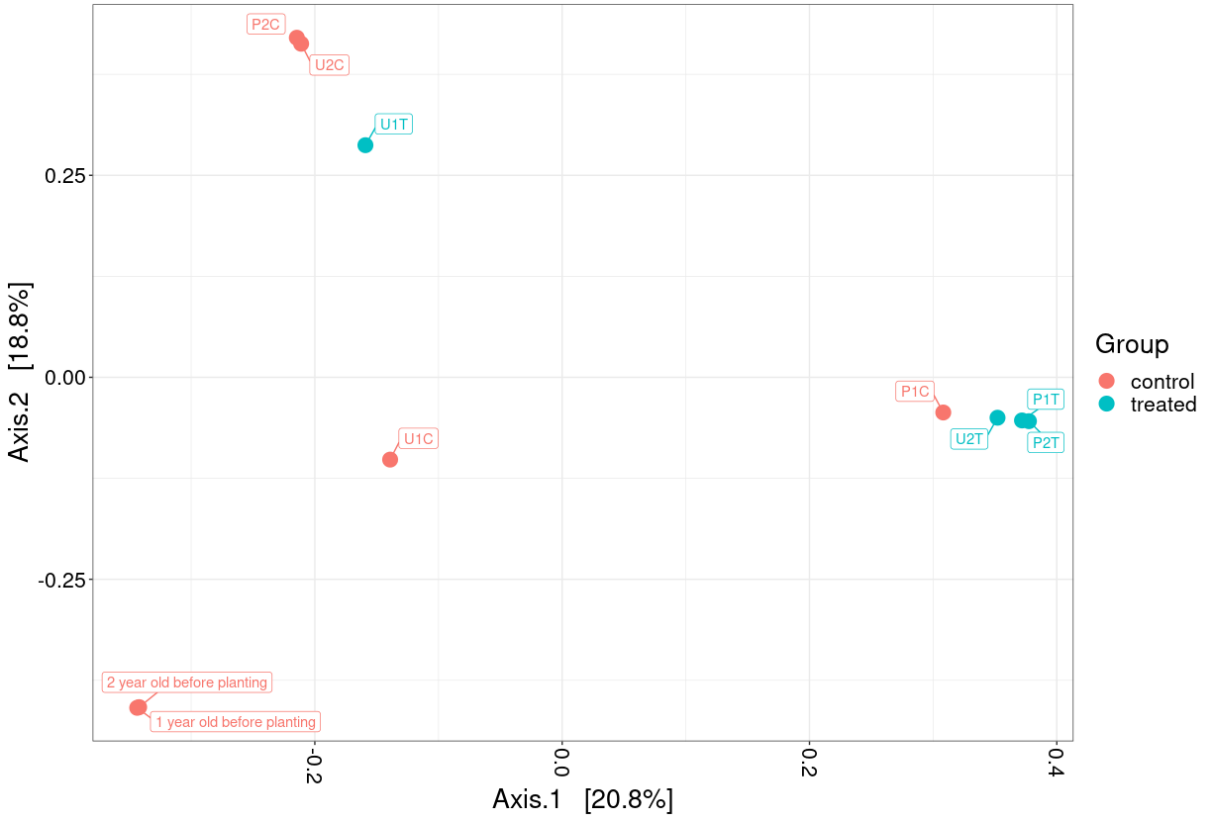

Figure 25. PCoA of the soil samples

4. Discussion

The results of this study provide important insights into the performance of *A. glutinosa* saplings in contaminated soil with HCH and the associated microbial abundance in soil and rhizosphere. Overall, the findings suggest that *A. glutinosa* seedlings are effective in accumulation of HCH-contaminated soil and can enhance microbial abundance in the rhizosphere.

The results indicate that the performance of *A. glutinosa* seedlings is influenced by the concentration of HCH in the soil. Specifically, the shoot and root dry weights of the seedlings were significantly lower in the highest concentration of HCH (200 mg/kg) compared to the lowest concentration (50 mg/kg). This finding is consistent with previous studies that have shown that high levels contamination in the soil can negatively impact plant growth and development (Singh et al., 2016).

The results also indicate that *A. glutinosa* saplings can enhance microbial abundance in the rhizosphere, as indicated by the higher microbial biomass in the rhizosphere soil compared to bulk soil. This finding is consistent with previous studies that have shown that plant roots can promote microbial growth and activity in the rhizosphere (Bais et al., 2006).

In addition, the results suggest that the performance of *A. glutinosa* saplings in phytoremediation is influenced by the duration of exposure to contaminated soil. Specifically, the two-year-old saplings showed significantly higher shoot and root dry weights compared to the one-year-old saplings in all concentrations of HCH. This finding is consistent with previous studies that have shown that longer exposure to contaminated soil can enhance the ability of plants to remediate contaminants (Baker et al., 1999).

The hormone analysis conducted in this study revealed significant changes in the levels of several hormones in the roots and shoots of alder seedlings exposed to HCH contamination.

The observed changes in hormone levels suggest that the plant response to HCH contamination involves a complex interplay between different hormone pathways. Auxins, ABA, SA AND JA are known to play important roles in plant growth and development, as well as in stress responses (Bais et al., 2006; Baker et al., 1999). The increased levels of these hormones in the roots of HCH-exposed seedlings may indicate a mechanism for coping with the toxic effects of HCH in the soil.

The decreased levels of abscisic acid in the roots of HCH-exposed seedlings may also be indicative of a stress response. Abscisic acid is known to play a key role in regulating plant responses to water stress, as well as in mediating other stress responses (Baker et al., 1999). Overall, the hormone analysis results provide valuable insights into the mechanisms underlying the plant response to HCH contamination. The observed changes in hormone levels suggest that the plant response is complex and involves

multiple pathways. However, further research is needed to fully understand the specific roles of each hormone in the response to HCH contamination, as well as to investigate potential crosstalk between different hormone pathways.

While the results of this study are promising, there are several limitations that should be acknowledged. First, the study was conducted in a greenhouse setting, which may not accurately reflect the conditions in natural environments. Second, the study focused on a single plant species, which may not be representative of other plant species that are commonly used in phytoremediation. Finally, the study did not investigate the mechanisms underlying the observed effects of *A. glutinosa* seedlings on microbial abundance in the rhizosphere.

In conclusion, this study provides valuable insights into the performance of *A. glutinosa* seedlings in phytoremediation of HCH-contaminated soil and their impact on microbial abundance in the rhizosphere. Future research should focus on investigating the mechanisms underlying these effects and exploring the potential of other plant species in phytoremediation of HCH-contaminated soil.

5. Summary

A. glutinosa trees are promising candidates for OCP removal. They are participating on HCH removal and increasing the removal efficiency by 6.79 - 24.42 %. Pruning has in many cases a negative effect on total biomass, abundance of the *lin* genes and removal efficiency. However, one-year-old plants have a better prediction for establishing short rotation coppice culture than older plants. Hormone analysis and evaluation by PCA method indicated that hormones can be used as stress markers, however, it depends on the age of the plant, the stress stimulus and the analyzed plant part. *LinA* which encodes dehydrochlorinase was most detected in soil samples, while rhizosphere samples were rich on *linB-RT* and *linD* as well. Treated one-year-old plants rhizosphere was rich in sulfur and iron reducing bacteria.

Based on the results, it can be concluded that the presence of HCH in soil has a negative effect on the biomass of 2-year-old plants only when they are pruned. The remediation efficiency of HCH-contaminated soil was increased by the presence of both 1-year-old and 2-year-old alder plants, with the highest efficiency observed in pruned 1-year-old alders. The plant uptake of HCH followed the trend of remediation efficiency, with the highest concentrations observed in the root biomass. HCH concentrations were affected by pruning, with higher concentrations in 1-year-old alders and lower concentrations in 2-year-old alders. HCH isomers were not detected in leaf tissue, and no metabolites were found in plant biomass. The presence of HCH in soil also resulted in changes in the hormonal profile of the plants, depending on the type of treatment. Overall, this experiment indicates that planting

may have a positive impact on the diversity and richness of the bacterial community, which may be beneficial for the removal of pollutants in the soil. However more investigation is required to completely comprehend the mechanisms behind these findings and to identify the potential uses of this strategy in environmental remediation.

Overall, the results suggest that plants have the potential to remediate HCH-contaminated soil and that different plant species have different abilities to take up HCH from the soil. Additionally, the results suggest that the composition of microbial communities in the rhizosphere and soil are different, and that plants can enhance the microbial abundance in the rhizosphere.

Overall findings suggest that plant age, HCH applications, and hormonal concentrations can influence plant biomass, removal efficiency, and microbial abundance in the rhizosphere and soil. These results highlight the complex interactions between plants, HCH applications, and microbial communities' patterns or relationships.

III. Phytoremediation Potential of Selected Plant Species for HCH Contaminated Sites and Impact on Rhizosphere Microbiome: A Laboratory Study.

1. Background

The objective of this study is to assess the effectiveness of selected plant species, including *Typha latifolia*, *Juncus effusus*, *Phragmites australis*, and *Alnus glutinosa*, as phytoremediators for HCH-contaminated environments. Laboratory experiments conducted under controlled growth chamber conditions provide a platform for evaluating plant performance in removing HCH contaminants. Simultaneously, we explore the intricate interplay between these plants and the rhizosphere microbiome, investigating both microbial communities' composition and the presence of genes associated with HCH degradation. The study aims to shed light on how rhizosphere microbiota influence plant performance in HCH-contaminated environments.

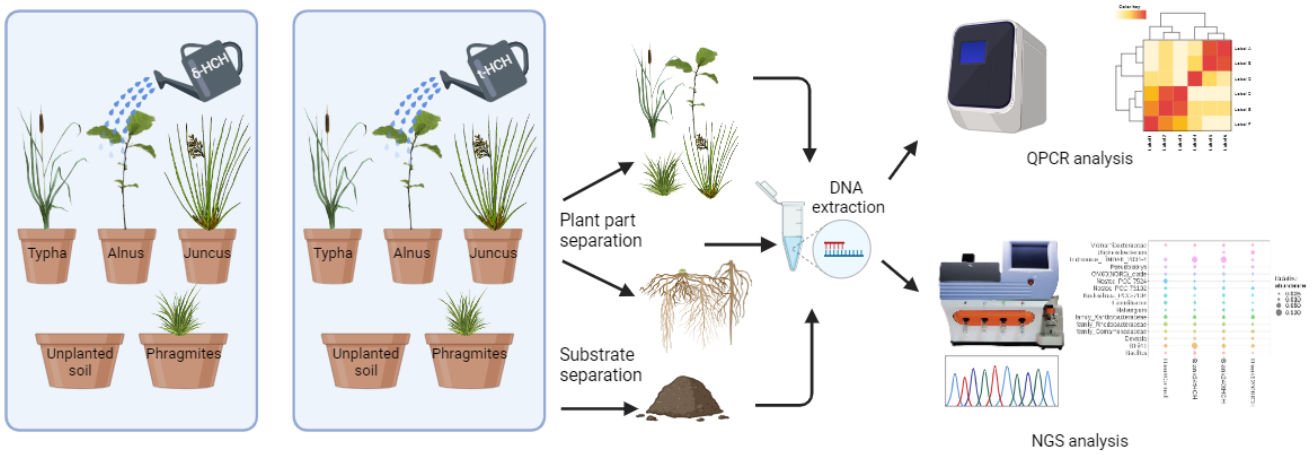

Figure 26. Graphical description of the experiment

2. Materials and methods

2.1 Experimental design

The bioaccumulation experiment was set up with 60 experimental units for targeted treatment involving δ-HCH and t HCH (Figure 26). These units were organized into five groups, encompassing four planted groups and one unplanted control group. Each group comprised 12 pots, further divided into four triplicates. The triplicates were exposed to three distinct pesticide concentrations (20, 200, 1000 µg·L-1), with one control triplicate. Wetland plant species: *Juncus effusus* (*J. effusus*), *Typha latifolia* (*T. latifolia*), and *Phragmites australis* (*P. australis*), were procured from Aarhus University (Denmark), while one-year-old *Alnus glutinosa* (*A. glutinosa*) seedlings were sourced from the Silva Taroucy Research Institute (RILOG, Czech Republic). For uniformity, similar-looking individual seedlings were selected, washed thoroughly, and planted in one-liter pots containing 800 ml of a mixed substrate, composed of sand, peat, and vermiculite in a 40%:30%:30% volume ratio. All materials originated from local sources and underwent chemical analysis to eliminate potential hexachlorocyclohexane (HCH) contamination. The prepared experimental units underwent a 28-day acclimatization in a greenhouse with controlled light (16h day/8h night) and temperature (min. 12°C), receiving regular irrigation and nutrition solutions. Following acclimatization, the plants were transferred to growth chambers, and their positions were altered weekly to mitigate chamber effects. The irrigation followed a predefined routine, and the light and temperature conditions were maintained at 16 hours/23°C day and 8 hours/17°C night, with a controlled relative air humidity of 70%.

2.2 Morphological and physiological measurements of plants

The experiment was conducted under the aforementioned climatic conditions. Morphological

parameters, encompassing plant weight, height, and chlorophyll content, were assessed biweekly. Plant height was determined as the distance from the soil surface to the stem's apex for *A.glutinosa* and *P. australis* , or to the highest point for *J. effusus* and *T. latifolia*. Additionally, *P. australis* and *J. effusus* shoots were marked for subsequent height measurements, while *T. latifolia* manifested as one or two shoots per pot. Recorded values represent triplicate averages. Plant weight was measured on the third day after the final irrigation. Stem thickness was evaluated using plant diameter, measured 5 cm above the soil with a caliper. Similar to height measurement, shoots of *P. australis* and *J. effusus* were marked. Chlorophyll content in fully developed top leaves was non-destructively determined using the Chlorophyll Meter SPAD 502 (Konica Minolta Inc., Tokyo, Japan). Photosynthetic measurements were conducted on fully developed leaves using the LI-6400 XT infrared gas analysis technique (IRGA) with a red-blue LED source (LI-COR Biosciences Inc., Lincoln, NE, USA). Measurements were carried out between 9 a.m. and 4 p.m. for two weeks before the experiment's conclusion. To ascertain the maximum light-saturated photosynthetic rate (Amax), the photon flux density was set at 1600 μmol PAR photons m^{-2}. s^{-1}. Measurements were conducted at a temperature of 25 °C, CO_2 concentration of 400 μmol. mol^{-1}, and airflow rate of 400 μmol. s^{-1}. Concurrently, stomatal conductance (gs), transpiration rate (E), and dark respiration (Rd) were determined. All values were recalibrated using specific leaf area (SLA; m2. $kgdw^{-1}$), derived from the ratio of the surface area of measured leaves to their dry biomass.

2.2 Chemical treatment

The t-HCH mixture (α: β: γ: δ = 1:1:1:1) and δ-HCH standards were purchased from Merck (St. Louis, Missouri, United States). The appropriate amount of each powder standard was weighed and dissolved in 96% ethanol to achieve the concentration of 1 $g \cdot L^{-1}$. The stock solutions were stored in the fridge at 4 °C for no longer than one month. The work solutions at the concentrations 20, 200, 1000 $\mu g \cdot L^{-1}$ were prepared fresh by diluting the stock solutions with the tap water right before irrigation. The plants and unplanted pots were treated weekly with the known volume of pesticide solutions and irrigated with nutrition solution once per two weeks.

2.3 Plant processing and analysis

All the soil and plant samples were collected at the end of the experiment. Before the following processing, plants were washed repeatedly with tap water to remove the soil residues and divided into the root and above-ground parts. All the plant parts were measured and group weighted, ground in the liquid nitrogen and store in the freezer until the analysis. The samples were subjected to two different extraction procedures: To determine HCH and ClB, the protocol described in Košková et al., 2022 was

applied (Košková et al., 2022). Here, acetone: hexane 1:1 (v/v) extracts were injected into GC/MS/MS with deuterium labelled γ-HCH internal standard.

The sample processing for the non-targeted analysis was performed as previously described by Souza et al (Perez de Souza et al., 2019). For the analysis, 100 mg of grounded biomass and 0.5 ml of extraction solution were used. The extraction solution was formed by pure methanol and water 8: 2 (v/v) with the isotopic labelled acetaminophen. Subsequently, the prepared samples were analysed by LC/HRMS. All plant biomass samples were analysed by IDA (Information dependent acquisition) and SWATH acquisitions (Analytics software, AB Sciex, MA, USA). IDA acquisition allows obtaining better quality spectra for subsequent identification using libraries (Natural Products HR-MS/MS 2.0, NIST 2017, AB Sciex, MA, USA). Analysis using SWATH acquisition allows data collection to perform fragmentation of all compounds present in the sample. These data were used to search for theoretical metabolites and their fragment spectra. Validation was carried out using the control.

For the molecular biology analysis, the substrate samples together with rhizosphere samples were collected. Substrate were mixed and 1 g of the sample was collected for molecular biology analysis. Rhizosphere soil obtained by shaking roots to remove bulk soils, and the remaining soils sticked to roots placed in a 50-ml test tube containing 35 ml of sterile phosphate buffer and then shaking for 5 min. The resultant solution was then centrifuged 10 min at 4,000 × g at a temperature of 4 °C to obtain biomass for DNA extraction.

2.4 Statistics

The software Origin, Version 2019b (OriginLab Corporation, Northampton, MA, USA) was used for statistical analysis and results visualization. The effect of plants on the HCH removal and plant biomass were evaluated using one-way ANNOVA at the significance level of 0.05, followed by the post hoc Tukey test. All the samples were analysed for homogeneity of variance using the Levene's test. The software MarketView 1.3.1. (AB Sciex, MA, USA) was applied for the supervised principal components - discriminant model (PCA-DA) to illustrate the metabolic variation between the control and treated group.

2.5 Molecular genetic analysis

DNA extraction, real-time quantitative PCR, amplicon 16S rRNA sequencing were described in previous study in section 1.5 of I. HCH Removal in constructed wetland beds

2.6 Bioinformatic analysis

The raw Ion Torrent reads were processed with QIIME 2 2021.8 software (Bolyen et al., 2019). Raw sequence data were demultiplexed and quality filtered using the q2-demux plugin followed by denoising with DADA2 (Callahan et al., 2016). Reads below 250 bp were removed. Taxonomy was assigned to ASVs using the q2-feature-classifier (Bokulich et al., 2018) classifysklearn naive Bayes taxonomy classifier against the Silva 138 database (Quast et al., 2013) and then Mitochondria and Chloroplast were removed. The accuracy of classification was evaluated against an artificial MOCK com-munity sample. QIIME 2 outputs were processed using the phyloseq R package (McMurdie and Holmes, 2013).

3. Results and discussion

3.1 Morphological and Physiological Parameters

The biomass results were variable but no statistically significant difference between the treated and control groups in both HCH exposures was observed (Figure 27). However, the presence of HCH resulted in the higher biomass production the case of *T. latifolia* and *A. glutinosa*. Similarly, for the plant height no statistically significant difference between the treated and control groups was observed. In the case of *J. effusus* and *P. australis* exposed to the highest δ-HCH concentration, the final observed plants were shorter, but it can still be only statistical deviation (Figure 28). The relative chlorophyll content was adversely affected but again without statistical significance (Figure 29). These results correlate with the conclusion of study that was focused on the relationship between the chlorophyll content and exposure to ClB and γ-HCH in the concentration higher than 10 $mg \cdot L^{-1}$ (Faure et al., 2012). Similarly, the results of photosynthetic parameters demonstrated the possible adverse effect of HCH (Figure 30- 33). γ-HCH has been described as the inhibitor of photosystem II in cyanobacterium *Anabaena* (Bueno et al., 2004). Due to time consumption of analysis, the photosynthetic measurements were always performed in triplicate on one plant of a given species from a given group. Therefore, a statistical evaluation cannot be fully used; rather, it is a screening of the impact on the plant species under study.

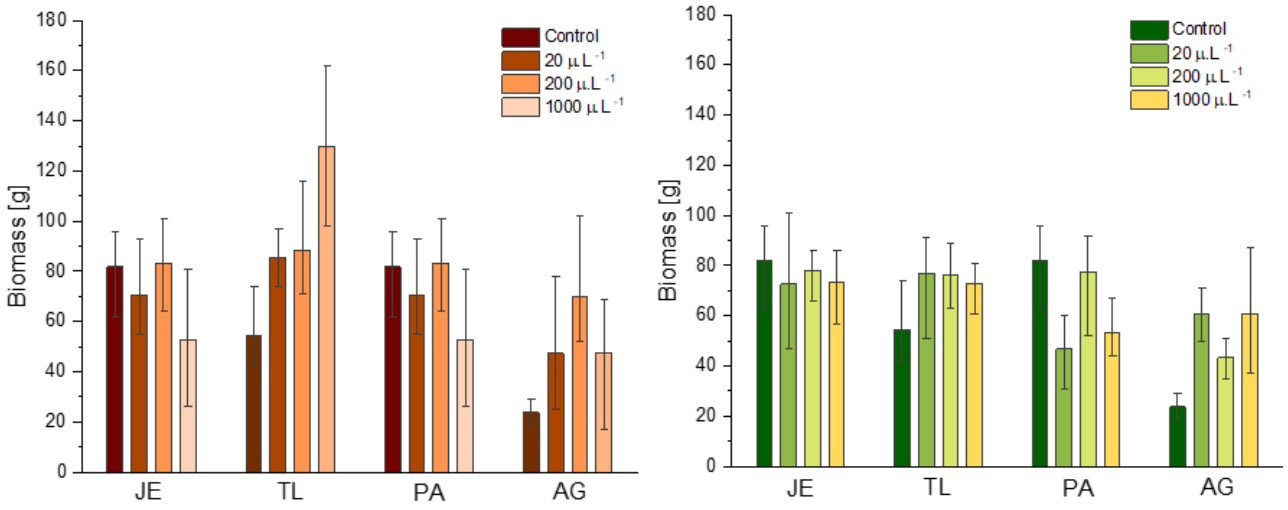

Figure 27.The total biomass for all plant species a) treated with δ-HCH; b) treated with t-HCH; JE - *Juncus effusus*, TL - *Typha latifolia*, PA - *Phragmites australis*, AG - *Alnus glutinosa*; Statistical assessment: one-way ANOVA, significance level α = 0.05; * p < 0,05, **p < 0.01, *** p < 0.001

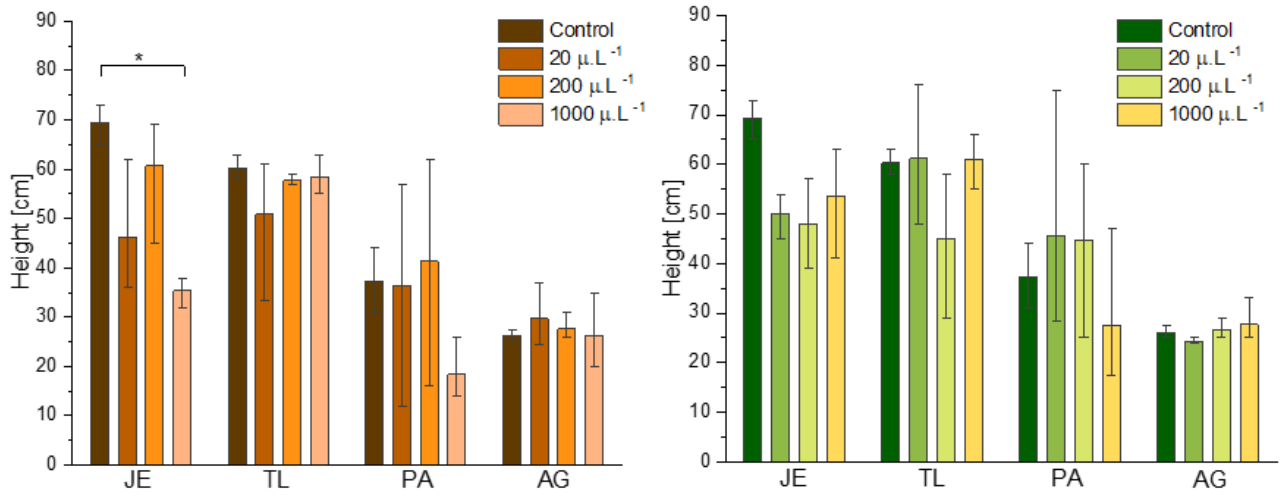

Figure 28. The total height for all plant species a) treated with δ-HCH; b) treated with t-HCH; JE - *Juncus effusus*, TL - *Typha latifolia*, PA - *Phragmites australis*, AG - *Alnus glutinosa*; Statistical assessment: one-way ANOVA, significance level α = 0.05; * p < 0,05, **p < 0.01, *** p < 0.001

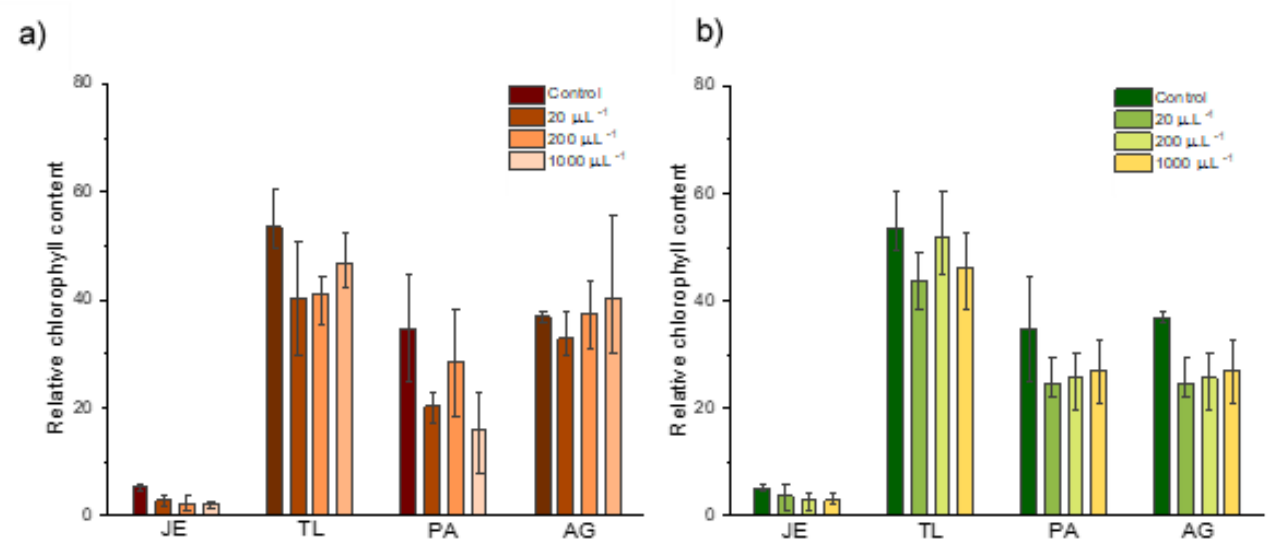

Figure 29. The relative chlorophyll content for all plant species a) treated with δ-HCH; b) treated with t-HCH; JE - *Juncus effusus*, TL - *Typha latifolia*, PA - *Phragmites australis*, AG - *Alnus glutinosa*; Statistical assessment: one-way ANOVA, significance level α= 0.05; * p < 0.05, **p < 0.01, *** p < 0.001

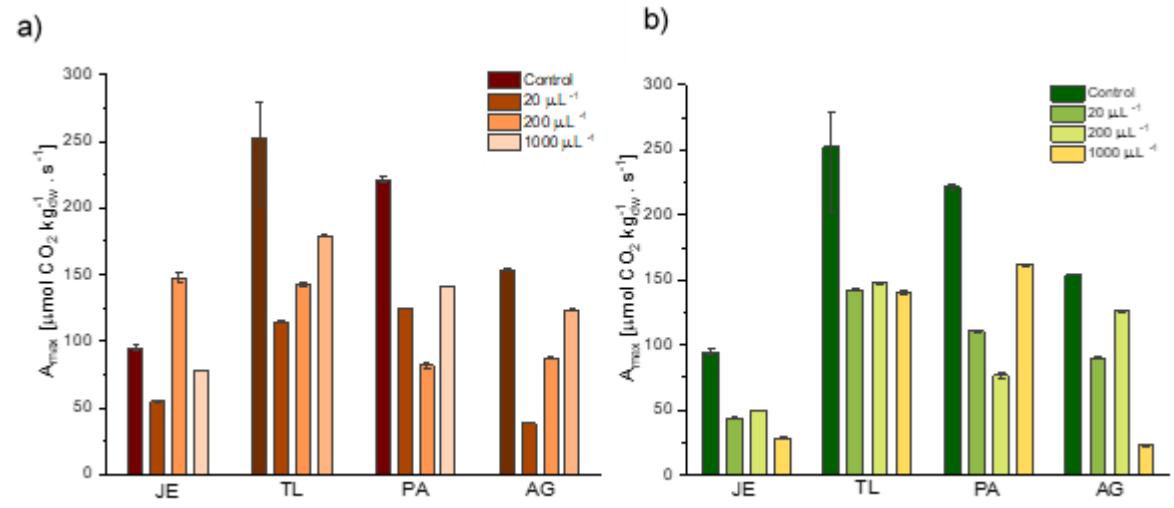

Figure 30. Photosynthetic measurements - Amax for all plant species a) treated with δ-HCH; b) treated with t-HCH; JE - *Juncus effusus*, TL - *Typha latifolia*, PA - *Phragmites australis*, AG - *Alnus glutinosa*

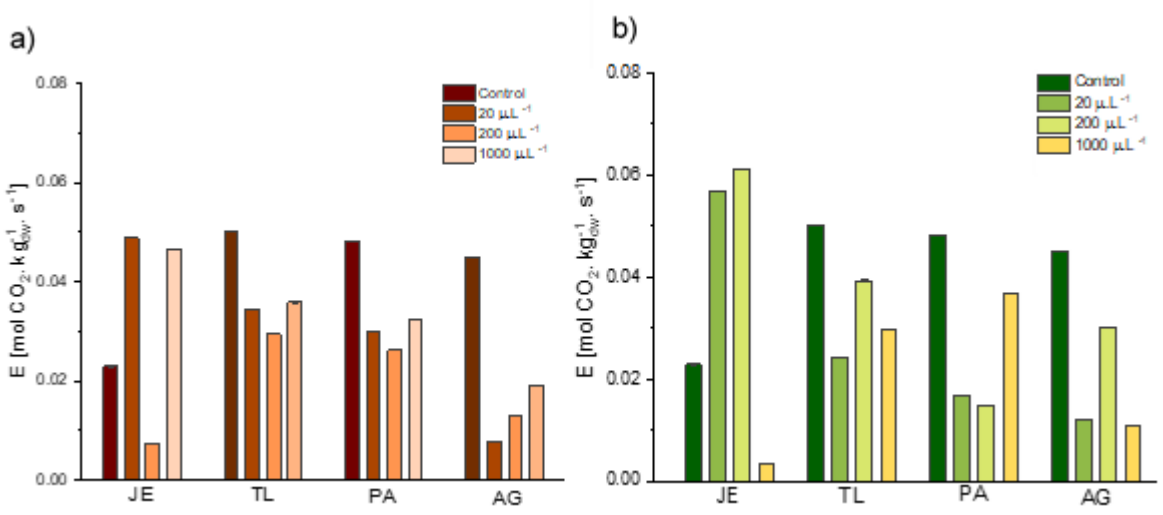

Figure 31. Photosynthetic measurements - E for all plant species a) treated with δ-HCH; b) treated with t-HCH; JE - *Juncus effusus*, TL - *Typha latifolia*, PA - *Phragmites australis*, AG - *Alnus glutinosa*

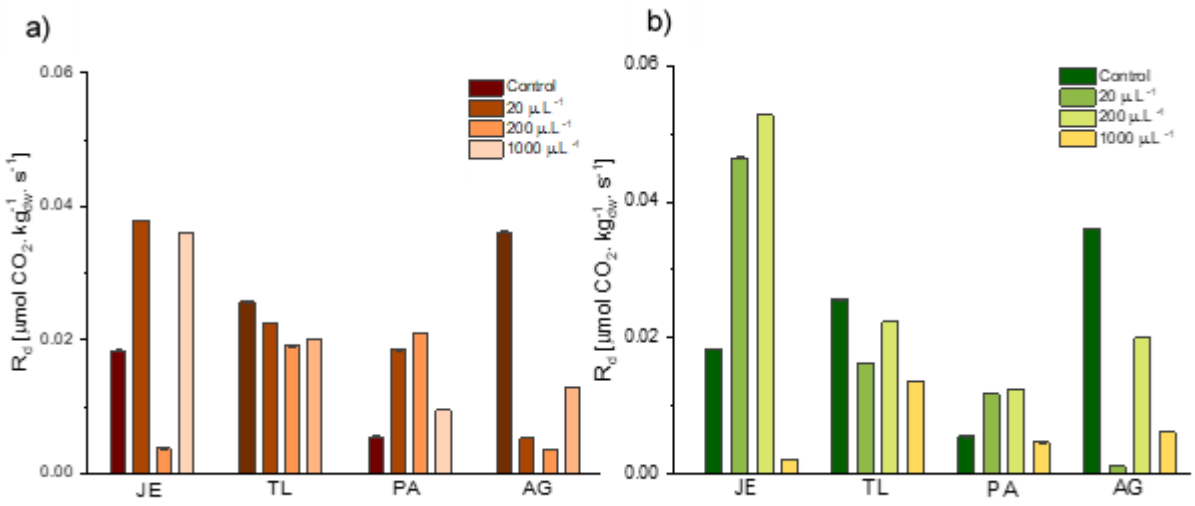

Figure 32. Photosynthetic measurements - Rd for all plant species a) treated with δ-HCH; b) treated with t-HCH; JE - *Juncus effusus*, TL - *Typha latifolia*, PA - *Phragmites australis*, AG - *Alnus glutinosa*

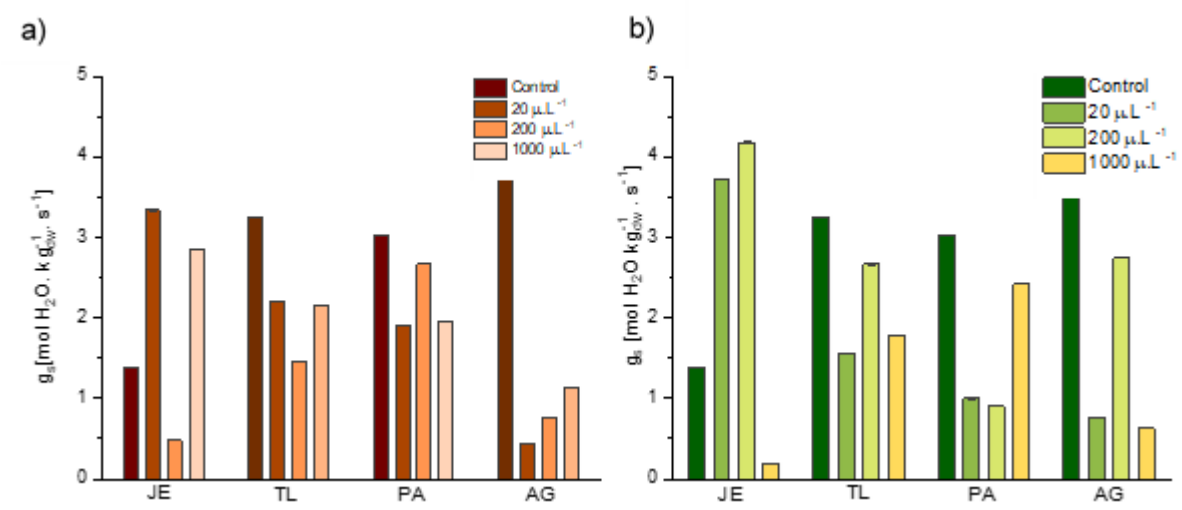

Figure 33. Photosynthetic measurements - gs for all plant species a) treated with δ-HCH; b) treated with t-HCH; JE - *Juncus effusus*, TL - *Typha latifolia*, PA - *Phragmites australis*, AG - *Alnus glutinosa*

3.2 Results of HCH Analysis

The study involved unplanted soil controls to observe HCH behaviour in the substrate, revealing a decrease in HCH concentration attributed to biotic and abiotic degradation, volatilization, and pot adsorption. Blank experiments indicated an average removal of approximately 25% of initial HCH amounts, with slightly lower removal (15%) for t-HCH. For planted experiments, HCH concentrations were determined in soil, roots, and aboveground parts, allowing estimation of missing HCH amounts potentially removed by plant mechanisms such as transformation and volatilization. Results, presented in Table 12 and Figure 34a for the δ-HCH group, highlighted significantly higher HCH removal in *J. effusus* and *A.glutinosa* compared to *T. latifolia* and PA. The positive impact of plants was most pronounced at a medium δ HCH concentration of 200 $\mu g \cdot L^{-1}$. Root biomass concentrations correlated with pesticide dose, with *A.glutinosa* exhibiting the highest HCH concentrations at all exposure levels. Isomer detection in plant species indicated the presence of α-HCH, β-HCH, and γ-HCH, with *A.glutinosa* displaying these isomers even at the lowest δ-HCH concentration. The results also revealed the presence of degradation products, such as 1,3-diClB, in roots, suggesting potential HCH degradation in the rhizosphere. Aboveground parts showed increasing HCH concentrations corresponding to applied doses, with *A.glutinosa* trunks exhibiting higher concentrations than leaves, attributed to volatilization. The study provides valuable insights into the efficacy of different plant species as phytoremediators and the complex dynamics of HCH removal and degradation products in the rhizosphere.

Table 12. Summary of HCH analysis results for the δ-HCH exposed group

δ-HCH	δ-HCH [μg·L^{-1}]	RE_{TOT} [% of HCH dose]	Sum of HCH in roots [% of HCH dose]	Sum of HCH in above-ground parts [% of HCH dose]	Metabolism degradation volatilization of HCH [%]
J. effusus	20	52	13	2.9	12
	200	66	11.0	1.9	47
	1000	53	6	10	24
T. latifolia.	20	33	4	2	13
	200	42	6	1	15
	1000	22	6	4	14
A. glutinosa	20	54	25	2.4	10.7
	200	66	22	2.2	40
	1000	46	22	4.4	23.1
P. australis	20	25	11	3	9
	200	38	8	2	35.9
	1000	8	6	5	0

The values are listed as the average of 9 measurements (3 samples of 3 parallel experiments). Standard deviation for the experimental set-up was determined to be 32 % of the reported values.

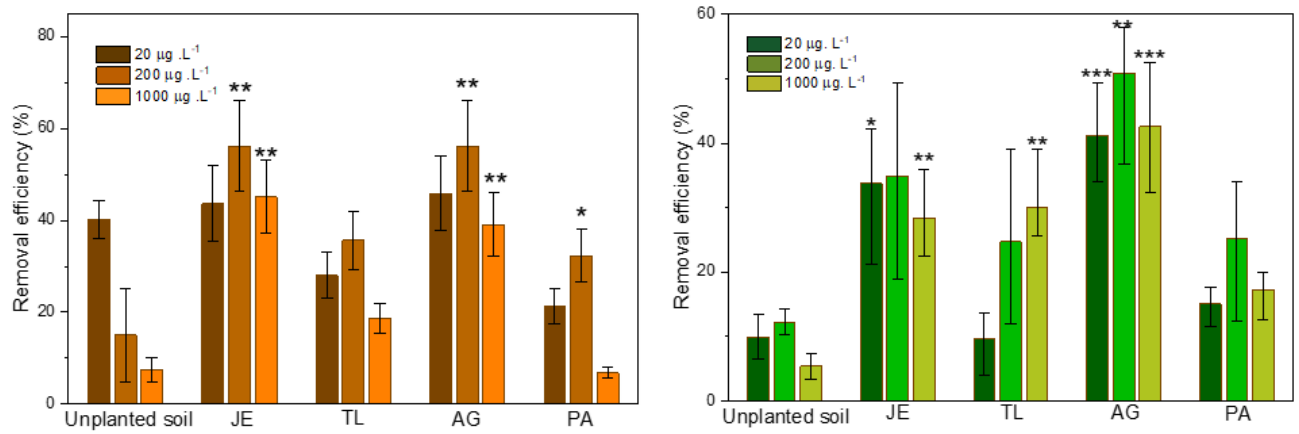

Figure 34. The total removal efficiency of all plants in the group exposed to a) δ-HCH and, b) t-HCH; statistical assessment of plant presence compared to unplanted control: one-way ANOVA, significance level α = 0.05; * p < 0,05, **p < 0.01, *** p < 0.001

The results of the growth substrate analysis for t-HCH are presented in Table 13 and Figure 34 (b), revealing lower HCH removal compared to δ-HCH. Notably, HCH removal was significantly higher for *J. effusus* and *A. glutinosa* compared to TL, with *P. australis* showing significant removal only at the highest HCH concentration. While there was no significant difference in isomer removal at the highest HCH concentration, lower concentrations exhibited a significant trend with the highest removal efficiency for α-HCH = δ-HCH > γ-HCH > β-HCH, consistent with previous studies highlighting the persistence of β-HCH. Root biomass analysis indicated the highest sum HCH concentrations in AG, PA, JE, and TL, with preferential uptake of β-HCH and δ-HCH in *T. latifolia* and *P. australis*. The degradation product 1,3-diClB was detected in root tissue, albeit below quantification limits. Aboveground parts exhibited lower concentrations than the δ-HCH group, with α-HCH and δ-HCH predominant at high t-HCH concentrations. β-HCH appeared to accumulate in the root system, while α-HCH and δ-HCH were transported to aboveground parts, suggesting a correlation with vapor pressure values and lipophilicity. All samples contained 1,3-diClB, with the highest concentration observed at 200 $\mu g \cdot L^{-1}$, indicating higher HCH degradation at this concentration. Comparing the t-HCH and δ-HCH exposure groups, the former showed lower total remediation efficiency. *A.glutinosa* and *J. effusus* demonstrated a positive effect, particularly at lower t-HCH concentrations, resembling the trends observed in the δ-HCH group. PA, however, retained most removed HCH in plant tissue, with ClB production intensifying at intermediate doses but decreasing at the highest dose. Overall, *A. glutinosa* and *J. effusus* emerged as the most effective species for HCH elimination from both water and solid substrate, suggesting their potential in phytoremediation efforts on contaminated sites. While AG's massive central root may limit its use in treatment wetlands, it could prove valuable for restoring contaminated fields or sites with restricted constructed wetland use.

Table 13. Summary of HCH analysis results for the t HCH exposed group

t-HCH	t-HCH dose [$\mu g \cdot L^{-1}$]	Total removal efficiency [% of HCH dose]	Sum of HCH in roots [% of HCH dose]	Sum of HCH in above-ground parts [% of HCH dose]	Metabolism degradation volatilization of HCH [%]
J. effusus	20	34	1.3	3.7	15
	200	35	14	2.3	14
	1000	29	17	1.7	9

T. latifolia.	20	10	0.5	1.0	0
	200	25	8	0.5	10
	1000	31	17	0.6	0
A. glutinosa	20	44	5.7	5.7	17
	200	51	20	1.1	18
	1000	43	24.9	2.1	12
P. australis	20	15	1.1	2.7	0
	200	25	21	0.8	0
	1000	18	18	0.4	0

The values are listed as the average values of 9 measurements (3 samples of 3 parallel experiments). Standard deviation for the experimental set-up was determined to be 32% of the reported values.

3.3 Non-targeted Analysis - Consequences of t-HCH Presence

Non-targeted analysis assessed changes in plant metabolism after exposure to technical-HCH (t-HCH). Polyphenols, including chlorogenic acid and flavonoids, exhibited qualitative diversity across plant species. The study identified potential markers for metabolic changes in response to t-HCH exposure. Additionally, the presence of HCH metabolites, such as monochlorophenyl-β-D-(6-O-malonyl) glucopyranoside (MCPGM), indicated plant-mediated degradation processes. The results underscored the potential of *A.glutinosa* and *J. effusus* for phytoremediation, offering valuable insights into their effectiveness in eliminating HCH from water and solid substrates.

3.4 Microbial abundance

In the substrate, discernable distinctions surfaced across plant species. In *A. glutinosa*, the 24 μg δ-HCH treatment induced a distinctive community composition (Figure 35). *J. effusus* displayed a convergence with control samples at this concentration (Figure 36). *P. australis* mirrored *A. glutinosa* and *J. effusus*, revealing a distinct composition under the 24 μg δ-HCH treatment (Figure 37). *T. latifolia*, conversely, exhibited a divergence in samples treated with 24 μg δ-HCH from both control and other treated samples (Figure 38).

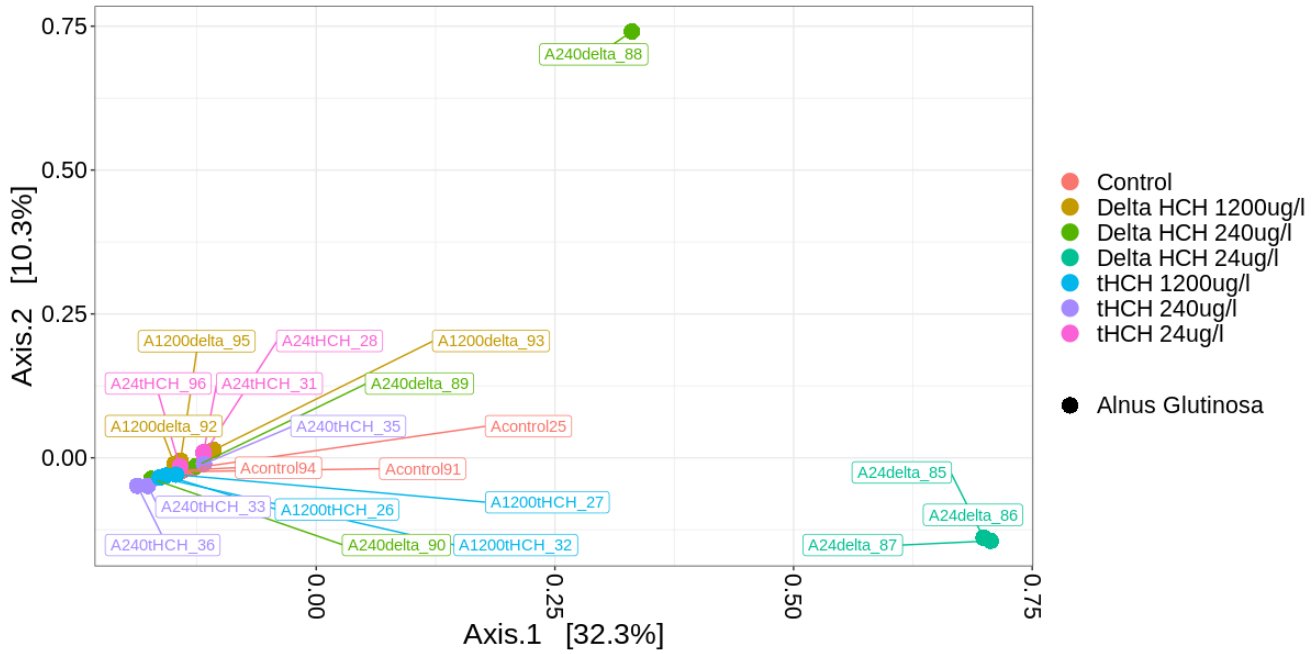

Figure 35. PCoA of the substrate samples planted with *A. glutinosa*

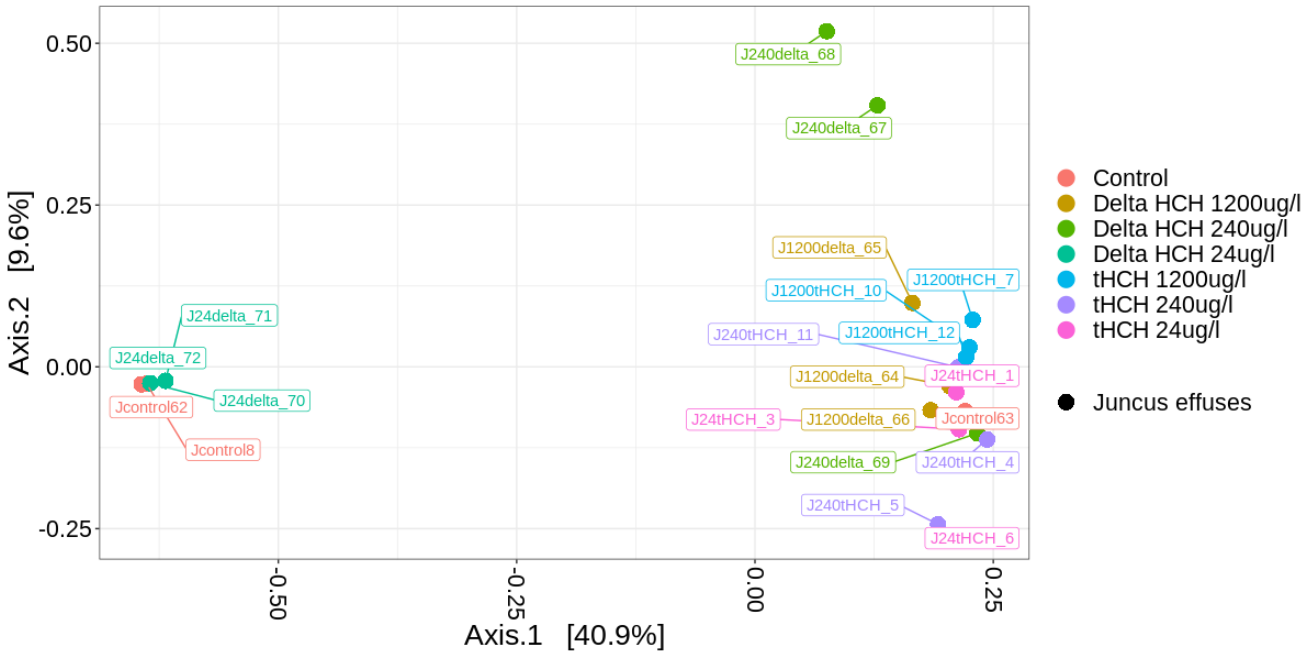

Figure 36. PCoA of the substrate samples planted with *J. effusus*

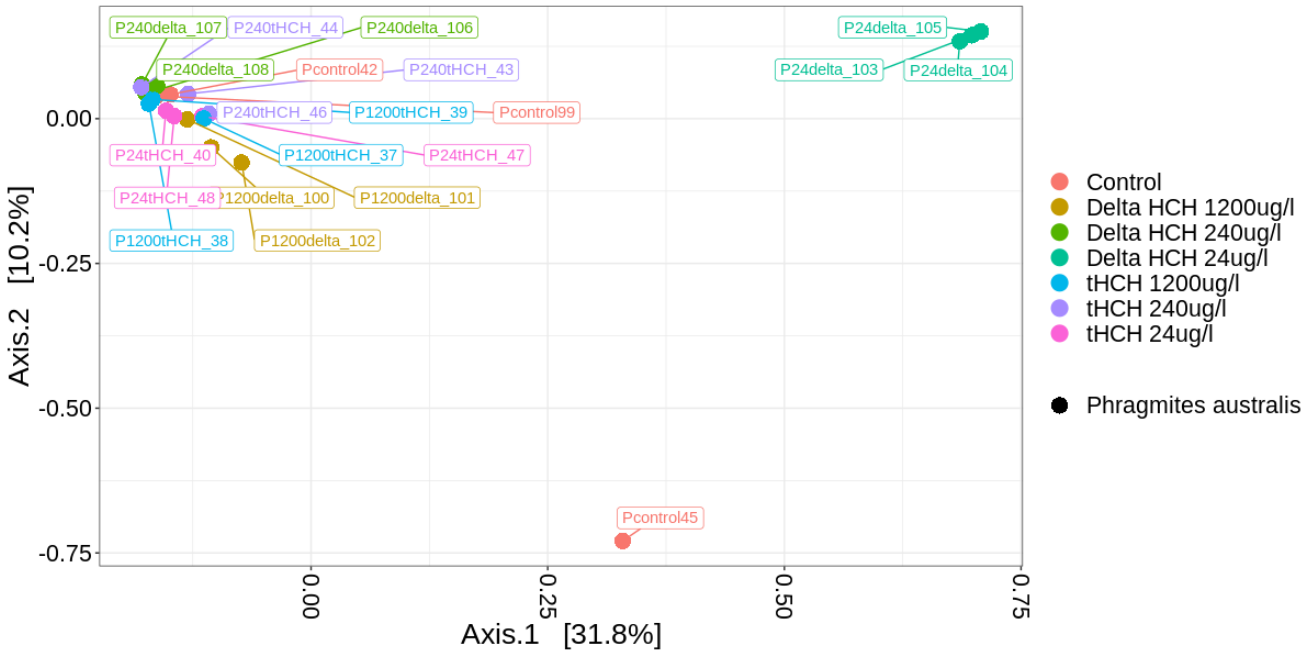

Figure 37. PCoA of the substrate samples planted with *P. australis*

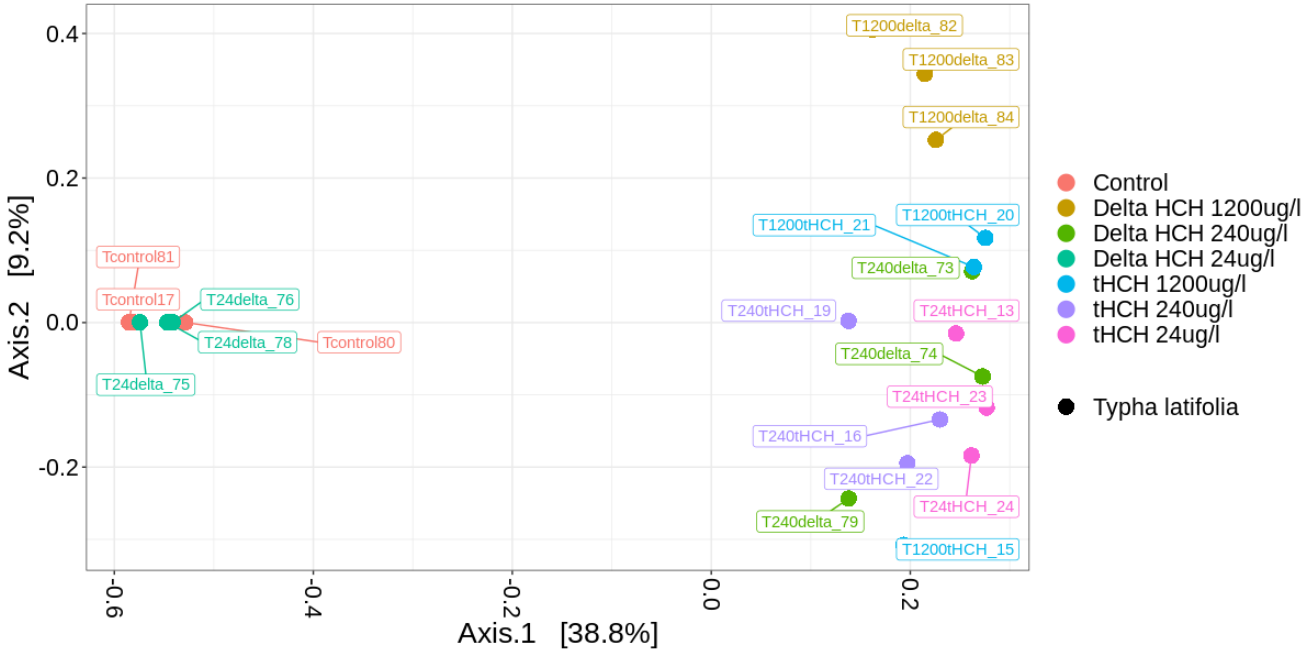

Figure 38. PCoA of the substrate samples planted with *T. latifolia*

Within the rhizosphere, distinct patterns persisted. *A.glutinosa* manifested a divergence in samples treated with 1200 µg δ-HCH, whereas control samples exhibited a differential composition (Figure 39). *J. effusus* evidenced a dissimilarity in samples treated with 1200 µg δ-HCH and 1200 µg t-HCH (Figure 40). *P. australis* exhibited a distinct community composition in samples treated with 1200 δ-HCH (Figure 41). In TL, solely the 1200 µg δ-HCH treatment engendered dissimilarity from other samples (Figure 42).

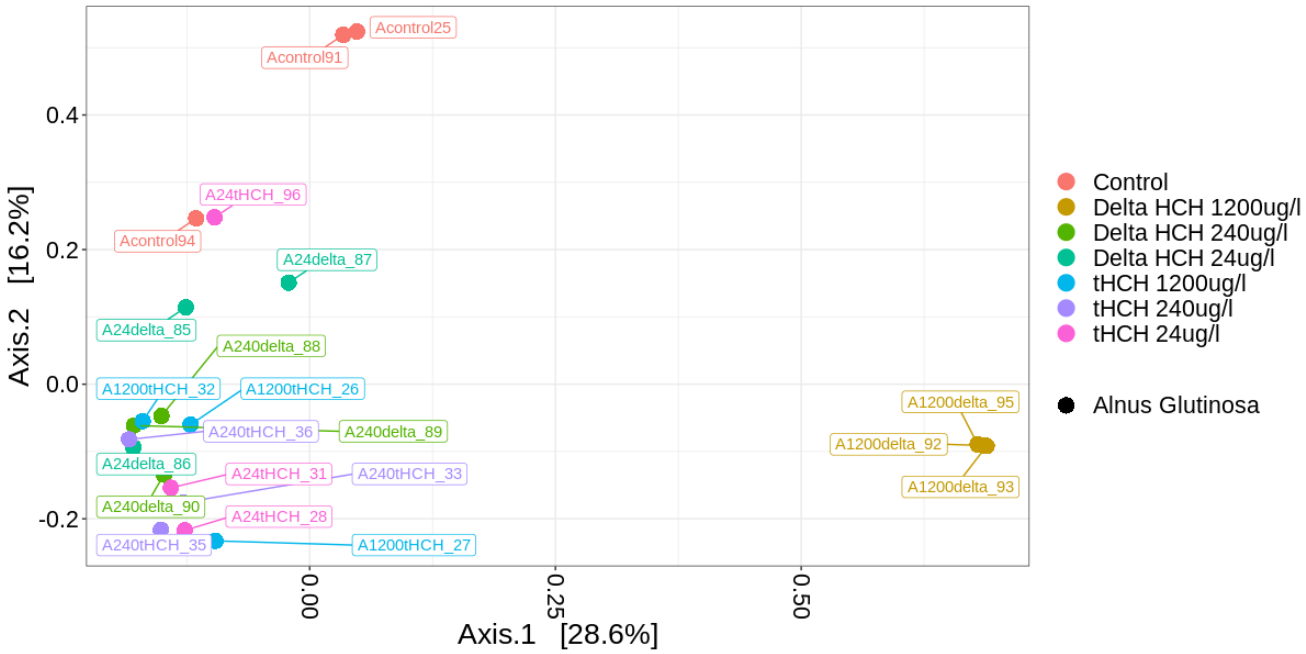

Figure 39. PCoA of the rhizophere samples planted with *A. glutinosa*

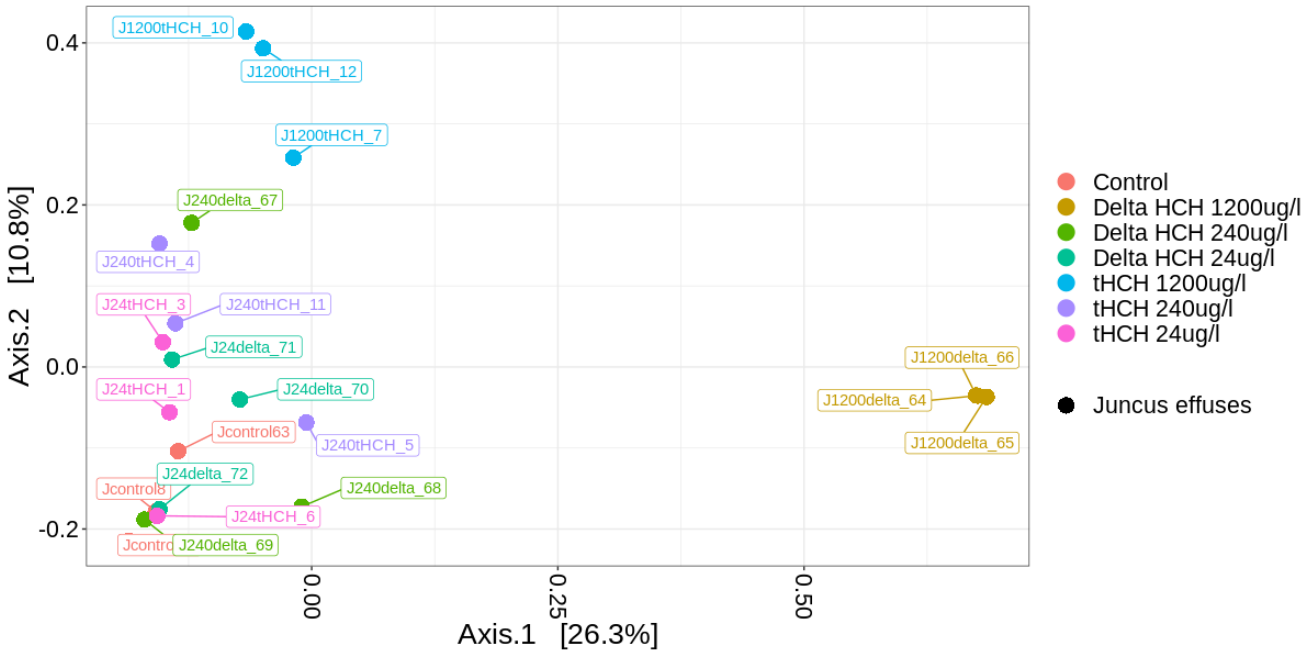

Figure 40. PCoA of the rhisophere samples planted with *J. effusus*

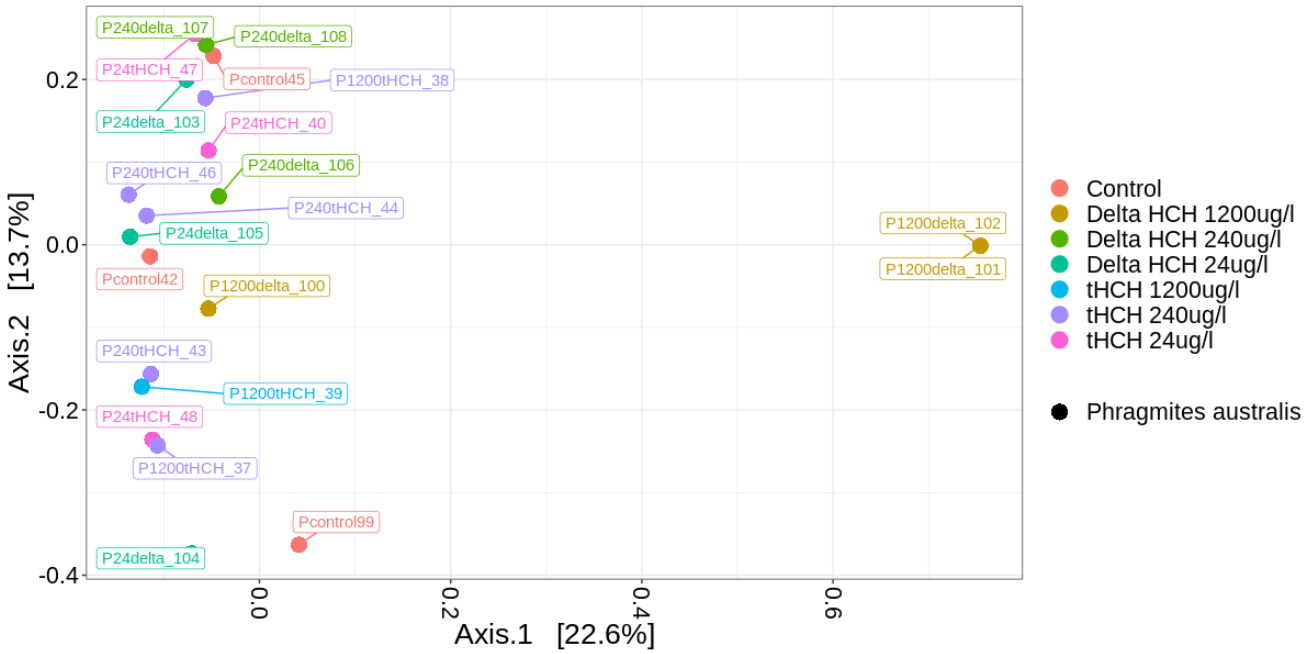

Figure 41. PCoA of the rhisophere samples planted with *P. australis*

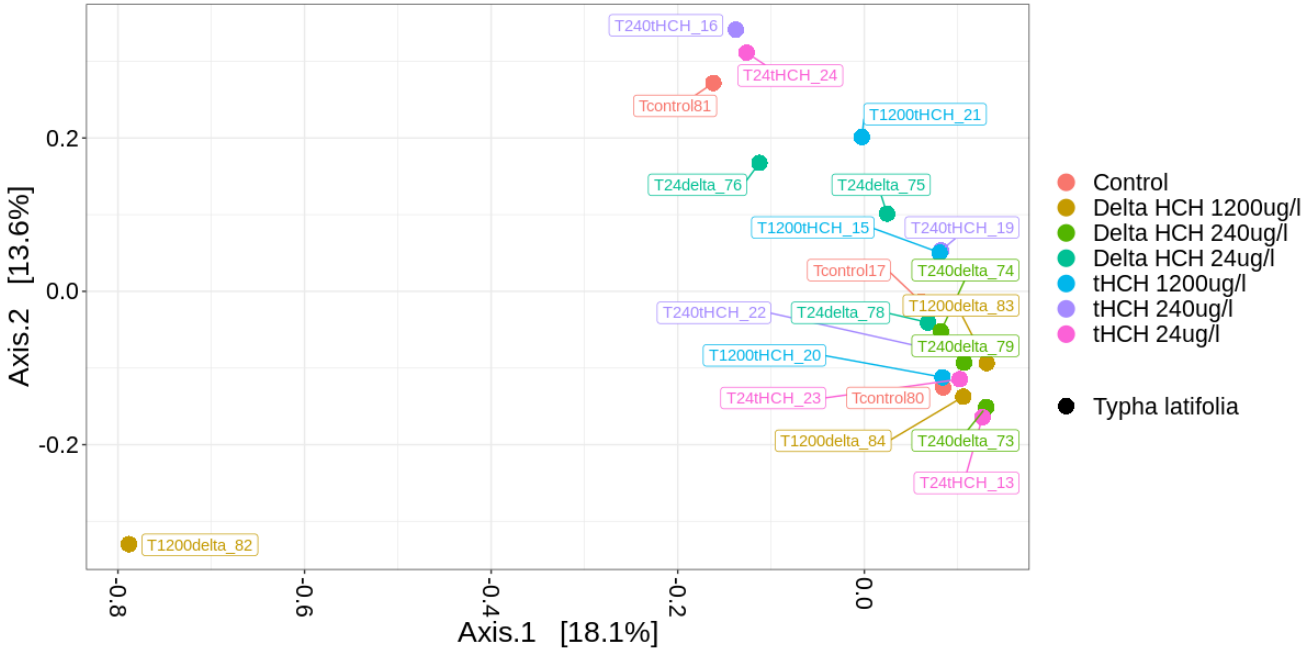

Figure 42. PCoA of the rhisophere samples planted with *T. latifolia*

Complementing these findings, NGS analysis elucidated noteworthy trends. *Trichormus* displayed heightened abundance in 240 µg-t-HCH treated samples in the absence of plants but exhibited a diminishing trend with escalating concentrations (Figure 43). In planted samples treated with δ-HCH, *Trichormus* prevalence peaked in 24 µg-treated samples, waning with higher concentrations (Figure 44). Additionally, differential trends were observed in the abundance of specific microbial taxa across plant species and HCH treatments.

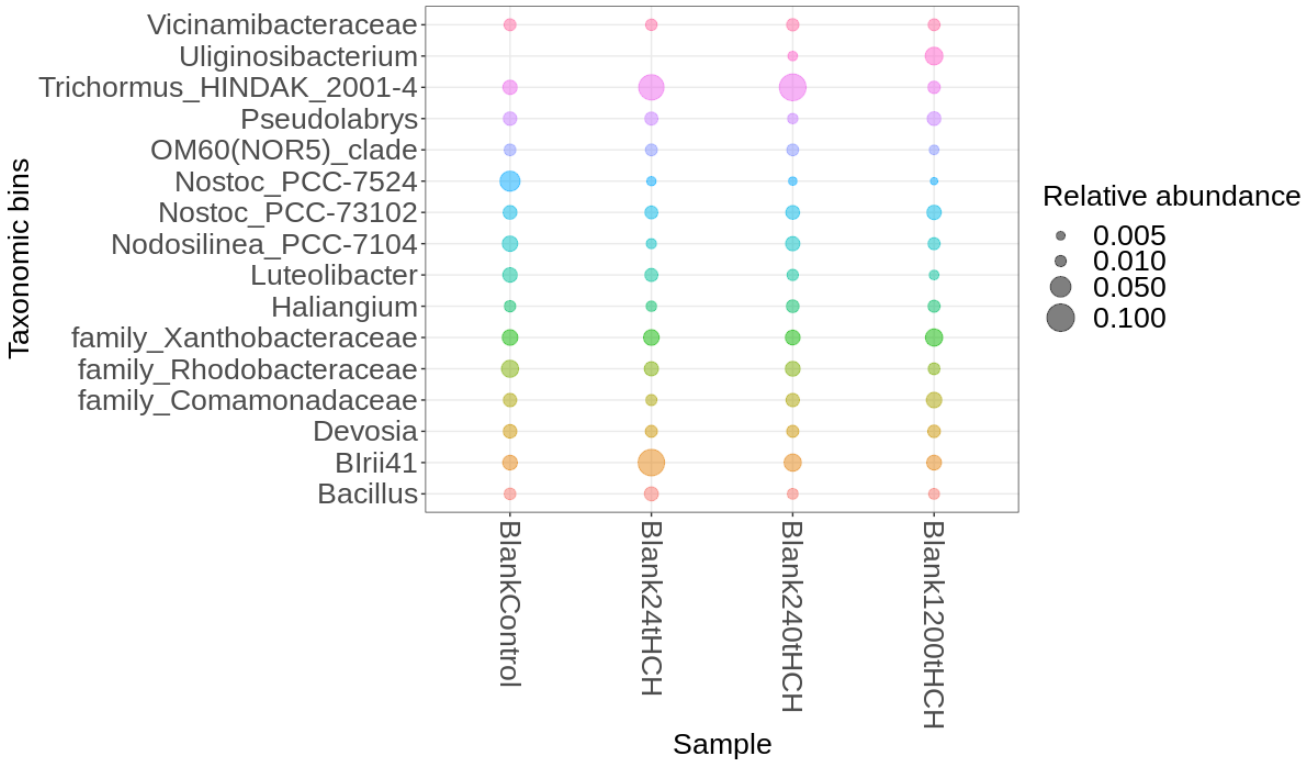

Figure 43. Relative abundance (mean > 0.01) of bacteria in substrate samples treated with t-HCH.

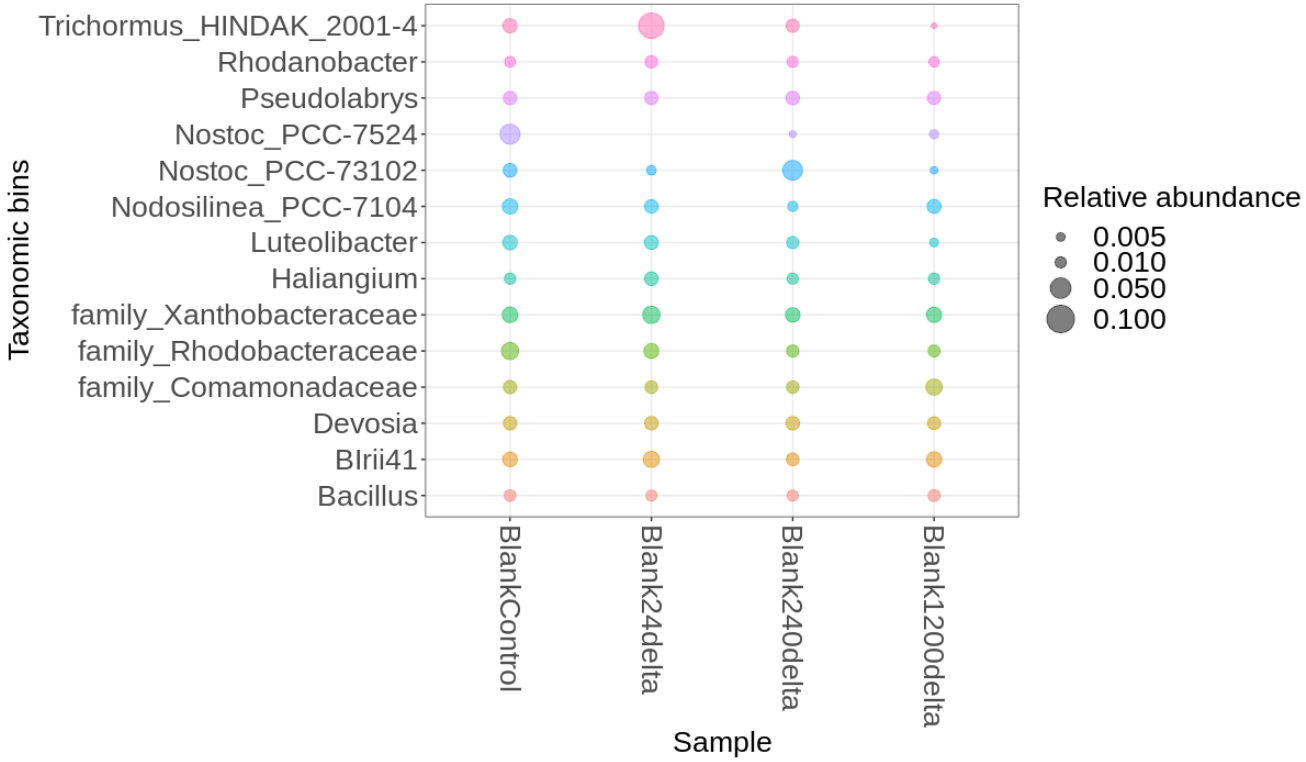

Figure 44. Relative abundance (mean > 0.01) of bacteria in substrate samples treated with δ-HCH.

3.5 Individual Plant Species Response

3.5.1 Substrate.

A. glutinosa

Family *Rhodocyclaceae* was not detected in control but increasing by increasing concentration of the t-HCH treatment (Figure 45). Same trend for *Dechloromonas*, in other hand *Calothrix*_PCC-6303 decreasing by increasing the concentration.

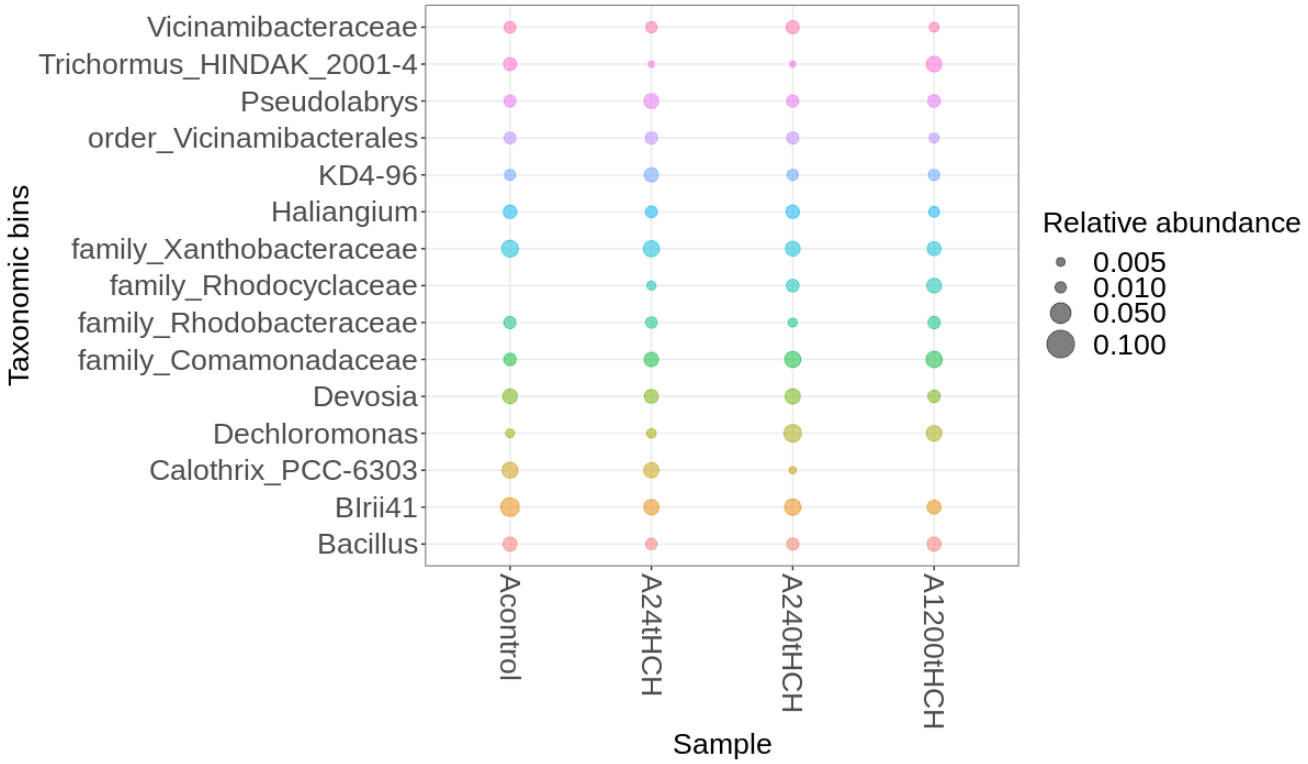

Figure 45. Relative abundance (mean > 0.01) of bacteria in *A. glutinosa* substrate samples treated with t-HCH.

In soil samples obtained from *A. glutinosa* saplings treated with δ-HCH, the discerned outcomes are as follows: *Uliginosibacterium*, absent in control samples, manifested a presence in treated samples, and its abundance exhibited an escalating trend corresponding to increasing concentration levels (Figure 46). Conversely, *Skermanella*, classified under the family *Comamonadaceae*, displayed a proclivity for heightened abundance in tandem with escalating concentrations. Conversely, *Deviosa* exhibited higher abundance in control samples, yet its prevalence demonstrated a decremental tendency with an augmentation in concentration levels.

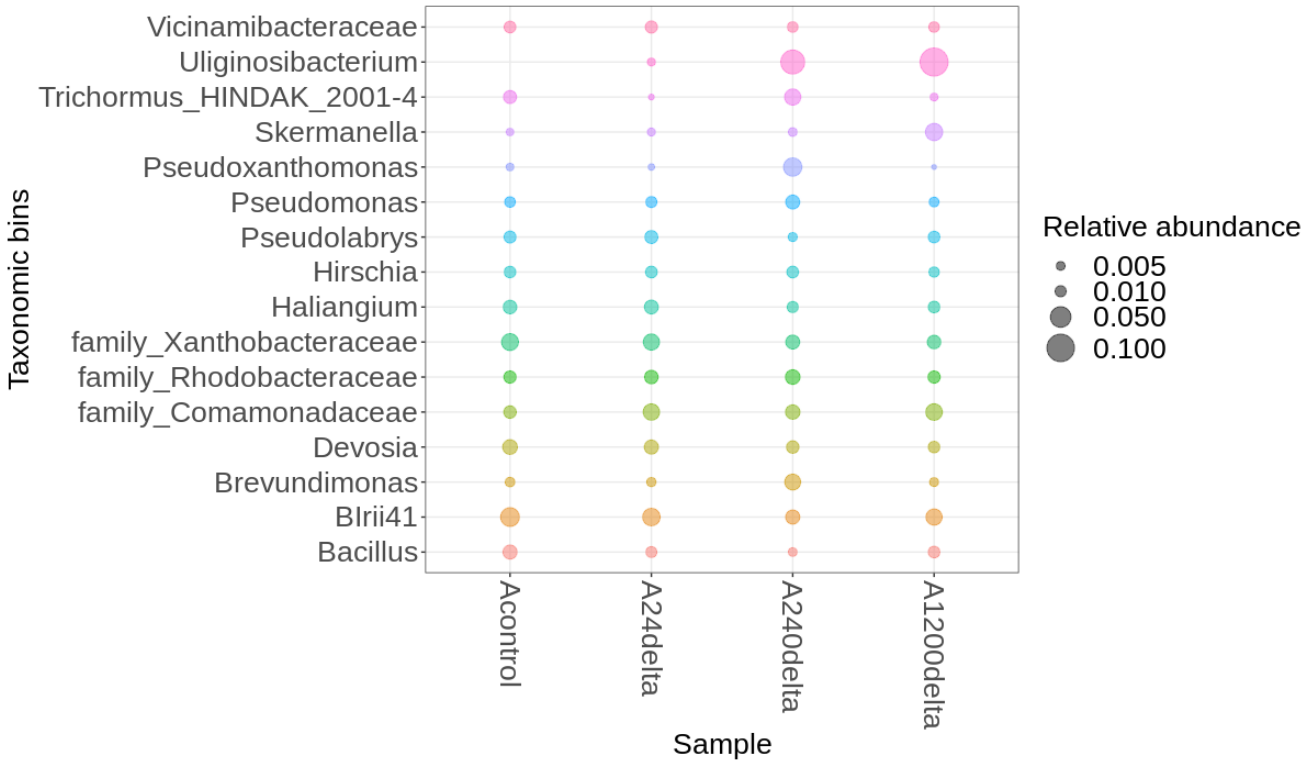

Figure 46. Relative abundance (mean > 0.01) of bacteria in *A. glutinosa* substrate samples treated with δ-HCH.

***J. effusus*:**

In substrate samples treated with t-HCH, the taxonomic entity *Nodosilinea_PCC-7104* exhibits a positive correlation with increasing concentration levels, signifying an augmentation in its abundance (Figure 47). This trend is mirrored in the cases of *Dechloromonas* and *Tolypothix*, with their abundances displaying an upward trajectory in tandem with escalating concentrations. Notably, *Skarmanella* achieves maximal prevalence in samples subjected to the highest concentration (1200 µg), implying a concentration-dependent relationship with its abundance. These findings provide insights into the taxonomic dynamics influenced by t-HCH concentration levels in the examined soil samples.

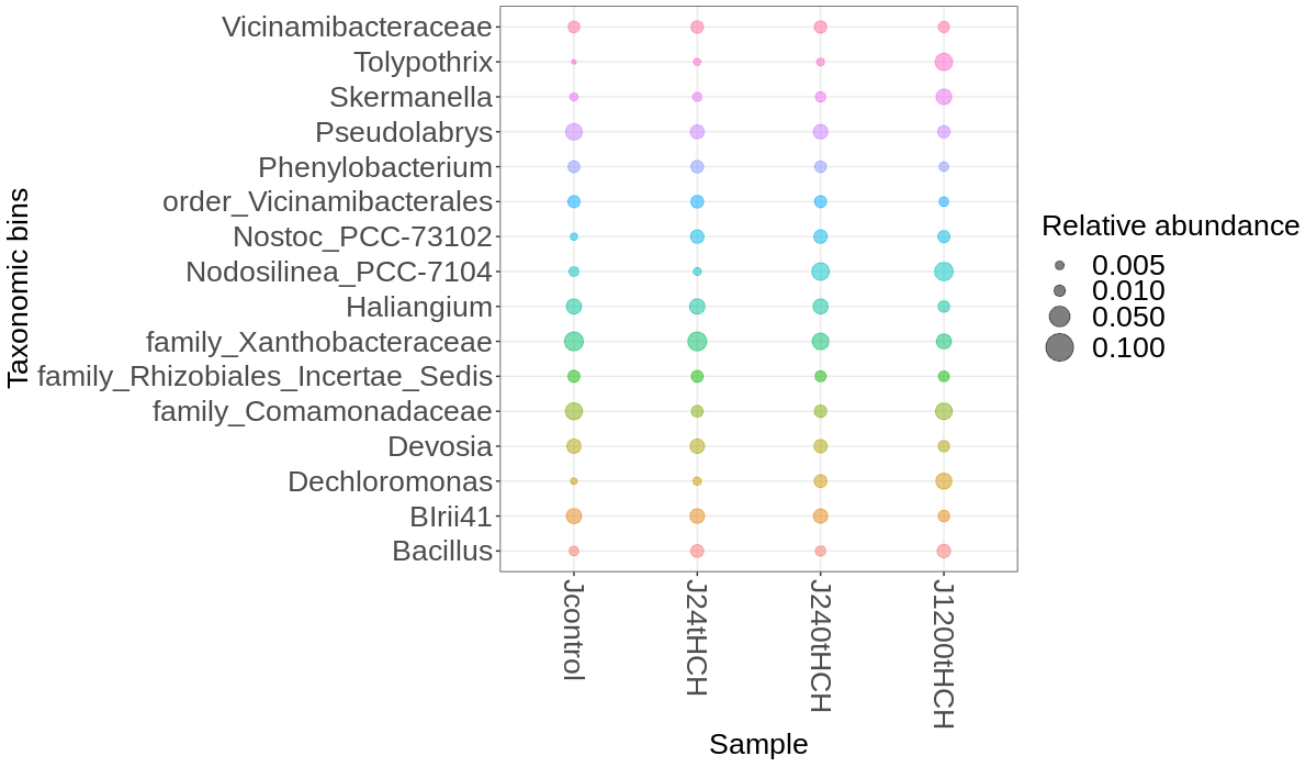

Figure 47. Relative abundance (mean > 0.01) of bacteria in *J. effusus* substrate samples treated with t-HCH.

The analysis of *J. effusus* effusus substrate samples treated with δ-HCH yielded noteworthy findings. Notably, the abundance of *Trichormus*, *Pseudolabrys*, *Xanthobacteria*, *Devosia*, and *Blrii41* exhibited maximal prevalence in control samples, demonstrating a diminishing trend with escalating concentration levels (Figure 48). Conversely, the abundance of *Skermanella*, *Dechloromonas*, and *family_Rhodobacteraceae* in control samples was comparatively minimal, displaying an increasing trend in correspondence with elevated concentrations. Furthermore, *Calothrix_PCC-6303* displayed an escalating trend in abundance corresponding to increasing concentrations, although it was not detected in samples treated with 1200 µg. These findings provide valuable insights into the dynamic interplay between microbial taxa and concentration levels in the planted soil samples.

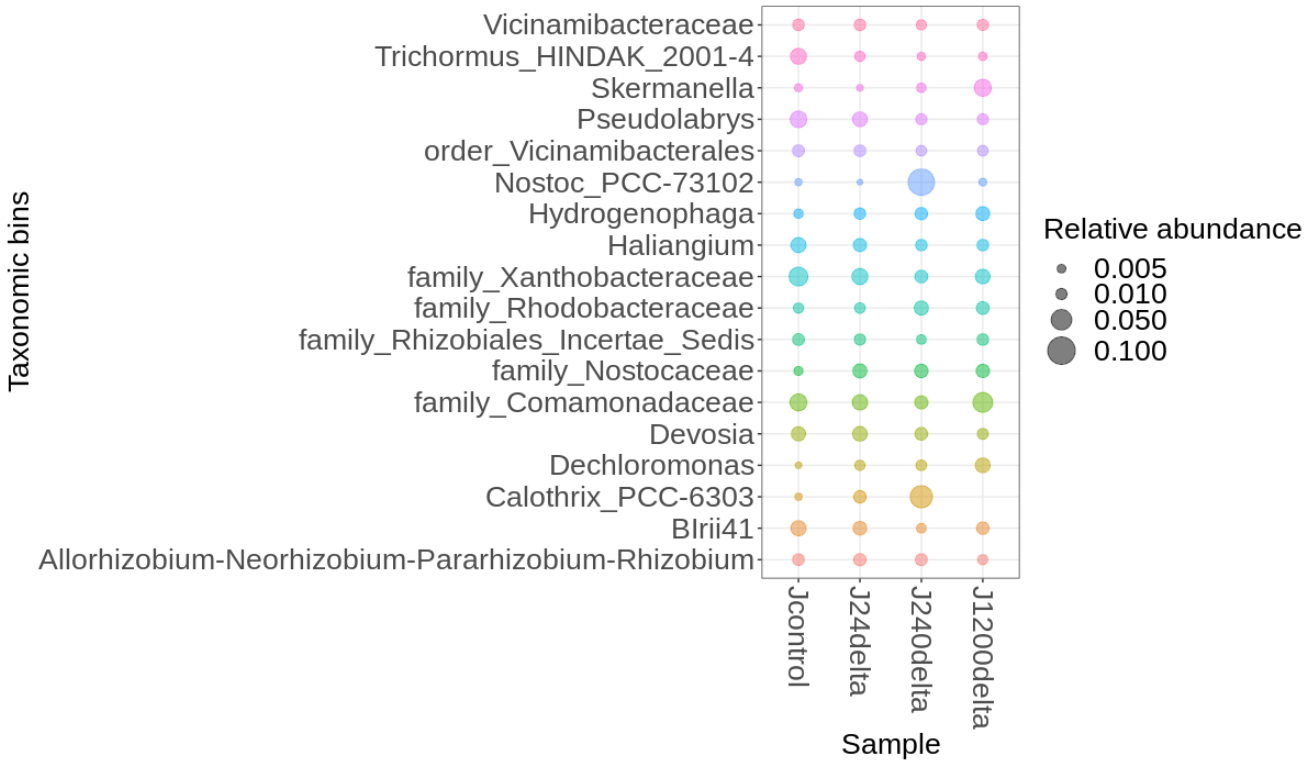

Figure 48. Relative abundance (mean > 0.01) of bacteria in *J. effusus* substrate samples treated with δ-HCH.

P. australis

In the context of soil samples planted with *P. australis* and subjected to t-HCH, the bacterial abundance exhibits relatively subtle variations across the samples, with some exceptions (Figure 49). Notably, the presence of *order_Cyanobacteriales* is discerned exclusively in control samples, lending a distinctive characteristic to the microbial composition in the absence of t-HCH exposure.

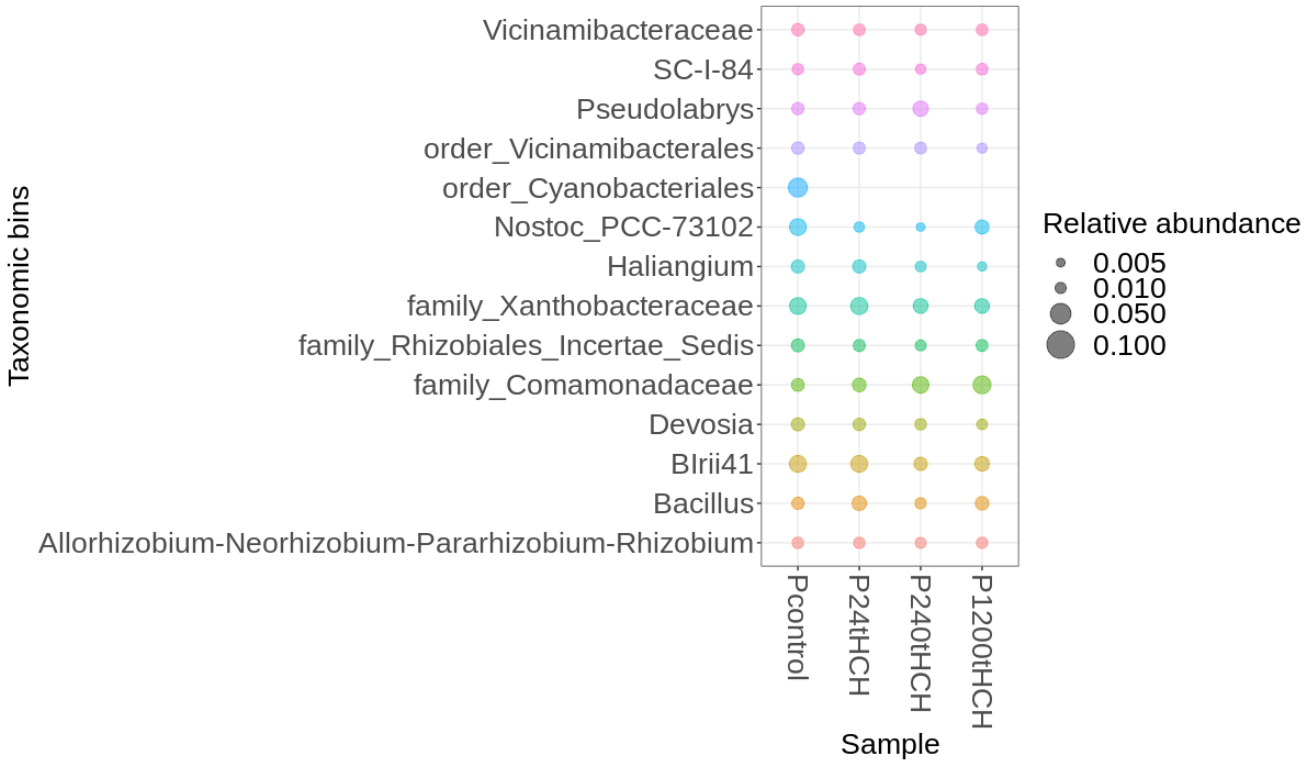

Figure 49. Relative abundance (mean > 0.01) of bacteria in *P. australis* substrate samples treated with t-HCH.

In the context of soil samples planted with *P. australis* and exposed to δ- HCH, the taxonomic *order_Cyanobacteriales* was observed solely in control samples and those treated with 24 µg, while its presence was not detected in other samples (Figure 50). Conversely, *Nostoc_PCC-73102* is predominantly identified in control samples, exhibiting a decremental trend with increasing concentration levels. *Trichormus* demonstrated an inclination to increase with rising concentrations, although it was not detected in samples treated with 1200 µg. These findings delineate distinctive microbial responses to varying concentrations of δ- HCH within the *P. australis* -inhabited soil matrix.

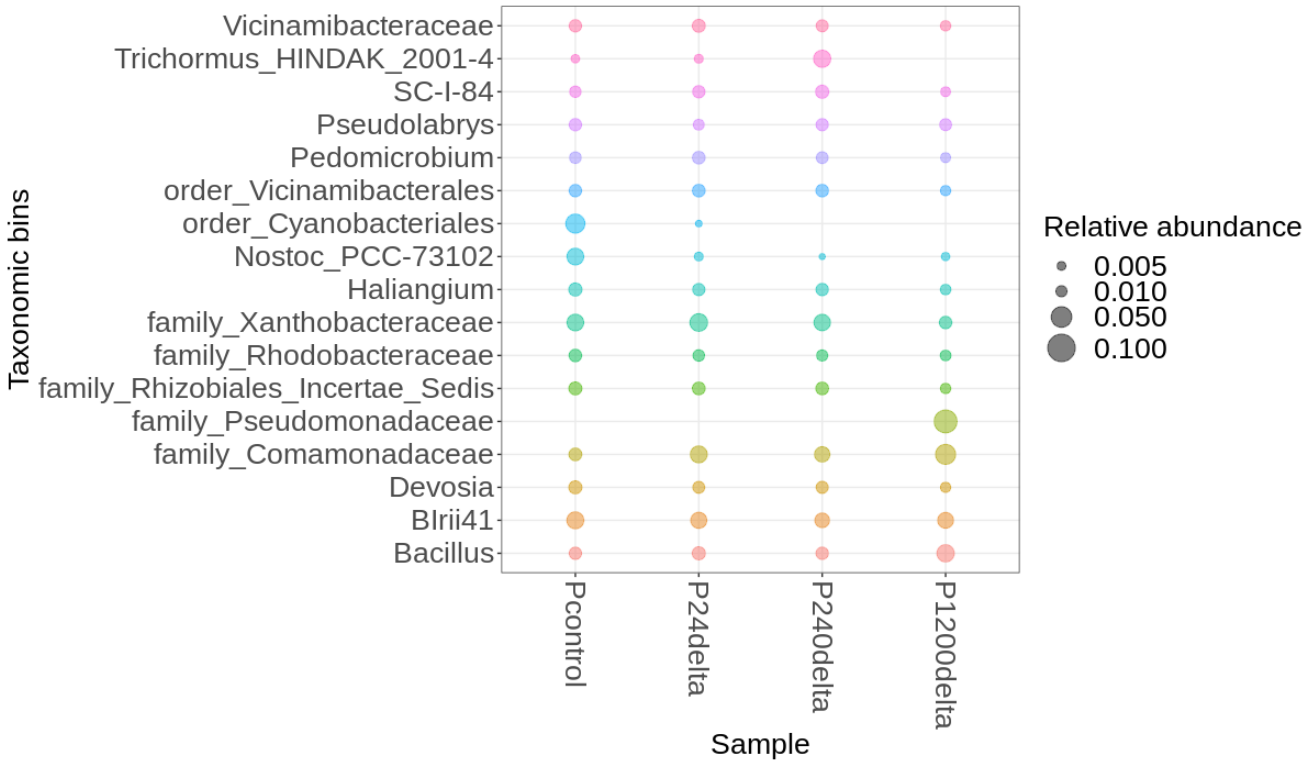

Figure 50. Relative abundance (mean > 0.01) of bacteria in *P. australis* substrate samples treated with δ-HCH.

T. latifolia

In the examination of soil samples planted with *T. latifolia* and subjected to t-HCH, the bacterial abundance reveals distinct patterns (Figure 51). Notably, *Trichormus* was most prevalent in control samples and those treated with 240 µg of δ- HCH in comparison to other samples. Conversely, the taxonomic *order_Cyanobacteriales* displayed an increasing trend with escalating concentrations, yet it is conspicuously absent in samples treated with 1200 µg. These findings delineate nuanced variations in microbial abundance within the *T. latifolia* -inhabited soil matrix in response to varying t-HCH concentrations.

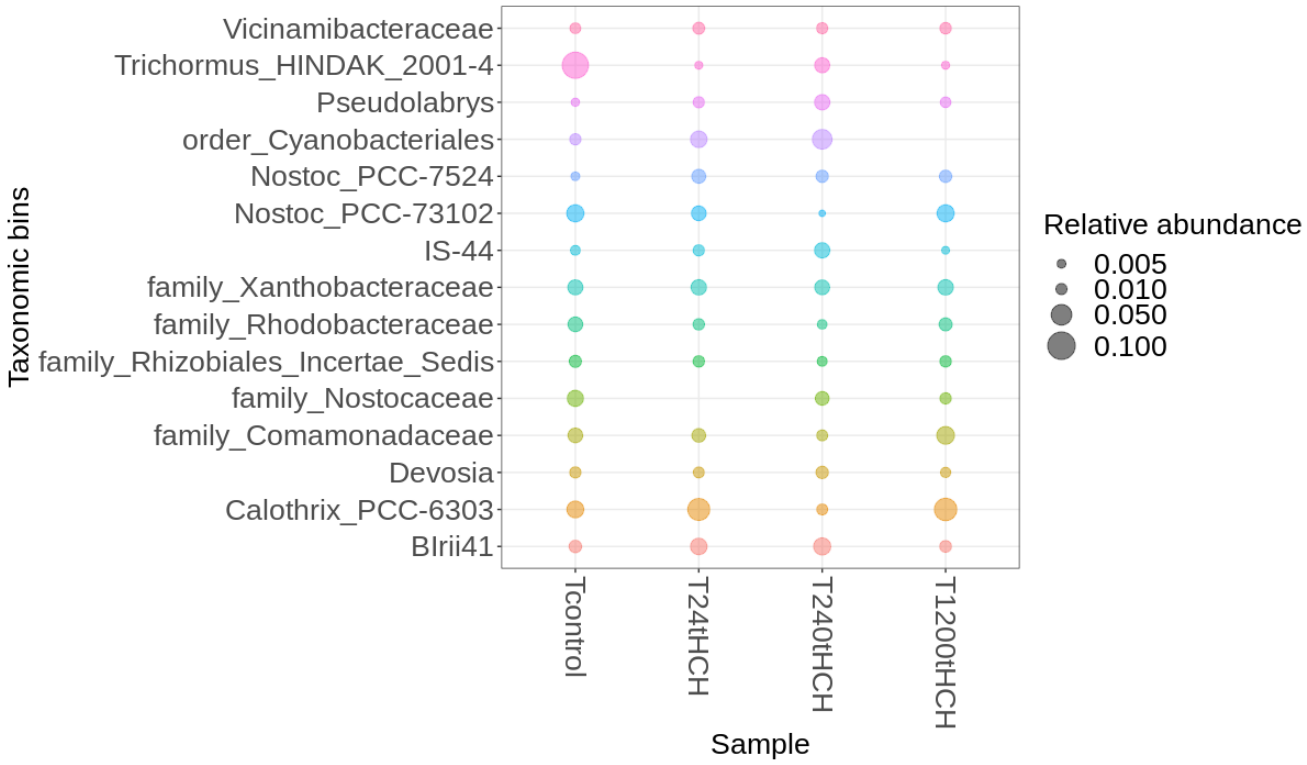

Figure 51. Relative abundance (mean > 0.01) of bacteria in *T. latifolia* substrate samples treated with t-HCH.

In the context of soil samples cultivated with *T. latifolia* and exposed to δ- HCH, the observed trends in bacterial abundance are as follows: *Calothrix_PCC-6303* exhibits a diminishing trend with increasing treatment concentrations, indicating a negative correlation (Figure 52). Conversely, *Trichormus* is most prevalent in control samples and those treated with 240 μg of δ- HCH compared to other treatment concentrations. These findings elucidate distinctive microbial dynamics within the *T. latifolia* -inhabited soil matrix under varying δ- HCH concentrations.

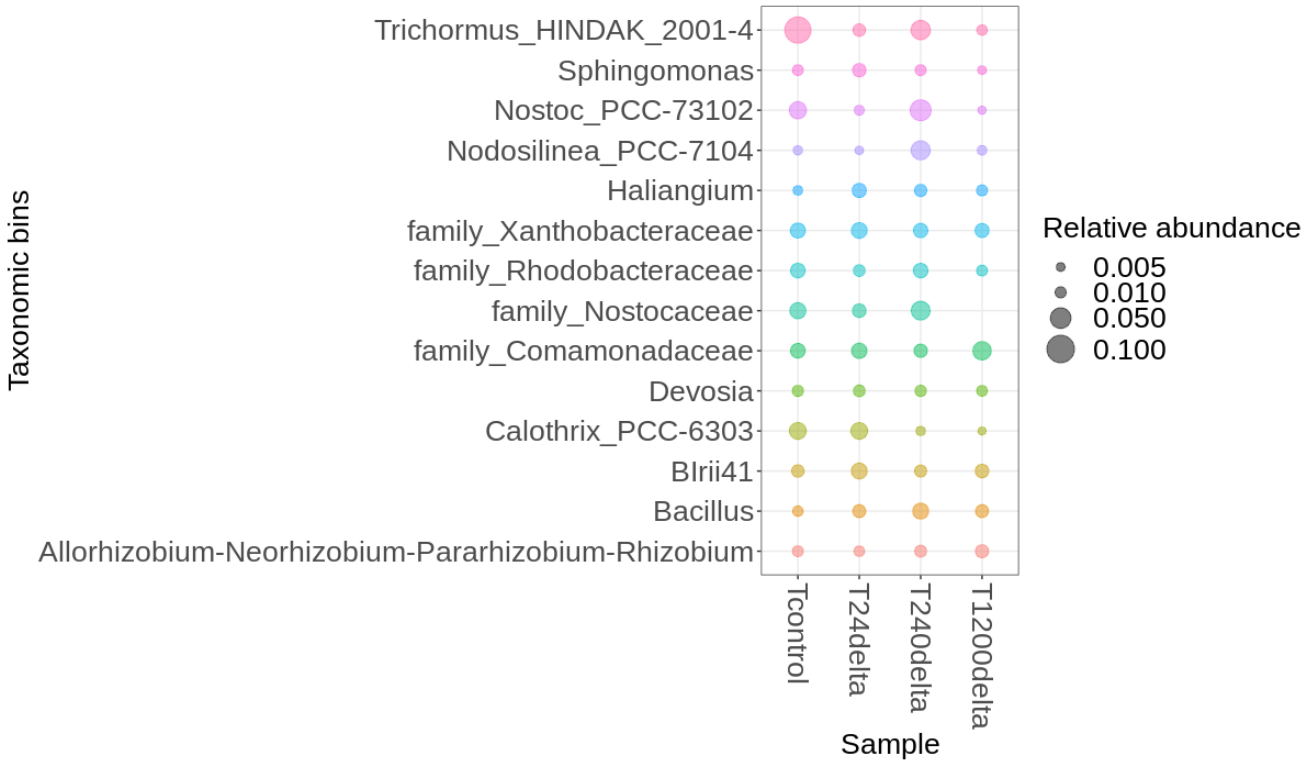

Figure 52. Relative abundance (mean > 0.01) of bacteria in *T. latifolia* substrate samples treated with δ-HCH.

3.5.2 Rhizosphere.

***A. glutinosa*:**

In the rhizosphere of *A.glutinosa* subjected to t-HCH, the analysis of control samples reveals notable variations in bacterial abundance, with *family_Sandaracinaceae, Steroidobacter*, *Streptomyces, Subgroup_10*, and *Acidibacter* emerging as the most abundant taxa in comparison to other samples (Figure 53). As the t-HCH concentration increases, a discernible decrease was observed in the abundance of *family_Sandaracinaceae, Subgroup_10, and Acidibacter*. Conversely, an opposing trend is evident in *Allorhizobium-Neorhizobium-Pararhizobium, family_Comamonadaceae*, *Limnobacter*, and *Sphingobium*, with their abundance showing an increase with rising t-HCH concentrations. Notably, *Dechloromonas* attained maximal prevalence in samples treated with 1200 µg of HCH, accentuating a concentration-dependent relationship with its abundance. These findings elucidate the dynamic microbial responses within the rhizosphere of A. glutinosa under varying t-HCH concentrations.

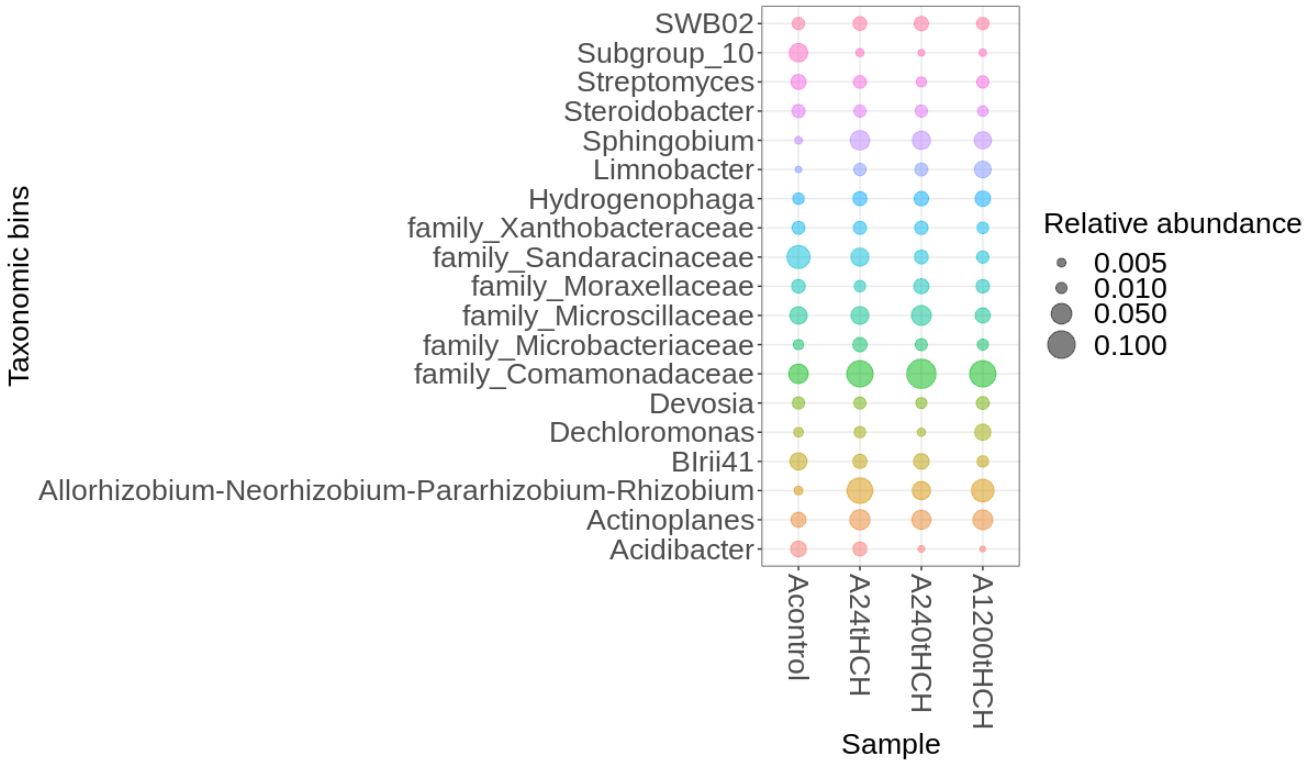

Figure 53. Relative abundance (mean > 0.01) of bacteria in *A. glutinosa* rhizosphere samples treated with t-HCH.

Within the rhizosphere of *A. glutinosa* subjected to δ-HCH, distinct trends in bacterial abundance are observed (Figure 54). Specifically, the taxa *Dechloromonas*, *Allorhizobium-Neorhizobium-Pararhizobium-Rhizobium*, *Limnobacter*, and *Sphingobium* exhibit an increasing trend corresponding to elevated treatment concentrations. Conversely, an opposite trend was discerned in the abundance of *Acidibacter*, *family_Rhodocyclaceae*, *family_Sandaracinaceae*, and *Subgroup_10*, with their prevalence decreased as the treatment concentration rises. These findings underscore the nuanced and concentration-dependent microbial dynamics within the rhizosphere of *A. glutinosa* under varying δ-HCH concentrations.

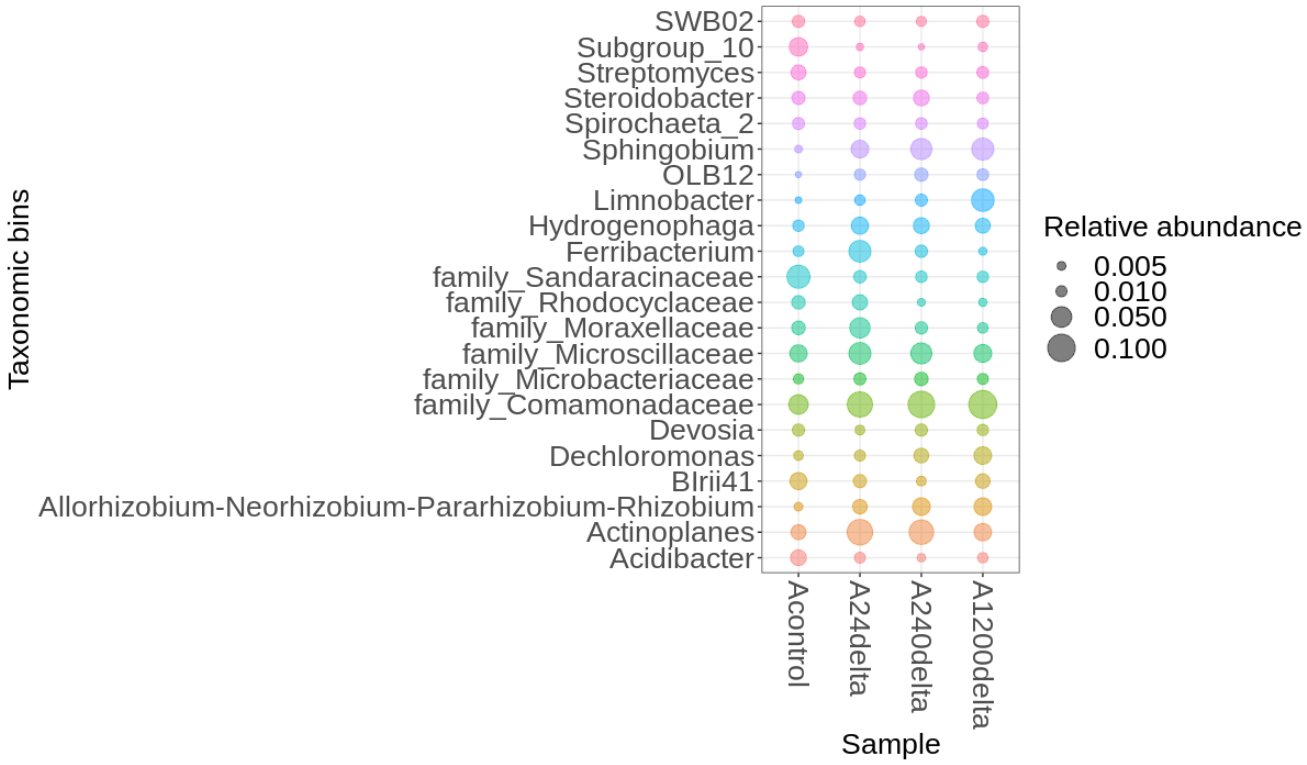

Figure 54. Relative abundance (mean > 0.01) of bacteria in *A. glutinosa* rhizosphere samples treated with δ-HCH.

J. effusus

In the rhizosphere of *J. effusus* subjected to t-HCH, notable distinctions in bacterial abundance are evident (Figure 55). *Ferribacterium* was exclusively detected in samples treated with 1200 µg, indicating a concentration-specific presence. Conversely, the abundances of *Flavobacterium*, *Hydrogenophaga*, and *Kineosporia* were higher in both control samples and those treated with 24 µg. In contrast, the abundances of *Nostoc_PCC-73102* and *Nodosilinea_PCC-7104* are comparatively low in control samples, exhibiting an increasing trend with rising t-HCH concentrations. These observations illuminate the intricate dynamics of microbial communities within the rhizosphere of *J. effusus* under varying t-HCH concentrations.

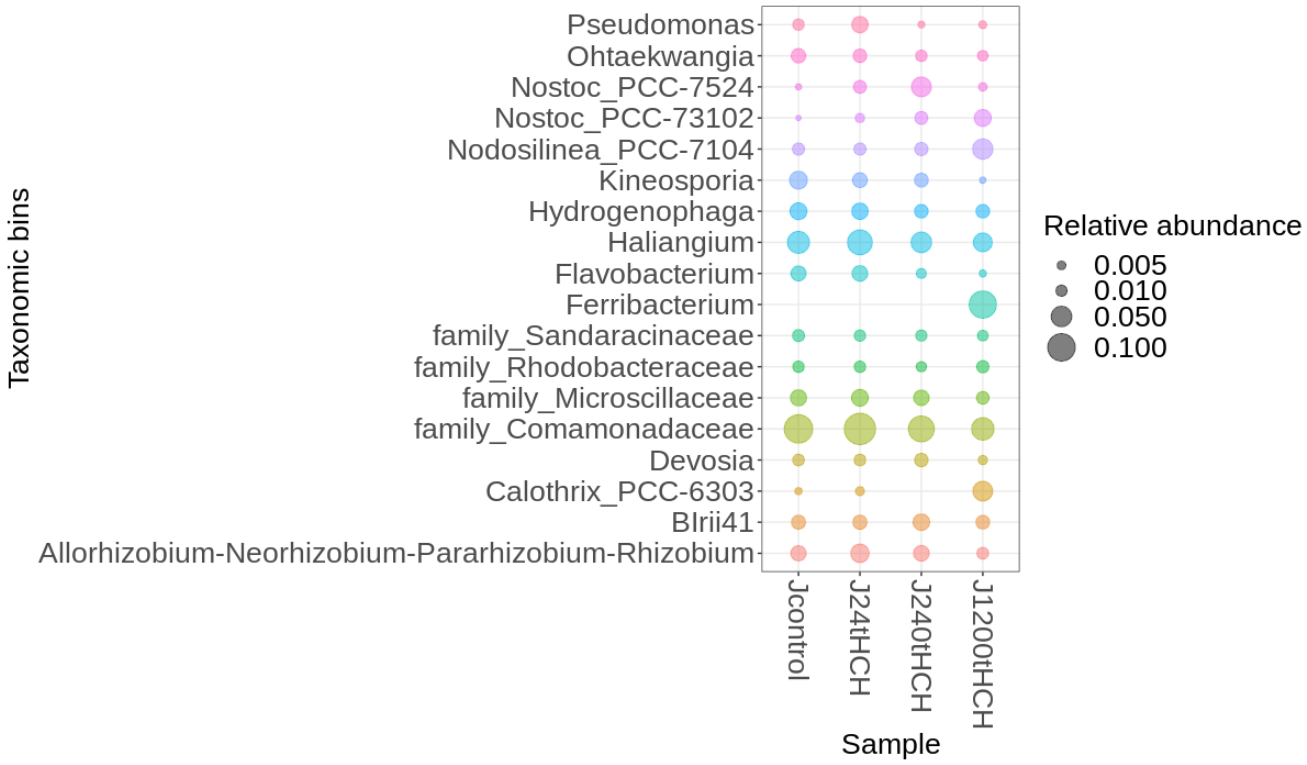

Figure 55. Relative abundance (mean > 0.01) of bacteria in *J. effusus* rhizosphere samples treated with t-HCH.

In the rhizosphere of *J. effusus* exposed to δ-HCH, the bacterial abundances exhibited no discernible overall trends, with a few exceptions (Figure 56). Notably, *Dechloromonas* was not detected in control samples but displayed an increasing trend with rising concentration levels. Conversely, *Flavobacterium* was predominantly detected in control samples compared to treated samples. Additionally, *Nodosilinea_PCC-7104* was primarily detected in samples treated with 24 µg, showing a decreasing trend with increasing treatment concentrations. These findings underscore the nuanced variations in microbial communities within the rhizosphere of *J. effusus* under varying δ- HCH concentrations, with certain taxa exhibiting distinctive responses.

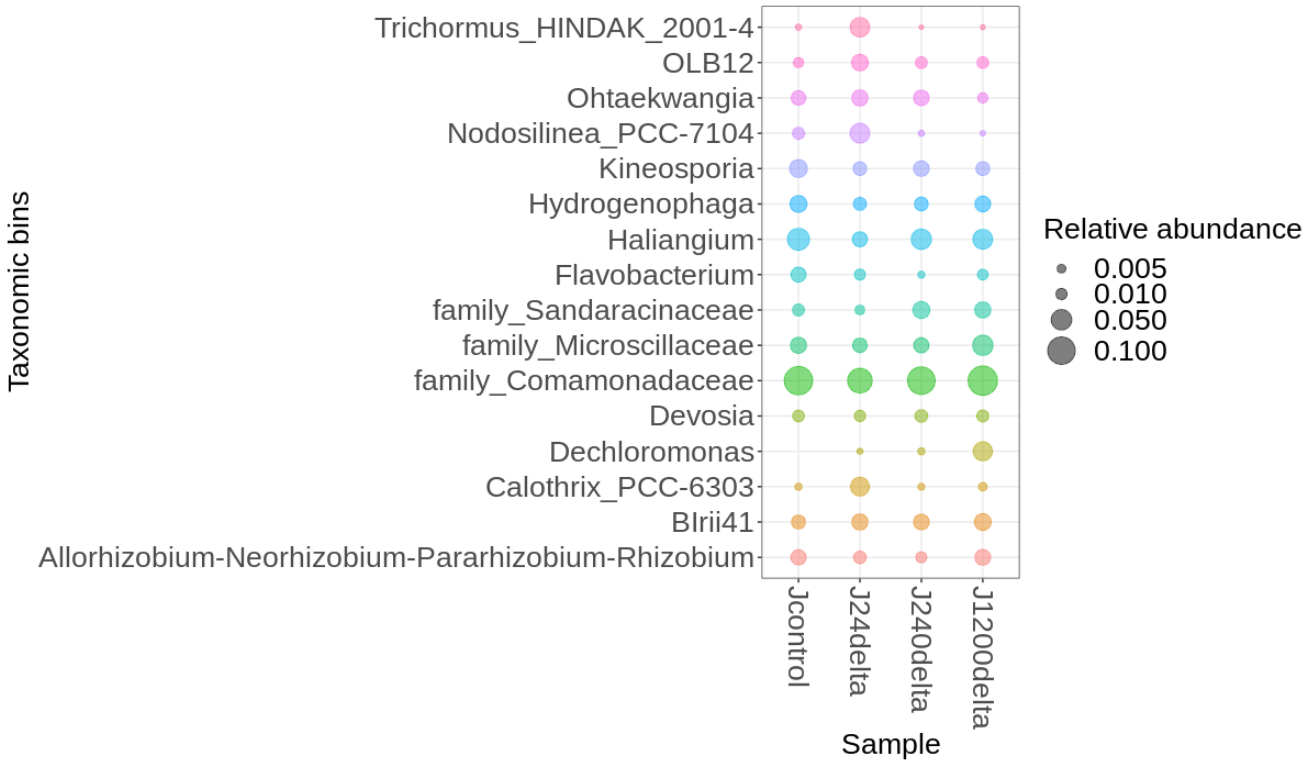

Figure 56. Relative abundance (mean > 0.01) of bacteria in J. EFFUSUS rhizosphere samples treated with δ-HCH.

P. australis

In the rhizosphere of *P. australis* subjected to t-HCH, certain bacterial taxa exhibit concentration-dependent trends (Figure 57). Notably, *Dechloromonas*, *family_Rhodocyclaceae*, *family_Sandaracinaceae*, and *Haliangium* displayed an increasing abundance with rising treatment concentrations. Conversely, Family_*Rhizobiales_Incertae_Sedis* was predominantly detected in control samples, demonstrating a decreasing trend with increasing treatment concentrations.

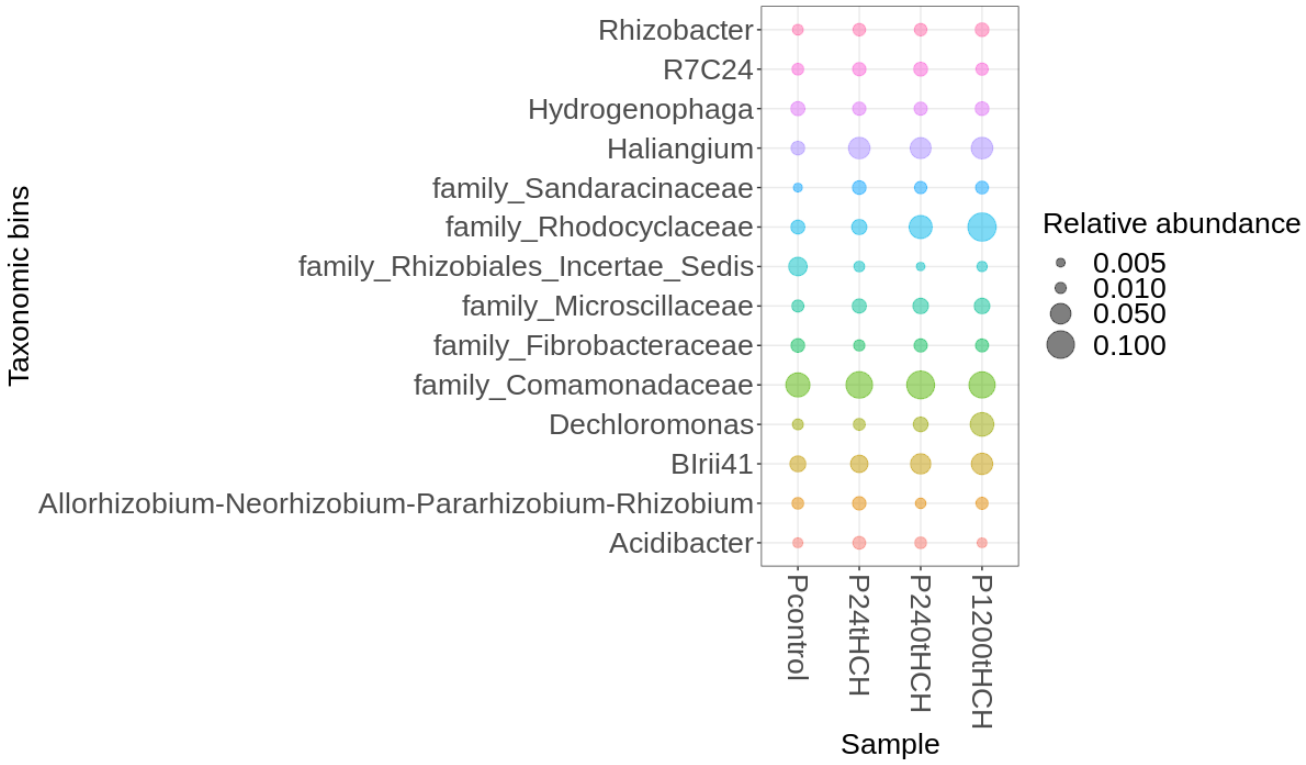

Figure 57. Relative abundance (mean > 0.01) of bacteria in *P. australis* rhizosphere samples treated with t-HCH.

In the rhizosphere of *P. australis* exposed to δ- HCH, control samples exhibited low abundance of *Dechloromonas* and *Haliangium* trends (Figure 58). The highest abundance of *Rhodocyclacae* and *Dechloromonas* was detected in samples treated with 24 µg compared to other treatment concentrations. *Flavobacterium* was detected in all samples, indicating its presence across varying δ- HCH concentrations.

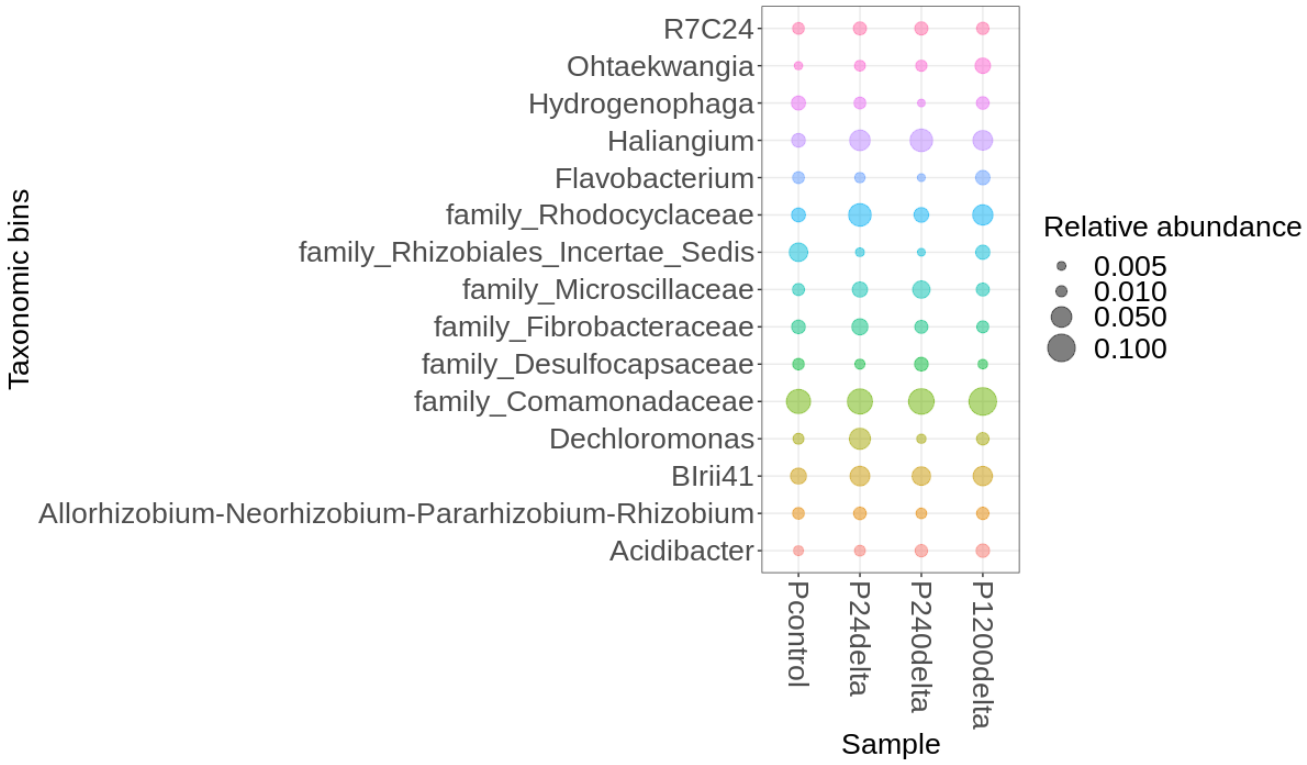

Figure 58. Relative abundance (mean > 0.01) of bacteria in *P. australis* rhizosphere samples treated with δ-HCH.

T. latifolia

In the rhizosphere of *T. latifolia* subjected to t-HCH, *Dechloromonas* was detected in all samples, and its abundance exhibited an increasing trend with rising treatment concentrations (Figure 59). Conversely, the abundances of Family_*Fibrobacteraceae* and *Methylotenera* demonstrate a decreasing trend with increasing treatment concentration.

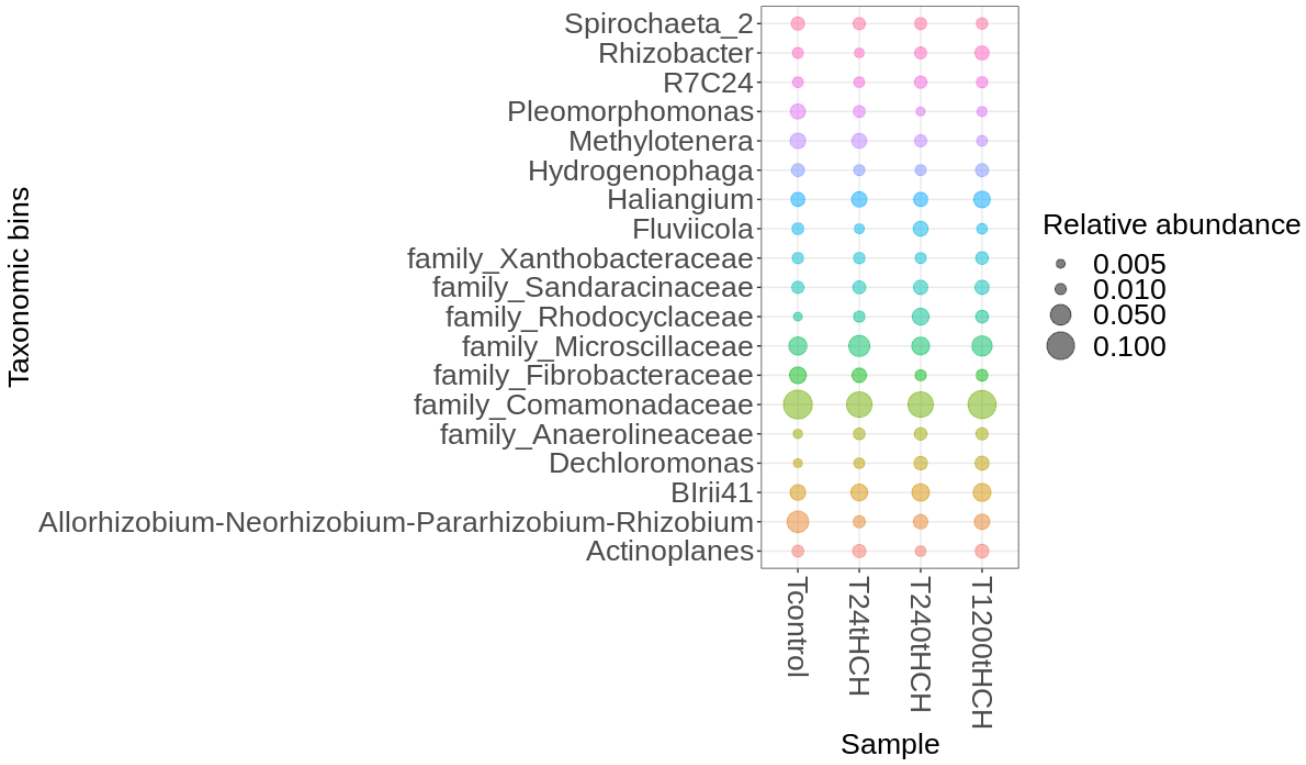

Figure 59. elative abundance (mean > 0.01) of bacteria in *T. latifolia* rhizosphere samples treated with t-HCH.

For the rhizosphere of *T. latifolia* exposed to δ- HCH, microbial abundance exhibited minimal differences between samples (Figure 60). Notably, the abundance of Family_*Fibrobacteraceae* was highest in control samples compared to other treated samples. Additionally, *Methylotenera* showed a decreasing trend with increasing treatment concentration. These findings highlight the nuanced variations in microbial communities within the rhizosphere of *T. latifolia* under the influence of both t-HCH and δ- HCH treatments.

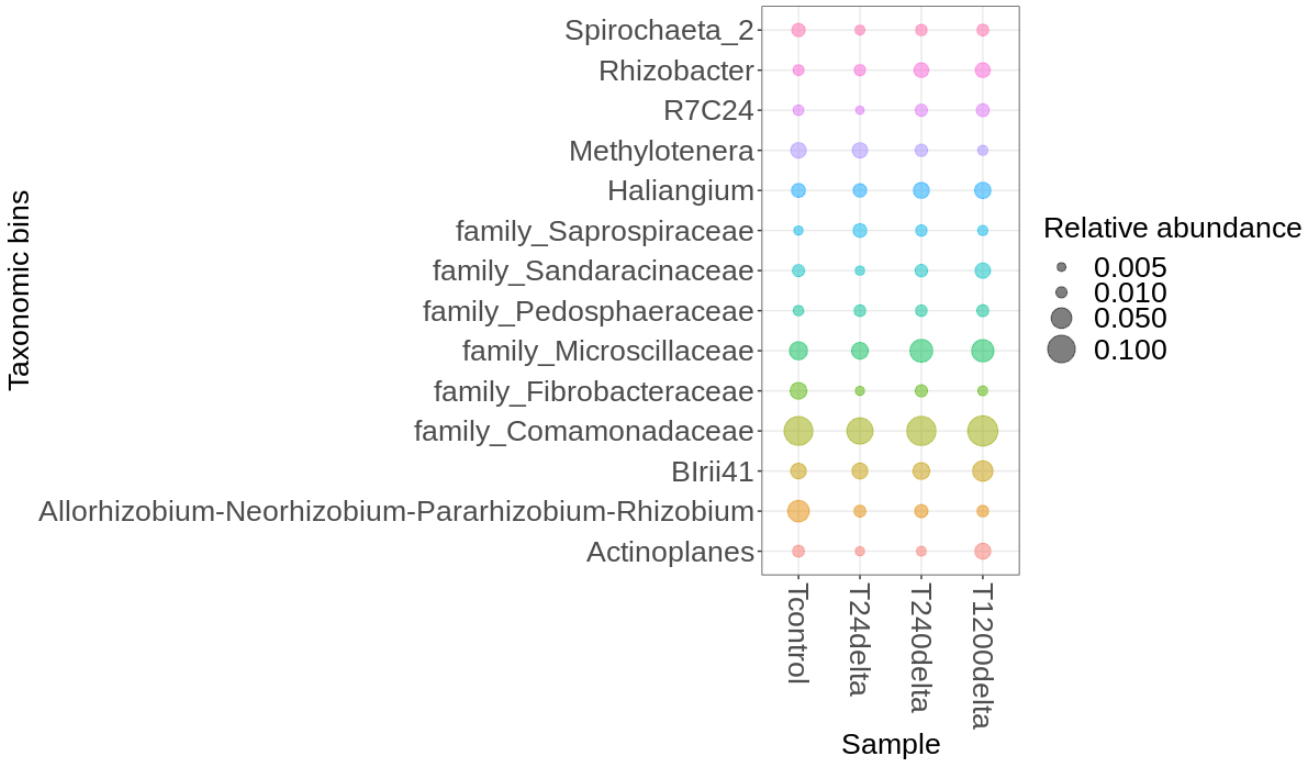

Figure 60. Relative abundance (mean > 0.01) of bacteria in *T. latifolia* rhizosphere samples treated with δ-HCH.

4. Summary

Capabilities of three wetland plants and one tree species in bioaccumulating and metabolizing HCH was evaluated. Despite the significant variability in the data and the use of artificial growth chamber conditions, the study yielded critical insights regarding the variability in HCH uptake among different species. HCH showed adverse effect on various physiological parameters in of the species. On the other hand, exposure to HCH resulted in an increase in total lipid (T. latifolia) and aboveground (A. glutinosa) biomass production. A higher phytoextraction efficiency was demonstrated for the δ-HCH isomer, with maximum removal rates of 50-70%, compared to 40-50% for the γ-HCH isomer at the same concentration. Furthermore, the presence of the plants enhanced the efficiency of HCH removal by 21-42% for δ-HCH and by 8-24% for γ-HCH, in comparison to controls without plants.

It is essential to note that the microbial community response is complex and influenced by the specific plant species and the type and concentration of the applied HCH compound. The intricacies of microbial community responses unveiled herein underscore the nuanced interplay between plant species, soil matrices, and HCH isomer concentrations. These findings contribute valuable insights into the ecologically pertinent dynamics of pollutant-microbe-plant interactions, enriching our understanding of the multifaceted implications of HCH exposure on plant-associated microbial communities.

In the rhizosphere of P. australis exposed to δ-HCH, control samples showed low abundance of *Dechloromonas* and *Haliangium*, while the highest abundance of *Rhodocyclaceae* and *Dechloromonas* was detected in samples treated with 24 μg, with *Flavobacterium* present across all concentrations. These observations underscore the intricate dynamics of bacterial communities within the rhizosphere of P. australis under the influence of both t-HCH and δ- HCH treatments. This study investigated the impact of HCH isomers on microbial communities in plant substrate and rhizosphere, revealing a consistent decrease in the abundance of the cyanobacterium *Trichormus* with rising HCH concentrations across diverse plant hosts. *Trichormus*'s consistent presence in non-polluted environments positions it as a potential ecological sentinel and bioindicator for environmental monitoring. The decline of Trichormus in the presence of HCH highlights the pollutant's disruptive effect on microbial communities, with potential repercussions for ecosystem processes. This underscores the importance of preserving microbial diversity, especially sensitive taxa like *Trichormus*, in environmental management and bioremediation strategies to maintain the integrity and functionality of native microbial ecosystems. The study concludes that *Trichormus* serves as a crucial component of microbial communities, alongside *Dechloromonas*, and its alteration by anthropogenic chemicals emphasizes the need for vigilant monitoring and comprehensive environmental protection strategies.

The study's findings offer practical applications for contaminated areas, indicating a correlation between pollutant dosage and phytoremediation effectiveness, where combined contamination inhibits HCH removal. For highly contaminated or chemically diverse sites, combined remediation methods are advised, with plant selection tailored to the remediation system. Wetland systems benefit from species like *J. effusus*, boasting high remediation efficiency, yet monoculture stands may lack resilience. Utilizing multiple plant species like *T. latifolia* and *P. australis* enhances sustainability and biodiversity. *A. glutinosa* shrubs/coppice culture, recommended for HCH-contaminated water treatment along riverbanks, can be effective due to regularly disturbed rooting. Additionally, A. glutinosa proves valuable in phytoscreening, with detectable HCH concentrations in stems, making it suitable for groundwater contamination monitoring.

CONCLUSIONS

The comprehensive investigation in this Ph.D. thesis clarifies that a multimodal strategy incorporating plant-mediated remediation, the Wetland+ system, or biochar wetland beds has great potential for reducing the effects of HCH contamination in soil and water environments.The efficiency of biochar wetland beds in removing HCH and related compounds underscores their potential as effective water purification systems, particularly in historically polluted sites, as demonstrated by their higher removal efficiency (98.2%) compared to control wetland beds (81.0%). Certainly, biochar as a sorbent has been acknowledged for its efficiency in adsorbing contaminants. However, it's important to note that biochar's effectiveness is tempered by its limited lifespan.More complex system the Wetland+ proved high and longer-term capacity to treat heavily contaminated water through a combination of chemical removal and biodegradation, with notable contributions from indigenous microbial communities. The Wetland+ system achieved 96.8% for ClB, and 81.7% for HCH removal.

First phytoremediation study investigated the persistence of HCH isomers in soil treated with alder trees and examines their uptake by the plants. Highest removal efficiency was observed in the group treated with β-HCH (90.26%), followed by α-HCH (64.85 %) and δ-HCH (57.08 %). All HCH isomers were found at highest proportions in the soil, with relatively little found in root biomass, suggesting that degradation of HCH isomers by soil bacteria occurs mainly through the aerobic upstream pathway.

The second experiment delves into the role of alder trees in phytoaccumulation and metabolizing HCH in soil, shedding light on the complex interactions between plant age, pruning, and pollutant removal efficiency. It is participating in HCH removal and increasing the removal efficiency by 6.79 - 24.42%. Key findings demonstrate that *A. glutinosa* contributes to HCH removal, with 1-year-old saplings showing particularly high potential for establishing short rotation coppice cultures, an approach that may offer a sustainable and efficient method for OCP remediation. *LinA*, which encodes dehydrochlorinase was most often detected in soil samples, while rhizosphere samples were rich in *LinB-RT* and *LinD* as well. The rhizosphere samples of the treated 1-year old saplings were rich in sulfur and iron-reducing bacteria.

Furthermore, last experiment elucidates the diverse capabilities of wetland plants and tree species in HCH phytoextraction, emphasizing the importance of considering plant physiology and microbial dynamics in remediation strategies. The negative effect of HCH was observed in most cases in the physiological parameters of all studied species. On the other hand, HCH led to an increase in the *T. latifolia* and *A. glutinosa* biomass. All species showed better phytoexctractability toward δ-HCH isomer than to t-HCH of the same load. Simultaneously, the presence of the plant increases the HCH removal

efficiency compared to the unplanted control, and a probable trans isomerization was also observed.

To sum up, these studies contribute to a deeper understanding of remediation technologies and ecological processes involved in mitigating HCH contamination. The findings presented herein not only advance scientific knowledge but also offer practical implications for designing sustainable remediation strategies and environmental policy. As such, this research serves as a foundation for future studies aimed at optimizing remediation technologies and promoting environmental recovery in contaminated areas.

Publications

(1) **Amirbekov A**, Mamirova A, Sevcu A, Spanek R, Hrabak P. HCH Removal in a Biochar-Amended Biofilter. Water. 2021; 13(23):3396. https://doi.org/10.3390/w13233396 (IF 3.4)

(2) Mamirova A, Pidlisnyuk V, **Amirbekov A**, Ševců A, Nurzhanova A. Phytoremediation potential of Miscanthus sinensis And. in organochlorine pesticides contaminated soil amended by Tween 20 and Activated carbon. *Environ Sci Pollut Res Int*. 2021;28(13):16092-16106. https://doi.org/10.1007/s11356-020-11609-y (IF 5.8)

(3) Košková S, Štochlová P, Novotná K, **Amirbekov A**, Hrabák P. Influence of delta-hexachlorocyclohexane (δ-HCH) to Phytophthora ×alni resistant Alnus glutinosa genotypes - Evaluation of physiological parameters and remediation potential. Ecotoxicol Environ Saf. 2022 Dec 1;247:114235. https://doi.org/10.1016/j.ecoenv.2022.114235 (IF 6.8)

(4) **Amirbekov A.,** Strojsova M., Nemecek J., Riha J., Hrabak P., Arias C., Sevcu A. and Černík M., 2023. Biodiversity in wetland+ system: a passive solution for HCH dump effluents. Water Science & Technology, p.wst 2023395. https://doi.org/10.2166/wst.2023.395 (IF 2.7)

(5) **Amirbekov A,** Vrchovecka S, Riha J, Petrik I, Friedecky D, Novak O, Cernik M, Hrabak P, Sevcu A. Assessing HCH isomer uptake in Alnus glutinosa: implications for phytoremediation and microbial response. Sci Rep. 2024 Feb 20;14(1):4187. https://doi.org/10.1038/s41598-024-54235-1 (IF 4.6)

(6) Vrchovecká S, **Amirbekov A**, Sázavská T, Arias CA, Jespersen EA, Černík M, Hrabák P. Chemical analysis of wetland plants to evaluate the bioaccumulation and metabolism of hexachlorocyclohexane (HCH). Sci Total Environ. 2024 Feb 20; 921:171141. https://doi.org/10.1016/j.scitotenv.2024.171141 (IF 9.8)

Conference participation

August 2018	17th Symposium for International Society for Microbial Ecology (ISME 17) Leipzig, Germany.
May 2019	Sustainable use and management of soil and water soils **AquaConSoil**. Antwerp, Belgium.
June 2019	8th International Symposium on wetland pollutant dynamics and control **WETPOL**.Aarhus, Denmark.
May 2020	Society of Environmental Toxicology and Chemistry **SETAC** Europe 30th annual meeting. Dublin. Ireland. *Online.*
June 2020 August 2021	Studentská konference FM. Liberec.
May 2021	Society of Environmental Toxicology and Chemistry **SETAC** Europe 31st annual meeting. Seville, Spain. *Online.*
September 2021	9th International Symposium on wetland pollutant dynamics and control **WETPOL**. Vienna, Austria. *Online.*
October 2021	7th Young Water Professionals Denmark's Annual Conference. Copenhagen, Denmark.
October 2022	**ECOpole**'22, Krakow, Poland.
November 2022	17th International conference on wetland systems for water pollution control **ICWS**, Lyon, France.
May 2023	Society of Environmental Toxicology and Chemistry **SETAC** Europe 33rd annual meeting. Dublin. Ireland.
September 2023	Sustainable use and management of soil and water soils **AquaConSoil**. Prague, Czechia.

References

Ahmad, M., Rajapaksha, A.U., Lim, J.E., Zhang, M., Bolan, N., Mohan, D., Vithanage, M., Lee, S.S., Ok, Y.S., 2014. Biochar as a sorbent for contaminant management in soil and water: A review. Chemosphere 99, 19–33. https://doi.org/10.1016/j.chemosphere.2013.10.071

Albuquerque, L., da Costa, M.S., 2014. The Family Gaiellaceae, in: Rosenberg, E., DeLong, E.F., Lory, S., Stackebrandt, E., Thompson, F. (Eds.), The Prokaryotes: Actinobacteria. Springer, Berlin, Heidelberg, pp. 357–360. https://doi.org/10.1007/978-3-642-30138-4_394

Ali, I., Asim, Mohd., Khan, T.A., 2012. Low cost adsorbents for the removal of organic pollutants from wastewater. J. Environ. Manage. 113, 170–183. https://doi.org/10.1016/j.jenvman.2012.08.028

Amirbekov, A., Mamirova, A., Sevcu, A., Spanek, R., Hrabak, P., 2021. HCH Removal in a Biochar-Amended Biofilter. Water 13, 3396. https://doi.org/10.3390/w13233396

Amirbekov, A., Strojsova, M., Nemecek, J., Riha, J., Hrabak, P., Arias, C., Sevcu, A., Černík, M., 2023. Biodiversity in wetland+ system: a passive solution for HCH dump effluents. Water Sci. Technol. wst2023395. https://doi.org/10.2166/wst.2023.395

Amirbekov, A., Vrchovecka, S., Riha, J., Petrik, I., Friedecky, D., Novak, O., Cernik, M., Hrabak, P., Sevcu, A., 2024. Assessing HCH isomer uptake in Alnus glutinosa: implications for phytoremediation and microbial response. Sci. Rep. 14, 4187. https://doi.org/10.1038/s41598-024-54235-1

Anderson, J.P., Badruzsaufari, E., Schenk, P.M., Manners, J.M., Desmond, O.J., Ehlert, C., Maclean, D.J., Ebert, P.R., Kazan, K., 2004. Antagonistic interaction between abscisic acid and jasmonate-ethylene signaling pathways modulates defense gene expression and disease resistance in Arabidopsis. Plant Cell 16, 3460–3479. https://doi.org/10.1105/tpc.104.025833

Anderson, T.A., Coats, J.R., 1995. Screening rhizosphere soil samples for the ability to mineralize elevated concentrations of atrazine and metolachlor. J. Environ. Sci. Health Part B 30, 473–484. https://doi.org/10.1080/03601239509372948

Arey, J.S., Green, W.H., Gschwend, P.M., 2005. The Electrostatic Origin of Abraham's Solute Polarity Parameter. J. Phys. Chem. B 109, 7564–7573. https://doi.org/10.1021/jp044525f

Atashgahi, S., Maphosa, F., Doğan, E., Smidt, H., Springael, D., Dejonghe, W., 2013. Small-scale oxygen distribution determines the vinyl chloride biodegradation pathway in surficial sediments of riverbed hyporheic zones. FEMS Microbiol. Ecol. 84, 133–142. https://doi.org/10.1111/1574-6941.12044

Bachmann, A., Walet, P., Wijnen, P., de Bruin, W., Huntjens, J.L., Roelofsen, W., Zehnder, A.J., 1988. Biodegradation of alpha- and beta-hexachlorocyclohexane in a soil slurry under different redox conditions. Appl. Environ. Microbiol. 54, 143–149. https://doi.org/10.1128/aem.54.1.143-149.1988

Baek, J.H., Baek, W., Ruan, W., Jung, H.S., Lee, S.C., Jeon, C.O., 2022. Massilia soli sp. nov., isolated from soil. Int. J. Syst. Evol. Microbiol. 72, 005227. https://doi.org/10.1099/ijsem.0.005227

Bais, H.P., Weir, T.L., Perry, L.G., Gilroy, S., Vivanco, J.M., 2006. The role of root exudates in rhizosphere interactions with plants and other organisms. Annu. Rev. Plant Biol. 57, 233–266. https://doi.org/10.1146/annurev.arplant.57.032905.105159

Bajpai, A., Shukla, P., Dixit, B.S., Banerji, R., 2007. Concentrations of organochlorine insecticides in edible oils from different regions of india. Chemosphere 67, 1403–1407. https://doi.org/10.1016/j.chemosphere.2006.10.026

Baker, A.J.M., McGrath, S.P., Reeves, R.D., Smith, J.A.C., 1999. Metal hyperaccumulator plants: a review of the ecology and physiology of a biological resource for phytoremediation of metal-polluted soils, in: Terry, N., Vangronsveld, J., Banuelos, G. (Eds.), . CRC Press, Boca Raton, Florida, pp. 85–107.

Bala, K., Geueke, B., Miska, M.E., Rentsch, D., Poiger, T., Dadhwal, M., Lal, R., Holliger, C., Kohler, H.-P.E., 2012. Enzymatic Conversion of ε-Hexachlorocyclohexane and a Heptachlorocyclohexane Isomer, Two Neglected Components of Technical Hexachlorocyclohexane. Environ. Sci. Technol. 46, 4051–4058. https://doi.org/10.1021/es204143x

Bala, K., Sharma, P., Lal, R., 2010. Sphingobium quisquiliarum sp. nov., a hexachlorocyclohexane (HCH)-degrading bacterium isolated from an HCH-contaminated soil. Int. J. Syst. Evol. Microbiol. 60, 429–433. https://doi.org/10.1099/ijs.0.010868-0

Balázs, H.E., Schmid, C.A.O., Cruzeiro, C., Podar, D., Szatmari, P.-M., Buegger, F., Hufnagel, G., Radl, V., Schröder, P., 2021. Post-reclamation microbial diversity and functions in hexachlorocyclohexane (HCH) contaminated soil in relation to spontaneous HCH tolerant vegetation. Sci. Total Environ. 767, 144653. https://doi.org/10.1016/j.scitotenv.2020.144653

Balázs, H.E., Schmid, C.A.O., Feher, I., Podar, D., Szatmari, P.-M., Marincaş, O., Balázs, Z.R., Schröder, P., 2018. HCH phytoremediation potential of native plant species from a contaminated urban site in Turda, Romania. J. Environ. Manage. 223, 286–296. https://doi.org/10.1016/j.jenvman.2018.06.018

Beesley, L., Moreno-Jiménez, E., Gomez-Eyles, J.L., Harris, E., Robinson, B., Sizmur, T., 2011. A review of biochars' potential role in the remediation, revegetation and restoration of contaminated soils. Environ. Pollut. 159, 3269–3282. https://doi.org/10.1016/j.envpol.2011.07.023

Bokulich, N.A., Kaehler, B.D., Rideout, J.R., Dillon, M., Bolyen, E., Knight, R., Huttley, G.A., Gregory Caporaso, J., 2018. Optimizing taxonomic classification of marker-gene amplicon sequences with QIIME 2's q2-feature-classifier plugin. Microbiome 6, 90. https://doi.org/10.1186/s40168-018-0470-z

Böltner, D., Moreno-Morillas, S., Ramos, J.-L., 2005. 16S rDNA phylogeny and distribution of lin genes in novel hexachlorocyclohexane-degrading Sphingomonas strains. Environ. Microbiol. 7, 1329–1338. https://doi.org/10.1111/j.1462-5822.2005.00820.x

Bolyen, E., Rideout, J.R., Dillon, M.R., Bokulich, N.A., Abnet, C.C., Al-Ghalith, G.A., Alexander, H., Alm, E.J., Arumugam, M., Asnicar, F., Bai, Y., Bisanz, J.E., Bittinger, K., Brejnrod, A., Brislawn, C.J., Brown, C.T., Callahan, B.J., Caraballo-Rodríguez, A.M., Chase, J., Cope, E.K., Da Silva, R., Diener, C., Dorrestein, P.C., Douglas, G.M., Durall, D.M., Duvallet, C., Edwardson, C.F., Ernst, M., Estaki, M., Fouquier, J., Gauglitz, J.M., Gibbons, S.M., Gibson, D.L., Gonzalez, A., Gorlick, K., Guo, J., Hillmann, B., Holmes, S., Holste, H., Huttenhower, C., Huttley, G.A., Janssen, S., Jarmusch, A.K., Jiang, L., Kaehler, B.D., Kang, K.B., Keefe, C.R., Keim, P., Kelley, S.T., Knights, D., Koester, I., Kosciolek, T., Kreps, J., Langille, M.G.I., Lee, J., Ley, R., Liu, Y.-X., Loftfield, E., Lozupone, C., Maher, M., Marotz, C., Martin, B.D., McDonald, D., McIver, L.J., Melnik, A.V., Metcalf, J.L., Morgan, S.C., Morton, J.T., Naimey, A.T., Navas-Molina, J.A., Nothias, L.F., Orchanian, S.B., Pearson, T., Peoples, S.L., Petras, D., Preuss, M.L., Pruesse, E., Rasmussen, L.B., Rivers, A., Robeson, M.S., Rosenthal, P., Segata, N., Shaffer, M., Shiffer, A., Sinha, R., Song, S.J., Spear, J.R., Swafford, A.D., Thompson, L.R., Torres, P.J., Trinh, P., Tripathi, A., Turnbaugh, P.J., Ul-Hasan, S., van der Hooft, J.J.J., Vargas, F., Vázquez-Baeza, Y., Vogtmann, E., von Hippel, M., Walters, W., Wan, Y., Wang, M., Warren, J., Weber, K.C., Williamson, C.H.D., Willis, A.D., Xu, Z.Z., Zaneveld, J.R., Zhang, Y., Zhu, Q., Knight, R., Caporaso, J.G., 2019. Reproducible, interactive, scalable and extensible microbiome data science using QIIME 2. Nat. Biotechnol. 37, 852–857. https://doi.org/10.1038/s41587-019-0209-9

Boyle, A.W., Häggblom, M.M., Young, L.Y., 1999. Dehalogenation of lindane (γ-hexachlorocyclohexane) by anaerobic bacteria from marine sediments and by sulfate-reducing bacteria. FEMS Microbiol. Ecol. 29, 379–387. https://doi.org/10.1111/j.1574-6941.1999.tb00628.x

Breivik, K., Pacyna, J.M., Münch, J., 1999. Use of α-, β- and γ-hexachlorocyclohexane in Europe, 1970–1996. Sci. Total Environ. 239, 151–163. https://doi.org/10.1016/S0048-9697(99)00291-0

Briggs, G.G., Bromilow, R.H., Evans, A.A., 1982. Relationships between lipophilicity and root uptake and translocation of non-ionised chemicals by barley. Pestic. Sci. 13, 495–504. https://doi.org/10.1002/ps.2780130506

Brittain, D.R.B., Pandey, R., Kumari, K., Sharma, P., Pandey, G., Lal, R., Coote, M.L., Oakeshott, J.G., Jackson, C.J., 2010. Competing SN2 and E2 reaction pathways for hexachlorocyclohexane degradation in the gas phase, solution and enzymes. Chem. Commun. 47, 976–978. https://doi.org/10.1039/C0CC02925D

Bromilow, R.H., Chamberlain, K., 1995. Principles governing uptake and transport of chemicals, in: Trapp, S., McFarlane, J.C. (Eds.), . CRC Press, Boca Raton, Florida, pp. 37–68.

Bueno, M., Fillat, M.F., Strasser, R.J., Maldonado-Rodriguez, R., Marina, N., Smienk, H., Gómez-Moreno, C., Barja, F., 2004. Effects of lindane on the photosynthetic apparatus of the cyanobacteriumanabaena. Environ. Sci. Pollut. Res. 11, 98–106. https://doi.org/10.1007/BF02979709

Buser, H.-Rudolf., Mueller, M.D., 1995. Isomer and Enantioselective Degradation of Hexachlorocyclohexane Isomers in Sewage Sludge under Anaerobic Conditions. Environ. Sci. Technol. 29, 664–672. https://doi.org/10.1021/es00003a013

Callahan, B.J., McMurdie, P.J., Rosen, M.J., Han, A.W., Johnson, A.J.A., Holmes, S.P., 2016. DADA2: High-resolution sample inference from Illumina amplicon data. Nat. Methods 13, 581–583. https://doi.org/10.1038/nmeth.3869

Calvelo Pereira, R., Camps-Arbestain, M., Rodríguez Garrido, B., Macías, F., Monterroso, C., 2006. Behaviour of α-, β-, γ-, and δ-hexachlorocyclohexane in the soil–plant system of a contaminated site. Environ. Pollut., Soil and Sediment Remediation (SSR) 144, 210–217. https://doi.org/10.1016/j.envpol.2005.12.030

Chakraborty, P., Zhang, G., Li, J., Sampathkumar, P., Balasubramanian, T., Kathiresan, K., Takahashi, S., Subramanian, A., Tanabe, S., Jones, K.C., 2019. Seasonal variation of atmospheric organochlorine pesticides and polybrominated diphenyl ethers in Parangipettai, Tamil Nadu, India: Implication for atmospheric transport. Sci. Total Environ. 649, 1653–1660. https://doi.org/10.1016/j.scitotenv.2018.07.414

Chaudhry, Q., Schröder, P., Werck-Reichhart, D., Grajek, W., Marecik, R., 2002. Prospects and limitations of phytoremediation for the removal of persistent pesticides in the environment. Environ. Sci. Pollut. Res. 9, 4. https://doi.org/10.1007/BF02987313

Chen, W., Wei, R., Ni, J., Yang, L., Qian, W., Yang, Y., 2018. Sorption of chlorinated hydrocarbons to biochars in aqueous environment: Effects of the amorphous carbon structure of biochars and the molecular properties of adsorbates. Chemosphere 210, 753–761. https://doi.org/10.1016/j.chemosphere.2018.07.071

Claesson, M.J., Wang, Q., O'Sullivan, O., Greene-Diniz, R., Cole, J.R., Ross, R.P., O'Toole, P.W., 2010. Comparison of two next-generation sequencing technologies for resolving highly complex microbiota composition using tandem variable 16S rRNA gene regions. Nucleic Acids Res. 38, e200–e200. https://doi.org/10.1093/nar/gkq873

Clifford, R.J., Milillo, M., Prestwood, J., Quintero, R., Zurawski, D.V., Kwak, Y.I., Waterman, P.E., Lesho, E.P., Gann, P.M., 2012. Detection of Bacterial 16S rRNA and Identification of Four Clinically Important Bacteria by Real-Time PCR. PLOS ONE 7, e48558. https://doi.org/10.1371/journal.pone.0048558

Cruz Viggi, C., Rossetti, S., Fazi, S., Paiano, P., Majone, M., Aulenta, F., 2014. Magnetite Particles Triggering a Faster and More Robust Syntrophic Pathway of Methanogenic Propionate Degradation. Environ. Sci. Technol. 48, 7536–7543. https://doi.org/10.1021/es5016789

Cui, L., Yin, C., Chen, T., Quan, G., Ippolito, J.A., Liu, B., Yan, J., Ding, C., Hussain, Q., Umer, M., 2019. Remediation of organic halogen- contaminated wetland soils using biochar. Sci. Total Environ. 696, 134087. https://doi.org/10.1016/j.scitotenv.2019.134087

Curl, E.A., Truelove, B., 2012. The Rhizosphere. Springer Science & Business Media.

Dadhwal, M., Singh, A., Prakash, O., Gupta, S.K., Kumari, K., Sharma, P., Jit, S., Verma, M., Holliger, C., Lal, R., 2009. Proposal of biostimulation for hexachlorocyclohexane (HCH)-decontamination and characterization of culturable bacterial community from high-dose point HCH-contaminated soils. J. Appl. Microbiol. 106, 381–392. https://doi.org/10.1111/j.1365-2672.2008.03982.x

Dakora, F.D., Phillips, D.A., 2002. Root exudates as mediators of mineral acquisition in low-nutrient environments, in: Adu-Gyamfi, J.J. (Ed.), Food Security in Nutrient-Stressed Environments: Exploiting Plants' Genetic Capabilities, Developments in Plant and Soil Sciences. Springer Netherlands, Dordrecht, pp. 201–213. https://doi.org/10.1007/978-94-017-1570-6_23

Deng, C., Huang, L., Liang, Y., Xiang, H., Jiang, J., Wang, Q., Hou, J., Chen, Y., 2019. Response of microbes to biochar strengthen nitrogen removal in subsurface flow constructed wetlands: Microbial community structure and metabolite characteristics. Sci. Total Environ. 694, 133687. https://doi.org/10.1016/j.scitotenv.2019.133687

Denyes, M.J., Langlois, V.S., Rutter, A., Zeeb, B.A., 2012. The use of biochar to reduce soil PCB bioavailability to Cucurbita pepo and Eisenia fetida. Sci. Total Environ. 437, 76–82. https://doi.org/10.1016/j.scitotenv.2012.07.081

Desai, M., Haigh, M., Walkington, H., 2019. Phytoremediation: Metal decontamination of soils after the sequential forestation of former opencast coal land. Sci. Total Environ. 656, 670–680. https://doi.org/10.1016/j.scitotenv.2018.11.327

Dettenmaier, E.M., Doucette, W.J., Bugbee, B., 2009. Chemical Hydrophobicity and Uptake by Plant Roots. Environ. Sci. Technol. 43, 324–329. https://doi.org/10.1021/es801751x

Directorate-General for Internal Policies of the Union (European Parliament), E.-C.M., 2017. Lindane (persistant organic pollutant) in the EU. [WWW Document]. URL http://op.europa.eu/en/publication-detail/-/publication/8e37ab69-bd13-11e6-a237-01aa75ed71a1 (accessed 5.24.21).

Dominguez, C.M., Parchão, J., Rodriguez, S., Lorenzo, D., Romero, A., Santos, A., 2016. Kinetics of Lindane Dechlorination by Zerovalent Iron Microparticles: Effect of Different Salts and Stability Study. Ind Eng Chem Res 55, 12776-12785,. https://doi.org/10.1021/acs.iecr.6b03434.

Dowd, S.E., Callaway, T.R., Wolcott, R.D., Sun, Y., McKeehan, T., Hagevoort, R.G., Edrington, T.S., 2008. Evaluation of the bacterial diversity in the feces of cattle using 16S rDNA bacterial tag-encoded FLX amplicon pyrosequencing (bTEFAP). BMC Microbiol. 8, 125. https://doi.org/10.1186/1471-2180-8-125

Erkmen, B., Kolankaya, D., 2006. Determination of organochlorine pesticide residues in water, sediment, and fish samples from the Meriç Delta, Turkey. Int. J. Environ. Anal. Chem. 86, 161–169. https://doi.org/10.1080/03067310500247926

Fahy, A., McGenity, T.J., Timmis, K.N., Ball, A.S., 2006. Heterogeneous aerobic benzene-degrading communities in oxygen-depleted groundwaters. FEMS Microbiol. Ecol. 58, 260–270. https://doi.org/10.1111/j.1574-6941.2006.00162.x

Faure, M., San Miguel, A., Ravanel, P., Raveton, M., 2012. Concentration responses to organochlorines in Phragmites australis. Environ. Pollut. 164, 188–194. https://doi.org/10.1016/j.envpol.2012.01.040

Gołębiewski, M., Deja-Sikora, E., Cichosz, M., Tretyn, A., Wróbel, B., 2014. 16S rDNA Pyrosequencing Analysis of Bacterial Community in Heavy Metals Polluted Soils. Microb. Ecol. 67, 635–647. https://doi.org/10.1007/s00248-013-0344-7

Gomez-Eyles, J.L., Sizmur, T., Collins, C.D., Hodson, M.E., 2011. Effects of biochar and the earthworm Eisenia fetida on the bioavailability of polycyclic aromatic hydrocarbons and potentially toxic elements. Environ. Pollut. 159, 616–622. https://doi.org/10.1016/j.envpol.2010.09.037

Grgić, M., Maletić, S., Beljin, J., Isakovski, M.K., Rončević, S., Tubić, A., Agbaba, J., 2019. Lindane and hexachlorobenzene sequestration and detoxification in contaminated sediment amended with carbon-rich sorbents. Chemosphere.

Gu, H., Yan, K., You, Q., Chen, Y., Pan, Y., Wang, H., Wu, L., Xu, J., 2021. Soil indigenous microorganisms weaken the synergy of Massilia sp. WF1 and Phanerochaete chrysosporium in phenanthrene biodegradation. Sci. Total Environ. 781, 146655. https://doi.org/10.1016/j.scitotenv.2021.146655

Gupta, S.K., Lal, D., Lata, P., Sangwan, N., Garg, N., Holliger, C., Lal, R., 2013. Changes in the bacterial community and lin genes diversity during biostimulation of indigenous bacterial community of hexachlorocyclohexane (HCH) dumpsite soil. Microbiology 82, 234–240. https://doi.org/10.1134/S0026261713020185

Ha, S., Vankova, R., Yamaguchi-Shinozaki, K., Shinozaki, K., Tran, L.-S.P., 2012. Cytokinins: metabolism and function in plant adaptation to environmental stresses. Trends Plant Sci. 17, 172–179. https://doi.org/10.1016/j.tplants.2011.12.005

Hedden, P., 2020. The Current Status of Research on Gibberellin Biosynthesis. Plant Cell Physiol. 61, 1832–1849. https://doi.org/10.1093/pcp/pcaa092

Heo, J., Won, M., Lee, D., Han, B.-H., Hong, S.-B., Kwon, S.-W., 2022. Duganella dendranthematis sp. nov. and Massilia forsythiae sp. nov., isolated from flowers. Int. J. Syst. Evol. Microbiol. 72, 005487. https://doi.org/10.1099/ijsem.0.005487

Hsu, P.-K., Dubeaux, G., Takahashi, Y., Schroeder, J.I., 2021. Signaling mechanisms in abscisic acid-mediated stomatal closure. Plant J. 105, 307–321. https://doi.org/10.1111/tpj.15067

Huntjens, J.L.M., Brouwer, W., Grobben, K., Jansma, O., Scheffer, F., Zehnder, A.J.B., 1988. Biodegradation of Alpha-Hexachlorocyclohexane by a Bacterium Isolated from Polluted Soil, in: Wolf, K., Van Den Brink, W.J., Colon, F.J. (Eds.), Contaminated Soil '88: Second International TNO/BMFT Conference on Contaminated Soil, 11–15 April 1988, Hamburg, Federal Republic of Germany. Springer Netherlands, Dordrecht, pp. 733–737. https://doi.org/10.1007/978-94-009-2807-7_118

Johnston-Monje, D., Gutiérrez, J.P., Lopez-Lavalle, L.A.B., 2021. Seed-Transmitted Bacteria and Fungi Dominate Juvenile Plant Microbiomes. Front. Microbiol. 12.

Kaur, I., Gaur, V.K., Regar, R.K., Roy, A., Srivastava, P.K., Gaur, R., Manickam, N., Barik, S.K., 2021. Plants exert beneficial influence on soil microbiome in a HCH contaminated soil revealing advantage of microbe-assisted plant-based HCH remediation of a dumpsite. Chemosphere 280, 130690. https://doi.org/10.1016/j.chemosphere.2021.130690

Kaushik, C.P., 1989. Loss of HCH from surface soil layers under subtropical conditions. Environ. Pollut. 59, 253–264. https://doi.org/10.1016/0269-7491(89)90230-3

Kidd, P.S., Prieto-Fernández, A., Monterroso, C., Acea, M.J., 2008. Rhizosphere microbial community and hexachlorocyclohexane degradative potential in contrasting plant species. Plant Soil 302, 233–247. https://doi.org/10.1007/s11104-007-9475-2

Košková, S., Štochlová, P., Novotná, K., Amirbekov, A., Hrabák, P., 2022. Influence of delta-hexachlorocyclohexane (δ-HCH) to Phytophthora ×alni resistant Alnus glutinosa genotypes − Evaluation of physiological parameters and remediation potential. Ecotoxicol. Environ. Saf. 247, 114235. https://doi.org/10.1016/j.ecoenv.2022.114235

Kotov, A.A., Kotova, L.M., Romanov, G.A., 2021. Signaling network regulating plant branching: Recent advances and new challenges. Plant Sci. 307, 110880. https://doi.org/10.1016/j.plantsci.2021.110880

Kumar, D., Pannu, R., 2018. Perspectives of lindane (γ-hexachlorocyclohexane) biodegradation from the environment: a review. Bioresour. Bioprocess. 5, 29. https://doi.org/10.1186/s40643-018-0213-9

Kumari, R., Subudhi, S., Suar, M., Dhingra, G., Raina, V., Dogra, C., Lal, S., van der Meer, J.R., Holliger, C., Lal, R., 2002. Cloning and Characterization of lin Genes Responsible for the Degradation of Hexachlorocyclohexane Isomers by Sphingomonas paucimobilis Strain B90. Appl. Environ. Microbiol. 68, 6021–6028. https://doi.org/10.1128/AEM.68.12.6021-6028.2002

Lal, R., Dogra, C., Malhotra, S., Sharma, P., Pal, R., 2006. Diversity, distribution and divergence of lin genes in hexachlorocyclohexane-degrading sphingomonads. Trends Biotechnol. 24, 121–130. https://doi.org/10.1016/j.tibtech.2006.01.005

Lal, R., Pandey, G., Sharma, P., Kumari, K., Malhotra, S., Pandey, R., Raina, V., Kohler, H.-P.E., Holliger, C., Jackson, C., Oakeshott, J.G., 2010. Biochemistry of Microbial Degradation of Hexachlorocyclohexane and Prospects for Bioremediation. Microbiol. Mol. Biol. Rev. MMBR 74, 58–80. https://doi.org/10.1128/MMBR.00029-09

Lamarche, O., Platts, J.A., Hersey, A., 2001. Theoretical prediction of the polarity/polarizability parameter π2H. Phys. Chem. Chem. Phys. 3, 2747–2753. https://doi.org/10.1039/B102708P

Lata, P., Lal, D., Lal, R., 2012. Flavobacterium ummariense sp. nov., isolated from hexachlorocyclohexane-contaminated soil, and emended description of Flavobacterium ceti Vela et al. 2007. Int. J. Syst. Evol. Microbiol. 62, 2674–2679. https://doi.org/10.1099/ijs.0.030916-0

Le Bris, M., 2017. Hormones in Growth and Development☆, in: Reference Module in Life Sciences. Elsevier. https://doi.org/10.1016/B978-0-12-809633-8.05058-5

Leoni, C., Volpicella, M., Fosso, B., Manzari, C., Piancone, E., Dileo, M.C.G., Arcadi, E., Yakimov, M., Pesole, G., Ceci, L.R., 2020. A Differential Metabarcoding Approach to Describe Taxonomy Profiles of Bacteria and Archaea in the Saltern of Margherita di Savoia (Italy). Microorganisms 8, 936. https://doi.org/10.3390/microorganisms8060936

Li, H., Jiang, W., Pan, Y., Li, F., Wang, C., Tian, H., 2021. Occurrence and partition of organochlorine pesticides (OCPs) in water, sediment, and organisms from the eastern sea area of Shandong Peninsula, Yellow Sea, China. Mar. Pollut. Bull. 162, 111906. https://doi.org/10.1016/j.marpolbul.2020.111906

Liang, Y., Liu, X., Singletary, M.A., Wang, K., Mattes, T.E., 2017. Relationships between the Abundance and Expression of Functional Genes from Vinyl Chloride (VC)-Degrading Bacteria and Geochemical Parameters at VC-Contaminated Sites. Environ. Sci. Technol. 51, 12164–12174. https://doi.org/10.1021/acs.est.7b03521

Liu, J., Wang, Z., Belchik, S., Edwards, M., Liu, C., Kennedy, D., Merkley, E., Lipton, M., Butt, J., Richardson, D., Zachara, J., Fredrickson, J., Rosso, K., Shi, L., 2012. Identification and Characterization of MtoA: A Decaheme c-Type Cytochrome of the Neutrophilic Fe(II)-Oxidizing Bacterium Sideroxydans lithotrophicus ES-1. Front. Microbiol. 3, 37. https://doi.org/10.3389/fmicb.2012.00037

Liu, X., Li, W., Kümmel, S., Merbach, I., Sood, U., Gupta, V., Lal, R., Richnow, H.H., 2021. Soil from a Hexachlorocyclohexane Contaminated Field Site Inoculates Wheat in a Pot Experiment to Facilitate the

Microbial Transformation of β-Hexachlorocyclohexane Examined by Compound-Specific Isotope Analysis. Environ. Sci. Technol. 55, 13812–13821. https://doi.org/10.1021/acs.est.1c03322

Liu, X., Peng, P., Fu, J., Huang, W., 2003. Effects of FeS on the Transformation Kinetics of γ-Hexachlorocyclohexane. Environ. Sci. Technol. 37, 1822–1828. https://doi.org/10.1021/es0259178

M. Homolková, M.K., P. Hrabák, Černík, M., 2015. Degradability of hexachlorocyclohexanes in water using ferrate (VI. Water Sci Technol 71, 405-411,. https://doi.org/10.2166/wst.2014.516.

Man, Y.B., Chow, K.L., Cheng, Z., Kang, Y., Wong, M.H., 2018. Profiles and removal efficiency of organochlorine pesticides with emphasis on DDTs and HCHs by two different sewage treatment works. Environ. Technol. Innov. 9, 220–231. https://doi.org/10.1016/j.eti.2017.12.004

Mano, Y., Nemoto, K., 2012. The pathway of auxin biosynthesis in plants. J. Exp. Bot. 63, 2853–2872. https://doi.org/10.1093/jxb/ers091

Maphosa, F., Vos, W.M. de, Smidt, H., 2010. Exploiting the ecogenomics toolbox for environmental diagnostics of organohalide-respiring bacteria. Trends Biotechnol. 28, 308–316. https://doi.org/10.1016/j.tibtech.2010.03.005

Marcus, Y., 1991. Linear solvation energy relationships. Correlation and prediction of the distribution of organic solutes between water and immiscible organic solvents. J. Phys. Chem. 95, 8886–8891. https://doi.org/10.1021/j100175a086

McMurdie, P.J., Holmes, S., 2013. phyloseq: An R Package for Reproducible Interactive Analysis and Graphics of Microbiome Census Data. PLOS ONE 8, e61217. https://doi.org/10.1371/journal.pone.0061217

Miya, R.K., Firestone, M.K., 2001. Enhanced Phenanthrene Biodegradation in Soil by Slender Oat Root Exudates and Root Debris. J. Environ. Qual. 30, 1911–1918. https://doi.org/10.2134/jeq2001.1911

Miyauchi, K., Suh, S.-K., Nagata, Y., Takagi, M., 1998. Cloning and Sequencing of a 2,5-Dichlorohydroquinone Reductive Dehalogenase Gene Whose Product Is Involved in Degradation of γ-Hexachlorocyclohexane by Sphingomonas paucimobilis. J. Bacteriol. 180, 1354–1359. https://doi.org/10.1128/JB.180.6.1354-1359.1998

Mohan, D., Sarswat, A., Ok, Y.S., Pittman, C.U., 2014. Organic and inorganic contaminants removal from water with biochar, a renewable, low cost and sustainable adsorbent – A critical review. Bioresour. Technol., Special Issue on Biosorption 160, 191–202. https://doi.org/10.1016/j.biortech.2014.01.120

Mohn, W.W., Mertens, B., Neufeld, J.D., Verstraete, W., Lorenzo, V.D., 2006. Distribution and phylogeny of hexachlorocyclohexane-degrading bacteria in soils from Spain. Environ. Microbiol. 8, 60–68. https://doi.org/10.1111/j.1462-2920.2005.00865.x

Monferrán, M.V., Echenique, J.R., Wunderlin, D.A., 2005. Degradation of chlorobenzenes by a strain of Acidovorax avenae isolated from a polluted aquifer. Chemosphere 61, 98–106. https://doi.org/10.1016/j.chemosphere.2005.03.003

Murthy, H.M.R., Manonmani, H.K., 2007. Aerobic degradation of technical hexachlorocyclohexane by a defined microbial consortium. J. Hazard. Mater. 149, 18–25. https://doi.org/10.1016/j.jhazmat.2007.03.053

Nagata, Y., Endo, R., Ito, M., Ohtsubo, Y., Tsuda, M., 2007. Aerobic degradation of lindane (γ-hexachlorocyclohexane) in bacteria and its biochemical and molecular basis. Appl. Microbiol. Biotechnol. 76, 741–752. https://doi.org/10.1007/s00253-007-1066-x

Nagata, Y., Miyauchi, K., Takagi, M., 1999. Complete analysis of genes and enzymes for γ-hexachlorocyclohexane degradation in Sphingomonas paucimobilis UT26. J. Ind. Microbiol. Biotechnol. 23, 380–390. https://doi.org/10.1038/sj.jim.2900736

Nagata, Y., Nariya, T., Ohtomo, R., Fukuda, M., Yano, K., Takagi, M., 1993. Cloning and sequencing of a dehalogenase gene encoding an enzyme with hydrolase activity involved in the degradation of gamma-hexachlorocyclohexane in Pseudomonas paucimobilis. J. Bacteriol. 175, 6403–6410. https://doi.org/10.1128/jb.175.20.6403-6410.1993

Nagata, Y., Prokop, Z., Sato, Y., Jerabek, P., Kumar, A., Ohtsubo, Y., Tsuda, M., Damborský, J., 2005. Degradation of β-Hexachlorocyclohexane by Haloalkane Dehalogenase LinB from Sphingomonas paucimobilis UT26. Appl. Environ. Microbiol. 71, 2183–2185. https://doi.org/10.1128/AEM.71.4.2183-2185.2005

Nechanická M, D.L., Dolinová I, 2018. Use of nanofiber carriers for monitoring of microbial biomass., in: Topical Issues of Rational Use of Natural Resources: Proceedings of Th. CRC Press, p. 361.

Němeček, J., Dolinová, I., Macháčková, J., Špánek, R., Ševců, A., Lederer, T., Černík, M., 2017. Stratification of chlorinated ethenes natural attenuation in an alluvial aquifer assessed by hydrochemical and biomolecular tools. Chemosphere 184, 1157–1167. https://doi.org/10.1016/j.chemosphere.2017.06.100

Oakley, A.J., Klvaňa, M., Otyepka, M., Nagata, Y., Wilce, M.C.J., Damborský, J., 2004. Crystal Structure of Haloalkane Dehalogenase LinB from Sphingomonas paucimobilis UT26 at 0.95 Å Resolution: Dynamics of Catalytic Residues,. Biochemistry 43, 870–878. https://doi.org/10.1021/bi034748g

Odedishemi Ajibade, F., Wang, H.-C., Guadie, A., Fausat Ajibade, T., Fang, Y.-K., Muhammad Adeel Sharif, H., Liu, W.-Z., Wang, A.-J., 2021. Total nitrogen removal in biochar amended non-aerated vertical flow constructed wetlands for secondary wastewater effluent with low C/N ratio: Microbial community structure and dissolved organic carbon release conditions. Bioresour. Technol. 322, 124430. https://doi.org/10.1016/j.biortech.2020.124430

Okai, M., Kubota, K., Fukuda, M., Nagata, Y., Nagata, K., Tanokura, M., 2010. Crystal Structure of γ-Hexachlorocyclohexane Dehydrochlorinase LinA from Sphingobium japonicum UT26. J. Mol. Biol. 403, 260–269. https://doi.org/10.1016/j.jmb.2010.08.043

Okeke, B.C., Siddique, T., Arbestain, M.C., Frankenberger, W.T., 2002. Biodegradation of gamma-hexachlorocyclohexane (lindane) and alpha-hexachlorocyclohexane in water and a soil slurry by a Pandoraea species. J. Agric. Food Chem. 50, 2548–2555. https://doi.org/10.1021/jf011422a

Oksanen, J., Kindt, R., Legendre, P., Hara, B., Simpson, G., Solymos, P., Henry, M., Stevens, H., Maintainer, H., Oksanen@oulu, jari, 2009. The vegan Package.

Osugi, A., Sakakibara, H., 2015. Q&A: How do plants respond to cytokinins and what is their importance? BMC Biol. 13, 102. https://doi.org/10.1186/s12915-015-0214-5

Paul, A., Ghosh, C., Boettinger, W.J., 2011. Diffusion Parameters and Growth Mechanism of Phases in the Cu-Sn System. Metall. Mater. Trans. A 42, 952–963. https://doi.org/10.1007/s11661-010-0592-9

Perez de Souza, L., Alseekh, S., Naake, T., Fernie, A., 2019. Mass Spectrometry-Based Untargeted Plant Metabolomics. Curr. Protoc. Plant Biol. 4, e20100. https://doi.org/10.1002/cppb.20100

Phenrat, T., Le, T.S.T., Naknakorn, B., Lowry, G.V., 2019. Chemical Reduction and Oxidation of Organic Contaminants by Nanoscale Zerovalent Iron, in: Phenrat, T., Lowry, G.V. (Eds.), Nanoscale Zerovalent Iron Particles for Environmental Restoration: From Fundamental Science to Field Scale Engineering Applications. Springer International Publishing, Cham, pp. 97–155. https://doi.org/10.1007/978-3-319-95340-3_3

Pinton, R., Varanini, Z., Nannipieri, P. (Eds.), 2007. The Rhizosphere: Biochemistry and Organic Substances at the Soil-Plant Interface, Second Edition, 2nd ed. CRC Press, Boca Raton. https://doi.org/10.1201/9781420005585

Planas-Riverola, A., Gupta, A., Betegón-Putze, I., Bosch, N., Ibañes, M., Caño-Delgado, A.I., 2019. Brassinosteroid signaling in plant development and adaptation to stress. Dev. Camb. Engl. 146, dev151894. https://doi.org/10.1242/dev.151894

Podlešáková, K., Fardoux, J., Patrel, D., Bonaldi, K., Novák, O., Strnad, M., Giraud, E., Spíchal, L., Nouwen, N., 2013. Rhizobial synthesized cytokinins contribute to but are not essential for the symbiotic interaction between photosynthetic Bradyrhizobia and Aeschynomene legumes. Mol. Plant-Microbe Interact. MPMI 26, 1232–1238. https://doi.org/10.1094/MPMI-03-13-0076-R

Proietti, S., Caarls, L., Coolen, S., Van Pelt, J.A., Van Wees, S.C.M., Pieterse, C.M.J., 2018. Genome-wide association study reveals novel players in defense hormone crosstalk in Arabidopsis. Plant Cell Environ. 41, 2342–2356. https://doi.org/10.1111/pce.13357

Quast, C., Pruesse, E., Yilmaz, P., Gerken, J., Schweer, T., Yarza, P., Peplies, J., Glöckner, F.O., 2013. The SILVA ribosomal RNA gene database project: improved data processing and web-based tools. Nucleic Acids Res. 41, D590–D596. https://doi.org/10.1093/nar/gks1219

Ramteke, P.W., Hans, R.K., 2008. Isolation of hexachlorocyclohexane (HCH) degrading microorganisms from earthworm got. J. Environ. Sci. Health Part A. https://doi.org/10.1080/10934529209375844

Richards, P.M., Liang, Y., Johnson, R.L., Mattes, T.E., 2019. Cryogenic soil coring reveals coexistence of aerobic and anaerobic vinyl chloride degrading bacteria in a chlorinated ethene contaminated aquifer. Water Res. 157, 281–291. https://doi.org/10.1016/j.watres.2019.03.059

Rigét, F., Bignert, A., Braune, B., Dam, M., Dietz, R., Evans, M., Green, N., Gunnlaugsdóttir, H., Hoydal, K.S., Kucklick, J., Letcher, R., Muir, D., Schuur, S., Sonne, C., Stern, G., Tomy, G., Vorkamp, K., Wilson, S., 2019. Temporal trends of persistent organic pollutants in Arctic marine and freshwater biota. Sci. Total Environ. 649, 99–110. https://doi.org/10.1016/j.scitotenv.2018.08.268

Rissato, S.R., Galhiane, M.S., Fernandes, J.R., Gerenutti, M., Gomes, H.M., Ribeiro, R., Almeida, M.V. de, 2015. Evaluation of *Ricinus communis* L. for the Phytoremediation of Polluted Soil with Organochlorine Pesticides. BioMed Res. Int. 2015, e549863. https://doi.org/10.1155/2015/549863

Sah, S.K., Reddy, K.R., Li, J., 2016. Abscisic Acid and Abiotic Stress Tolerance in Crop Plants. Front. Plant Sci. 7.

Saxena, A., Anand, S., Dua, A., Sangwan, N., Khan, F., Lal, R., 2013. Novosphingobium lindaniclasticum sp. nov., a hexachlorocyclohexane (HCH)-degrading bacterium isolated from an HCH dumpsite. Int. J. Syst. Evol. Microbiol. 63, 2160–2167. https://doi.org/10.1099/ijs.0.045443-0

Schloss, P.D., Westcott, S.L., Ryabin, T., Hall, J.R., Hartmann, M., Hollister, E.B., Lesniewski, R.A., Oakley, B.B., Parks, D.H., Robinson, C.J., Sahl, J.W., Stres, B., Thallinger, G.G., Horn, D.J.V., Weber, C.F., 2009. Introducing mothur: Open-Source, Platform-Independent, Community-Supported Software for Describing and Comparing Microbial Communities. Appl. Environ. Microbiol. 75, 7537–7541. https://doi.org/10.1128/AEM.01541-09

Schnoor, J.L., Light, L.A., McCutcheon, S.C., Wolfe, N.L., Carreia, L.H., 2008. Phytoremediation of organic and nutrient contaminants [WWW Document]. ACS Publ. https://doi.org/10.1021/es00007a002

Schwitzguébel, J.-P., Meyer, J., Kidd, P., 2006. Pesticides Removal Using Plants: Phytodegradation Versus Phytostimulation, in: Mackova, M., Dowling, D., Macek, T. (Eds.), Phytoremediation Rhizoremediation. Springer Netherlands, pp. 179–198. https://doi.org/10.1007/978-1-4020-4999-4_13

Sharma, P., Raina, V., Kumari, R., Malhotra, S., Dogra, C., Kumari, H., Kohler, H.-P.E., Buser, H.-R., Holliger, C., Lal, R., 2006. Haloalkane Dehalogenase LinB Is Responsible for β- and δ-Hexachlorocyclohexane Transformation in Sphingobium indicum B90A. Appl. Environ. Microbiol. 72, 5720–5727. https://doi.org/10.1128/AEM.00192-06

Shaw, L.J., Burns, R.G., 2005. Rhizodeposition and the enhanced mineralization of 2,4-dichlorophenoxyacetic acid in soil from the Trifolium pratense rhizosphere. Environ. Microbiol. 7, 191–202. https://doi.org/10.1111/j.1462-2920.2004.00688.x

Silvani, L., Cornelissen, G., Hale, S.E., 2019. Sorption of α-, β-, γ- and δ-hexachlorocyclohexane isomers to three widely different biochars: Sorption mechanisms and application. Chemosphere 219, 1044–1051. https://doi.org/10.1016/j.chemosphere.2018.12.070

Šimura, J., Antoniadi, I., Široká, J., Tarkowská, D., Strnad, M., Ljung, K., Novák, O., 2018. Plant Hormonomics: Multiple Phytohormone Profiling by Targeted Metabolomics. Plant Physiol. 177, 476–489. https://doi.org/10.1104/pp.18.00293

Sineli, P.E., Tortella, G., Dávila Costa, J.S., Benimeli, C.S., Cuozzo, S.A., 2016. Evidence of α-, β- and γ-HCH mixture aerobic degradation by the native actinobacteria Streptomyces sp. M7. World J. Microbiol. Biotechnol. 32, 81. https://doi.org/10.1007/s11274-016-2037-0

Singh, S., Parihar, P., Singh, R., Singh, V.P., Prasad, S.M., 2016. Heavy Metal Tolerance in Plants: Role of Transcriptomics, Proteomics, Metabolomics, and Ionomics. Front. Plant Sci. 6, 1143. https://doi.org/10.3389/fpls.2015.01143

Ssekagiri, A., Sloan, W.T., Umer Zeeshan Ijaz, 2017. microbiomeSeq: An R package for analysis of microbial communities in an environmental context. https://doi.org/10.13140/RG.2.2.17108.71047

Stockholm Convention - an overview | ScienceDirect Topics [WWW Document], n.d. URL https://www.sciencedirect.com/topics/earth-and-planetary-sciences/stockholm-convention (accessed 6.21.21).

Suar, M., Meer, J.R. van der, Lawlor, K., Holliger, C., Lal, R., 2004. Dynamics of Multiple lin Gene Expression in Sphingomonas paucimobilis B90A in Response to Different Hexachlorocyclohexane Isomers. Appl. Environ. Microbiol. 70, 6650–6656. https://doi.org/10.1128/AEM.70.11.6650-6656.2004

Tedersoo, L., Suvi, T., Jairus, T., Ostonen, I., Põlme, S., 2009. Revisiting ectomycorrhizal fungi of the genus Alnus: differential host specificity, diversity and determinants of the fungal community. New Phytol. 182, 727–735. https://doi.org/10.1111/j.1469-8137.2009.02792.x

Thiem, D., Gołębiewski, M., Hulisz, P., Piernik, A., Hrynkiewicz, K., 2018. How Does Salinity Shape Bacterial and Fungal Microbiomes of Alnus glutinosa Roots? Front. Microbiol. 9.

Tischer, S., Hübner, T., 2002. Model Trials for Phytoremediation of Hydrocarbon-Contaminated Sites by the Use of Different Plant Species. Int. J. Phytoremediation 4, 187–203. https://doi.org/10.1080/15226510208500082

Torondel, B., Ensink, J.H.J., Gundogdu, O., Ijaz, U.Z., Parkhill, J., Abdelahi, F., Nguyen, V.-A., Sudgen, S., Gibson, W., Walker, A.W., Quince, C., 2016. Assessment of the influence of intrinsic environmental and geographical factors on the bacterial ecology of pit latrines. Microb. Biotechnol. 9, 209–223. https://doi.org/10.1111/1751-7915.12334

Trantírek, L., Hynková, K., Nagata, Y., Murzin, A., Ansorgová, A., Sklenář, V., Damborský, J., 2001. Reaction Mechanism and Stereochemistry of γ-Hexachlorocyclohexane Dehydrochlorinase LinA*. J. Biol. Chem. 276, 7734–7740. https://doi.org/10.1074/jbc.M007452200

Tuteja, N., 2007. Abscisic Acid and Abiotic Stress Signaling. Plant Signal. Behav. 2, 135–138. https://doi.org/10.4161/psb.2.3.4156

Verma, H., Bajaj, A., Kumar, R., Kaur, J., Anand, S., Nayyar, N., Puri, A., Singh, Y., Khurana, J.P., Lal, R., 2017. Genome Organization of Sphingobium indicum B90A: An Archetypal Hexachlorocyclohexane (HCH) Degrading Genotype. Genome Biol. Evol. 9, 2191–2197. https://doi.org/10.1093/gbe/evx133

Vrålstad, T., Schumacher, T., Taylor, A.F.S., 2002. Mycorrhizal synthesis between fungal strains of the Hymenoscyphus ericae aggregate and potential ectomycorrhizal and ericoid hosts. New Phytol. 153, 143–152. https://doi.org/10.1046/j.0028-646X.2001.00290.x

Vrchovecká, S., Amirbekov, A., Sázavská, T., Arias, C.A., Jespersen, E.A., Černík, M., Hrabák, P., 2024. Chemical analysis of wetland plants to evaluate the bioaccumulation and metabolism of hexachlorocyclohexane (HCH). Sci. Total Environ. 921, 171141. https://doi.org/10.1016/j.scitotenv.2024.171141

Waadt, R., Seller, C.A., Hsu, P.-K., Takahashi, Y., Munemasa, S., Schroeder, J.I., 2022. Plant hormone regulation of abiotic stress responses. Nat. Rev. Mol. Cell Biol. 23, 680–694. https://doi.org/10.1038/s41580-022-00479-6

Wacławek, S., 2019. Chemical oxidation and reduction of hexachlorocyclohexanes: A review. Water Res 162, 302-319,. https://doi.org/10.1016/j.watres.2019.06.072.

Wacławek, S., Silvestri, D., Hrabák, P., Padil, V.V.T., Torres-Mendieta, R., Wacławek, M., Černík, M., Dionysiou, D.D., 2019. Chemical oxidation and reduction of hexachlorocyclohexanes: A review. Water Res. 162, 302–319. https://doi.org/10.1016/j.watres.2019.06.072

Wang, C.-W., Chang, S.-C., Liang, C., 2019. Persistent organic pollutant lindane degradation by alkaline cold-brew green tea. Chemosphere 232, 281–286. https://doi.org/10.1016/j.chemosphere.2019.05.187

Wegner, C.-E., Liesack, W., 2017. Unexpected Dominance of Elusive Acidobacteria in Early Industrial Soft Coal Slags. Front. Microbiol. 8.

Wypych, G., 2001. Handbook of solvents. ChemTec Publishing.

Xu, X., Shi, Z., Li, D., Rey, A., Ruan, H., Craine, J.M., Liang, J., Zhou, J., Luo, Y., 2016. Soil properties control decomposition of soil organic carbon: Results from data-assimilation analysis. Geoderma 262, 235–242. https://doi.org/10.1016/j.geoderma.2015.08.038

Yang, K., Wu, W., Jing, Q., Zhu, L., 2008. Aqueous Adsorption of Aniline, Phenol, and their Substitutes by Multi-Walled Carbon Nanotubes. Environ. Sci. Technol. 42, 7931–7936. https://doi.org/10.1021/es801463v

Yuan, K., Rashotte, A.M., Wysocka-Diller, J.W., 2011. ABA and GA signaling pathways interact and regulate seed germination and seedling development under salt stress. Acta Physiol. Plant. 33, 261–271. https://doi.org/10.1007/s11738-010-0542-6

Zanewich, K.P., Rood, S.B., 1994. Endogenous gibberellins in flushing buds of three deciduous trees: alder, aspen, and birch. J. Plant Growth Regul. USA.

Zhang, Qiong, Zhou, C., Zhang, Quan, Qian, H., Liu, W., Zhao, M., 2013. Stereoselective Phytotoxicity of HCH Mediated by Photosynthetic and Antioxidant Defense Systems in Arabidopsis thaliana. PLOS ONE 8, e51043. https://doi.org/10.1371/journal.pone.0051043

Zhao, G., Xu, Y., Li, W., Han, G., Ling, B., 2007. PCBs and OCPs in human milk and selected foods from Luqiao and Pingqiao in Zhejiang, China. Sci. Total Environ. 378, 281–292. https://doi.org/10.1016/j.scitotenv.2007.03.008

Zheng, X., Jahn, M.T., Sun, M., Friman, V.-P., Balcazar, J.L., Wang, J., Shi, Y., Gong, X., Hu, F., Zhu, Y.-G., 2022. Organochlorine contamination enriches virus-encoded metabolism and pesticide degradation associated auxiliary genes in soil microbiomes. ISME J. 16, 1397–1408. https://doi.org/10.1038/s41396-022-01188-w

Zimmerman, A.R., Gao, B., Ahn, M.-Y., 2011. Positive and negative carbon mineralization priming effects among a variety of biochar-amended soils. Soil Biol. Biochem. 43, 1169–1179. https://doi.org/10.1016/j.soilbio.2011.02.005

Zürcher, E., Liu, J., di Donato, M., Geisler, M., Müller, B., 2016. Plant development regulated by cytokinin sinks. Science 353, 1027–1030. https://doi.org/10.1126/science.aaf7254